# Abstract

The Chromodomain Helicase DNA Binding Protein (CHD) family consists of a group of nine known proteins that function in controlling DNA dynamics and transcription. The CHD family member of interest in this work, *Chromodomain helicase DNA-binding protein 7* (*chd7*), has been implicated in human CHARGE (*c*oloboma of the eye, *h*eart defects, *a*tresia of the choanae, *r*etardation of growth and/or development, *g*enital and/or urinary abnormalities, and *e*ar abnormalities and deafness) Syndrome and Idiopathic Scoliosis, however little is known about the roles this gene plays during development.

Using zebrafish as a model system, morpholino antisense technology, whole mount *in situ* hybridization (WISH), and a relatively new protocol, RNA-Seq, we provide evidence of several developmental defects resulting from Chd7 knockdown as well as describe several genes that exhibit significant differential expression upon Chd7 knockdown. We provide evidence that zebrafish embryos highly express *chd7* in the retina, brain and somite boundaries. We demonstrate that a reduction in Chd7 synthesis results in laterality defects in the expression of somitogenesis genes, consistent with the hypothesis that this chromatin remodeler is necessary for the proper development of the long axis of the body and may be involved in the onset of human scoliosis. We show that the presence of Chd7 is crucial for proper neural, retinal and vertebral development in zebrafish and that loss of function of Chd7 resulted in several morphological defects similar to those observed in human patients with CHARGE syndrome.

Finally, this work is the first transcriptome-wide study analyzing genetic changes in response to knockdown of a member of the Chromodomain Helicase DNA Binding Protein family. Using RNA-Seq we were able to identify and quantify differentially

expressed genes in *chd7* morphant zebrafish embryos compared to control morphant zebrafish embryos. These data were consistent with our knockdown experiments as well as with putative roles for Chd7 in human diseases.

In an effort to make a broader impact, we extended the use of zebrafish beyond scientific research and described several different methods of using zebrafish in the undergraduate laboratory classroom. First, we described the use of WISH in the classroom to help students form connections between molecular and organismal biology and then described the use of two model organisms, zebrafish and *C. elegans*, in the classroom to help students understand how genes and the environment interact to affect organismal development.

Cumulatively, this work is an example of interdisciplinary study both in the research laboratory as well as in the classroom. It involves the intensive study of a chromatin remodeler, Chd7, and makes important connections between Chd7 knockdown in zebrafish and human diseases. It also describes the pedagogical advantages of model organisms with respect to providing a rich and integrative experience for undergraduate biology majors.

# Roles for Chd7 in zebrafish development with implications for human disease

By
Nicole Lynn McDaniels
B.S. SUNY University at Buffalo, 2007

DISSERTATION

Submitted in partial fulfillment of the requirements for the
degree of Doctor of Philosophy in Biology
in the Graduate School of Syracuse University

May 2012

# Acknowledgements

This dissertation is a cumulation of my studies in the lab of Dr. R. Craig Albertson to obtain my degree of Doctor of Philosophy in Biology at Syracuse University. Much time and effort of my own and of many others have gone into the construction of this work. As a result several parts of this work have been peer reviewed and published. Chapter 1 was published in *Developmental Dynamics* in 2011. Chapter 2 is currently in press for *PLoS One*. Chapter 4 was published in the *Journal of Visualized Experiments* in 2011.

Just one person cannot complete a work of this capacity. There are several people I would like to thank for their help in the process. Firstly, my advisor, Dr. R. Craig Albertson, for without Craig's expertise and guidance none of this would have been possible. Craig, I thank you whole-heartedly. I would also like to thank my committee members: Dr. Jeffrey Amack, Dr. Michael Cosgrove, Dr. Eleanor Maine, Dr. Melissa Pepling, and Dr. Jason Wiles. Each member of my committee contributed to this work in their own way, but it was the combination of backgrounds, knowledge and materials from this group of people that really helped to shape the body of my work and my educational experience.

Special thanks to Dr. Jeffrey Amack and Dr. Katherine Lewis for the use of their morpholino injection equipment. Thanks to Dr. Eleanor Maine and Dr. Jason Wiles for their help with the pedagogical work described in Chapters 4 and 5. I would also like to thank the Department of Biology staff and my fellow graduate students for their help and support along the way.

Chapter 2 was written in collaboration with Dr. Kessen Patten and the lab of Dr. Florina Moldovan at the University of Montreal. Dr. Patten and colleagues performed the

work analyzing defects in *chd7* morphant zebrafish heart, otolith, retina, ganglia, and facial nerve development as well as defects in vertebral mineralization. Our collaboration allowed us to suggest the use of *chd7* zebrafish morphants as a model system to study human CHARGE Syndrome. My interactions with Dr. Patten have been invaluable. I appreciate his willingness to work together and the expertise he brought to our study.

Finally, I would like to thank my family. Thanks to my parents, Neil and Diane Jacobs, for their support and guidance throughout my education. I would not be the person I am today without them. Thanks to my sister, Shannon Jacobs, for listening to me talk about my work and always being interested. And thank you to my husband, Shaun McDaniels, for his support and love and for putting up with me. No matter how nervous or stressed I was, Shaun always believed in me. Lastly, all of my friends and family not named here, thanks for being there and for being proud of me. You all have really helped make this a rewarding experience.

# Table of Contents

# List of Illustrative Materials

# Introduction

The processes that are initiated with the combination of genetic material in sexually reproducing organisms and result in the formation of a living organism in all of its complexities are both intriguing and amazing. These processes are taking place all around us in myriad different types of organisms every day. We collectively refer to these processes as development. Developmental biology is the study of how living things go from single cell embryos to complex organisms, and is studied in several different capacities, from genetic interactions to phenotypic output.

The overarching goal of this field is to understand the steps required to form a normal, healthy organism. Many human diseases can be attributed to defects in one or more of these steps. It is for this reason that the critical study and understanding of developmental processes is essential. Research in developmental biology can contribute to advances in medicine, gene therapy, and genetics. The work described herein is an example of experimental research designed to lead to a better understanding of vertebrate development by the intensive study of one gene with many important roles during early development.

**Laboratory based inquiry: Roles for *chd7* in zebrafish development**

The gene and corresponding protein of interest for this work is *chromodomain helicase DNA binding protein 7* (*chd7*). Chd7 is a chromatin remodeler, responsible for modulating the structure of the chromatin, therefore controlling the availability of genetic material for transcription. *Chd7* became a gene of interest to us after mutations in *CHD7* were shown to be associated with human idiopathic scoliosis (Gao et al., 2007) and

human CHARGE Syndrome (Vissers et al., 2004). We decided to examine this gene in more detail using the experimentally tractable zebrafish (*Danio rerio*) system.

The zebrafish was chosen as our model for several reasons. Zebrafish are relatively cheap and easy to breed and maintain in a laboratory setting. Fertilization is external, meaning the researcher can visually monitor embryonic development without disturbing the mother. Also, they mature quickly and early development occurs at a relatively rapid rate, with the embryos beginning to resemble a fish, with the precursors of most major organ systems, in less than 24 hours. The zebrafish genome has been sequenced and myriad literature is available describing zebrafish development and genetics. Finally, because the gene of interest was shown to play a role in spinal deformity, it was important to use a vertebrate model.

The work performed in this study was two-fold. First, gene specific studies and a reverse genetic approach were employed using methods such as whole mount *in situ* hybridization (WISH) and morpholino antisense knockdown to determine changes in response to Chd7 loss on a gene-by-gene basis. Secondly, a global approach was used to examine transcriptome-wide changes in zebrafish embryos upon loss of Chd7.

Our first goal was to obtain a general understanding of when and where *chd7* normally functions during zebrafish development. To this end, a *chd7* riboprobe was designed and WISH was performed on wild type zebrafish at several different stages of embryonic and larval development. These patterns, described in more detail in Chapters 1 and 2, were consistent with the *chd7* expression patterns of other vertebrates previously studied. This is evidence that our *chd7* riboprobe construction was accurate and

successful as well as evidence that *chd7* is evolutionarily conserved across vertebrate species.

To determine the role for *chd7* in proper zebrafish development, antisense morpholino technology was then used to knockdown Chd7 expression by suppressing the proper transcription of *chd7* mRNA. Zebrafish embryos were injected at the 1-2 cell stage with *chd7* splice blocking or translation blocking morpholinos. Injected embryos were allowed to develop, and gross phenotypic defects were analyzed. Functions of Chd7 during zebrafish development were inferred based on the loss of proper structural development in *chd7* morphants. This work is also described in greater detail in Chapters 1 and 2. Breifly, morpholino injected zebrafish embryos exhibit flattened heads, pericardial edema, as well as kinks, curvature and improper segmentation along the long axis of the body. In addition, defects in cranial neural crest development and migration are evident based on aberrant pharyngeal arch formation in *chd7* morphants.

Once we characterized more general functions of Chd7 in zebrafish, we went on to investigate a role for Chd7 during the earliest part of spinal development, somitogenesis. Somitogenesis is a complex genetic process involving the communication and coordination of many genes and proteins. During somitogenesis, paired tissue masses, termed somites, are formed in an anterior to posterior direction on either side of the neural tube. The somites consist of three different tissue types, the dermatome, the myotome, and the sclerotome. Following somitogenesis, the cells that compose the somites migrate ventro-laterally, and differentiate into several different structures including bone, muscle, and dermis. Sclerotomal tissue will develop into (among other bones) the vertebrae that compose the spine.

We used prior knowledge of the somitogenesis pathway constructed through the study of several different vertebrates to study the roles of Chd7 during zebrafish somitogenesis. Using a combination of morpholino antisense technology and WISH, we first knocked down proper production of Chd7 in zebrafish. Next, we fixed the *chd7* morphants at the 13 somite stage, about halfway through somitogenesis. Finally, we performed WISH to visualize the expression of selected somitogenesis genes that represent discrete stages of this process. More details on the somitogenesis signal transduction pathway and the genes selected for WISH can be found in Chapter 1. Broadly, the outcome of our study showed that upon Chd7 knockdown the expression patterns of several different genes involved in somitogenesis downstream of the formation of the anterior-posterior (A-P) axis were abnormal. Specifically, many somitogenesis genes exhibited an asymmetric expression pattern in the developing somites, whereas in wild type and control morphant zebrafish expression was symmetric.

Another interesting phenotype observed was the loss of proper A-P polarity in genes, leading to improper somite border formation, as discussed in Chapter 2. This border defect was also apparent later in development as exhibited by improper segmental vasculature formation. These data lend support for the idea that loss of Chd7 during spinal formation may contribute to spinal deformity. Based on our data and the previous data associating human *CHD7* with scoliosis (Gao et al., 2007), we suggest that zebrafish *chd7* morphants may be useful for research programs conducted to better understand human spinal deformities.

In collaboration with the lab of Dr. Florina Moldovan at the University of Montreal, we next studied the defects in zebrafish *chd7* morphants as they pertain to

human CHARGE Syndrome. CHARGE (*coloboma* of the eye, *h*eart defects, *a*tresia of the choanae, *r*etardation of growth, *g*enital abnormalities, *e*ar abnormalities and deafness) Syndrome is a debilitating disease in humans marked by several developmental defects. In Chapter 2 we provide evidence of defects in eye, otolith, and heart development in *chd7* morphants as well as in cranial neural crest cell development and migration, parallel to human CHARGE Syndrome symptoms. Based on this evidence we suggest the use of *chd7* zebrafish morphants as models for human CHARGE Syndrome.

The last part of this project took a more global approach to the study of roles for Chd7 during zebrafish development. A combination of morpholino antisense technology and RNA-seq was used to determine transcriptome-wide changes in zebrafish embryos upon loss of Chd7. RNA-seq is a relatively new approach using next generation sequencing technologies to explore transcriptome dynamics. Next generation sequencing is a novel high-throughput sequencing method that provides a rapid and cost-effective means to generate vast amounts of sequence information (Marguerat and Bahler, 2010), and this technology has revolutionized the way we study gene regulation. With the ability to obtain information about gene expression, as reflected in the transcriptome, we can better understand transcriptional gene regulation. In addition, RNA-seq can be used to compare transcriptome samples between different cell types or organisms under different treatment conditions to determine variation in transcripts.

For our purposes, we again used morpholino injection to knock down Chd7 in zebrafish embryos and fixed *chd7* morphants at the 13 somite stage. We then isolated the RNA from three biological replicates of *chd7* morphants and control morphants. The RNA was converted into double stranded cDNA libraries, fragmented, and adaptors

necessary for the binding of sequencing primers were ligated to the ends of the fragmented cDNA strands. Each cDNA strand was sequenced in a high-throughput manner on the Illumina machine at the University of Oregon. Sequencing data was analyzed using Galaxy, a web-based platform providing tools for RNA-seq data analysis.

We found over 2000 genes that were differentially expressed in *chd7* morphants compared to control morphants. Due to the plethora of data, we were not able to describe each differentially expressed gene in detail. Rather we listed the top 20 up- and downregulated genes in *chd7* morphants as well as described some differentially expressed genes that support previous studies. Some interesting differentially expressed genes included members of the *hox* gene family, *vox*, *vent*, other pattening genes, several Wnt receptors, an Fgf receptor, and several genes that play roles in Notch signaling. These all support our previous evidence of patterning and somitogenesis defects as discussed in Chapters 1 and 2.

Additionally, several genes whose loss of proper functions could potentially lead to the defects observed in CHARGE Syndrome were found to be differentially expressed in *chd7* morphants. Some examples include *gnl3*, involved in retina development (Schmitt et al., 2009), and *atp1a1*, which functions in heart tube, cardiac cell (Shu et al., 2003; Langenbacher et al., 2011), otolith, and otic vesicle development (Blasiole et al., 2006). Finally, several genes that function in neural crest cell development and migration and cartilage development were differentially expressed in *chd7* morphants.

In summary, using a relatively new protocol, RNA-Seq, we have accumulated useful data and were able to show several connections between genes with significantly different expression levels and *chd7* morphant zebrafish phenotypes, making our data

useful in supplementing previous work with Chd7 (Jacobs-McDaniels and Albertson, 2011; Patten et al., 2012). This work is discussed in detail in Chapter 3.

**Pedagogy: Zebrafish in the classroom**

The study of developmental biology is not only emerging as a significant and essential component of laboratory–based inquiry, but can also be a powerful tool in the classroom. To prepare future scientists, as well as citizen scientists, it is essential that undergraduate students obtain a well-rounded and integrative training.

As an instructor it is a perpetual challenge to come up with cutting-edge, budget friendly laboratory activities that promote student engagement and critical thinking, but are also contemporary and provide students with the skills they need to become proficient in understanding a field that is rapidly evolving. Interdisciplinary research that combines ideas and methods from several different areas of study is growing in popularity in research institutions worldwide. For example, within developmental biology, two subfields are gaining popularity and acceptance: Ecological developmental biology, or "eco-devo" which combines the fields of ecology and development to help understand the impacts of environmental events on organismal development (Gilbert and Epel, 2009); and Evolutionary developmental biology, or "evo-devo" which combines the studies of evolution and development to determine ancestral relationships between organisms as well as how different developmental processes have evolved (Carroll et al., 2005).

At the college level it is becoming more important now than ever before to provide students with a well-rounded scientific education. To aid in this accomplishment, we have produced resources for instructors that give examples of cutting-edge laboratory

experiences for college students. These resources are based on a combination of our experiences in the laboratory classroom and the research laboratories at Syracuse University.

First, with the help of a relatively new video publisher, the Journal of Visualized Experiments (JoVE), we made publicly available both a written protocol and video demonstration of WISH. WISH is a popular and relatively straight-forward technique often used in developmental biology laboratories to visualize gene expression. While the use of WISH as a pedagogical tool is not novel in and of itself, we used WISH in a Comparative Vertebrate Biology laboratory, an upper level course at Syracuse University, as a means to help students make connections between molecular and organismal biology. As a laboratory activity, we performed WISH using probes for several different genes and different strains of zebrafish embryos, had the students analyze gene expression patterns in these embryos, and make conclusions based on their previously obtained knowledge of anatomy, development and genetics. Students showed much interest and enthusiasm for this laboratory experience.

The inclusion of a molecular level technique in an otherwise organismal-level course allowed for the connection to be made between genes and phenotype or anatomy. This novel teaching technique provided students in the Comparative Vertebrate Biology course with an appreciation for how anatomical structures develop and evolve, and what can result on an organismal level when developmental processes are defective at the molecular level. This is discussed in greater detail in Chapter 4.

In an effort to provide students with an even more interdisciplinary learning experience, as a part of an Integrative Biology Laboratory course, we extended the

experience detailed above and used two model systems, a nematode, *Caenorhabditis elegans* (*C. elegans*), and the zebrafish (*Danio rerio*). The goal here was to provide students with an experience using live model organisms as well as allow students to observe the effects of gene-by-environmental interactions on development. Over several laboratory sessions, students were given the opportunity to observe live zebrafish development at the embryonic and larval stages, observe gene expression patterns in zebrafish embryos using WISH (as described above), study non-model systems including African cichlid fishes and Antarctic notothenioids (to gain an appreciation for the diversity in developmental systems), observe the life cycle of live *C. elegans*, and study the effects of genetic mutations and the environment on germline development in *C. elegans* (to gain an appreciation for Gene x Environment interactions).

Using a combination of lecture and lab activities, students were first introduced to zebrafish as a model system, the zebrafish life cycle, and how to properly maintain zebrafish in the laboratory. To demonstrate genetic regulation of development, the zebrafish line containing an *fgf8* mutation, named *acerebellar,* or "*ace*" was used because *ace* mutants display dysmorphic bone development, among other defects. To show our students how shifts in development precede and predict changes in adult morphology African cichlids and Antarctic notothenioids were used because they exhibit striking natural variations in bone development. Following the fish laboratory module, the nematode worm *C. elegans*, was introduced and employed in an activity to help emphasize the general importance of environmental factors in development. These lab-based exercises were augmented by problem-based learning assignments.

The outcome of this experience was the production of students with an

understanding of and experience in handling live organisms of two different model systems. In addition, these laboratory exercises provided a hands-on experience for students to gain an integrative biological understanding of how genetics and the environment work in tandem in the production of an organism's phenotype. We feel interdisciplinary courses and laboratory modules such as these help to produce well-rounded students and to better prepare them to perform independent laboratory research with faculty members. Detailed descriptions of the exercises used in this lab as well as their outcomes can be found in Chapter 5.

**Conclusions**

This work is the product of intense laboratory study examining zebrafish development, focusing specifically on a chromatin remodeler, Chd7, as well pedagogical work aimed at making laboratory courses in the field of biology more contemporary and interdisciplinary. The field of epigenetics, the study of heritable changes in gene expression patterns or phenotype as a result of changes beyond the DNA sequence, is quickly gaining popularity. The laboratory research described here combines the field of epigenetics with the field of development, to aid in the understanding of how regulation of gene expression is vital for proper organismal development. The pedagogical portion of this work provides cutting-edge examples of how laboratory activities can be enhanced at the college level to produce well-rounded, experienced students.

Cumulatively, this work is an example of interdisciplinary study both in the research laboratory as well as in the classroom. It is a combination of learning through experimentation, learning through questioning, and learning in the classroom, all

necessary to help us better understand the living world. Using these different educational methods, the goal of this body of work is to provide an appreciation and a better understanding of the many different aspects of what we call Science.

# Chd7 plays a critical role in controlling left-right symmetry during zebrafish somitogenesis

**Nicole L. Jacobs-McDaniels[1], R. Craig Albertson[1, 2]**

Affiliation: [1]Department of Biology, Syracuse University

[2]Department of Biology, University of Massachusetts

**ABSTRACT**

Somitogenesis is a complex process during early vertebrate development involving interactions between many factors to form a bilateral somite series. A role for chromatin remodelers in somitogenesis has not yet been demonstrated. Here we investigate the function of *chromodomain helicase DNA binding protein 7* (*chd7*) during zebrafish somitogenesis. We show that Chd7 deficiency leads to asymmetric segmentation of the presomitic mesoderm (PSM), as revealed by expression of the somitogenesis genes, *cdx1a, dlc, her7, mespa* and *ripply1*. Moreover, we show that abrogation of Chd7 results in the loss of asymmetric expression of *spaw* in the lateral plate mesoderm, which is consistent with more general laterality defects. Based on the observation that insufficient Chd7 leads to left-right asymmetry defects during PSM segmentation, and because *CHD7* has been linked to human spinal deformities, we suggest that zebrafish *chd7* morphants may be a good *in vivo* model to examine the pathophysiology of these diseases.

## INTRODUCTION

With recent advances in our understanding of epigenetic processes (Srinivasan et al., 2008; Radman-Livaja and Rando, 2010), new roles for chromatin remodelers in regulating organismal development have emerged (Pray-Grant et al., 2005; Marfella et al., 2006; Takada et al., 2007; Thompson et al., 2008; Gaspar-Maia et al., 2009; Randall et al., 2009; Bajpai et al., 2010; Scimone et al., 2010). The chromodomain helicase DNA-binding proteins (CHDs) are highly conserved from yeast to humans (Marfella and Imbalzano, 2007), and yet functional roles for most members of this family in organismal development and homeostasis remain poorly understood. The CHD family is distinguished by two signature sequence motifs: tandem chromodomains located in the N-terminal region, and the SNF2-like ATPase domain located in the central region of the protein structure (Marfella and Imbalzano, 2007). Each protein in the CHD family also has a more or less well defined C-terminal DNA-binding motif, but all are predicted to have abilities to interact with DNA, directly or indirectly (Hall and Georgel, 2007). CHD proteins regulate transcription by using energy from ATP to disrupt nucleosomes, thereby altering the structure of the chromatin (Tran et al., 2000; Wang and Zhang, 2001; Stockdale et al., 2006), and are thought to be important regulators of developmental processes (Pray-Grant et al., 2005; Marfella et al., 2006; Takada et al., 2007; Thompson et al., 2008; Gaspar-Maia et al., 2009; Randall et al., 2009; Bajpai et al., 2010; Scimone et al., 2010). Defects in members of the CHD family have also been implicated in several human diseases including neuroblastomas (Thompson et al., 2003; White et al., 2005), Dermatomyositis (Ge et al., 1995), CHARGE (*c*oloboma of the eye, *h*eart defects, *a*tresia of the choanae, *r*etardation of growth and/or development, *g*enital and/or urinary

abnormalities, and *e*ar abnormalities and deafness) Syndrome (Vissers et al., 2004), and Idiopathic Scoliosis (Gao et al., 2007).

Chromodomain helicase DNA-binding protein 7 (Chd7) is one of nine known proteins in the CHD family, and is categorized into the third of three CHD subfamilies. Chd7 is the largest protein in the CHD family and has only recently been described (Gao et al., 2007; Bajpai et al., 2010; Schnetz et al., 2010; Zentner et al., 2010). Binding of Chd7 has been correlated with methylation of histone H3 at lysine 4 (H3K4me), and based on this and several other features, it is suggested that Chd7 may function in enhancer mediated transcription (Schnetz et al., 2009). Mutations in *CHD7* are known to cause CHARGE Syndrome, in which over 60% of those afflicted develop later onset scoliosis (Doyle and Blake, 2005). It has also recently been demonstrated that a scoliosis-associated *CHD7* haplotype is centered over exons 2-4 in humans. Resequencing revealed a polymorphism that predicts disruption of a possible binding site for caudal-type (cdx) homeodomain-containing transcription factors (Gao et al., 2007). Scoliosis affects about 6 million Americans (National Scoliosis Foundation). Physiologically, spinal defects can lead to back and neck pain, and asymmetric human morphologies. Improperly developed vertebrae can put pressure on and/or puncture internal organs. In short, humans with spinal defects can have a range of difficulties in day to day living. Currently, there is no concrete cause for the most common type of scoliosis, Idiopathic Scoliosis, and therefore no animal model with which to study its pathophysiology. Based on previous work relating *CHD7* to human spinal deformity, the focus of our work was to determine the roles for Chd7 in zebrafish (*Danio rerio*) somitogenesis using antisense morpholino knockdown and gene expression analyses.

Development of the spine in vertebrates begins with somitogenesis in which individualization of metameric subunits (i.e., somites) takes place through a series of complex and hierarchical molecular interactions. Myriad genes are involved in somitogenesis (Stickney et al., 2000; Holley, 2007). For the experiments described herein, a simplified pathway consisting of a reduced set of somitogenesis genes was used to evaluate a role for Chd7 in mediating this process (Fig. 1). Specifically, somitogenesis was divided into three main patterning events: (1) the establishment of anterior-posterior (A-P) polarity, (2) the segmentation clock, and (3) the establishment of segmental anterior-posterior polarity. During the first stage, Retinoic Acid (RA) and Fibroblast Growth Factor 8 (Fgf8) act to establish the A-P axis within the presomitic mesoderm (PSM), with RA establishing anterior fate and Fgf8 maintaining the undifferentiated state of the posterior PSM (Dubrulle et al., 2001). A role for RA in maintaining left-right bilateral symmetry of the PSM has also recently been established (Kawakami et al., 2005). The canonical Wnt signaling pathway is responsible for joining RA/Fgf8 signaling with segmentation clock genes (Aulehla and Herrmann, 2004), as well as activating caudal-related genes that promote posterior morphogenesis (Shimizu et al., 2005). The segmentation clock consists of many genes, mostly members of the Notch signaling pathway, that are expressed first in the tailbud, then in a wave-like pattern along the PSM, moving anteriorly, to direct somite formation. This "wave" of gene expression oscillates such that each wave front contributes to the formation of one somite pair (Stickney et al., 2000; Holley, 2007; Mara and Holley, 2007; Sparrow et al., 2007). Finally, reminiscent of *Drosophila* segment polarity genes, the expressions of patterning genes within each somite defines the A-P segmental polarity within this tissue. The

process of somitogenesis is therefore important for the proper segmentation of the PSM, and is the first stage of vertebral development.

Here we demonstrate that a reduction in Chd7 synthesis results in laterality defects in the expression of somitogenesis genes, consistent with the hypothesis that this chromatin remodeler is necessary for the proper development of the long axis of the body. We suggest that these insights may contribute to an understanding of the etiologies of spinal deformity in zebrafish, which could be relevant to human health and disease.

## RESULTS

### *Chd7* shows strong expression in the brain, tail bud and somite borders of zebrafish embryos

To determine where *chd7* was expressed in wild type zebrafish, whole mount *in situ* hybridization (WISH) was performed. Digoxigenin labeled riboprobes were designed and synthesized complimentary to *chd7* mRNA. Upon the completion of WISH, embryos were embedded and sectioned into 35 μm sections for a more thorough analysis of expression patterns. Our initial results indicate that *chd7* is ubiquitously expressed during early stages of somitogenesis, but becomes more tissue specific toward the conclusion of somitogenesis (data not shown). Specifically, strong expression of *chd7* was observed throughout the brain, in the eyes and the otic vesicle, in the tail bud, and in the borders of mid to posterior somites by mid-segmentation stages (Fig. 2; Supplementary Fig. 1). Sense control riboprobes did not exhibit specific binding (Supplementary Fig. 1). Expression studies in other model organisms and in humans have reported similar patterns of tissue-specific *chd7* expression (Bosman et al., 2005; Lalani et al., 2006; Aramaki et al., 2007; Hurd et al., 2007; Kulkarni et al., 2008), which suggests that patterns of *chd7* expression have been highly conserved during vertebrate evolution.

### Chd7 morpholino knockdown

To better understand the roles for *chd7* in zebrafish development, antisense translation blocking and splice blocking morpholinos (MOs) were designed and injected into AB wild type zebrafish embryos at the 1-2 cell stage. To test the reliability of the MO knockdown, a dosage dependence study was performed. Zebrafish embryos were injected

with approximately 1 nl of 2 ng/nl, 4 ng/nl, or 6 ng/nl concentrations of *chd7* translation blocking or splice blocking MOs. The injected embryos were allowed to grow for 48 hours, and then the number of larvae with defects and the severity of the defects were quantified. Obvious phenotypic defects included a flattening of the top of the head, curves or kinks along the long axis of the body, and pericardial edema. An extreme defect also occurred in a small number of MO injected embryos, which included the complete truncation of the posterior body. To quantify defects induced by *chd7* MO injection, injected fish were categorized as "control", "mild", "moderate", or "severe" based on exhibited phenotypes (Fig. 3A). In concordance with the expected results, the frequency and severity of defects increased with increasing MO concentrations. Few embryos injected with control MO exhibited physical defects, and the number of defective embryos did not increase with increasing control MO concentrations (data not shown). We also tested for any differences between standard control MO and *chd7* 5bp mismatch control MO. The phenotypic ratios were largely indistinguishable between the two types of controls (Fig. 3B).

To verify that the *chd7* MO was knocking down the expression of Chd7 by preventing proper translation of *chd7* mRNA, RT-PCR was performed using *chd7* splice blocking MO injected zebrafish at 48 hpf (hours post fertilization). The splice blocking MO was designed to bind *chd7* mRNA at the junction across the 3' end of exon 2 and the 5' end of intron 2. To test for loss of proper *chd7* mRNA processing, PCR primers were designed to bind cDNA at sites corresponding to the 5' end of exon 2 and the 3' end of exon 3 of the *chd7* mRNA. Intron 2 of zebrafish *chd7* was predicted to be 252 base pairs (bp) long (Ensembl Zv9). To verify that the splice blocking MO prevented proper

splicing of intron 2, PCR products were visualized using gel electrophoresis. As expected, the resulting PCR products from the *chd7* morphant embryos were approximately 250bp longer than the PCR products of control MO injected zebrafish (Fig. 3C). This is evidence that intron 2 was not properly spliced out of the *chd7* morphant mRNA during mRNA processing, which should lead to improper protein construction at the translational level and therefore flawed protein function. The band corresponding to the PCR product of uninjected wild type zebrafish at 48 hpf was the same size as the control MO injected fish at the same age (Fig. 3C).

Injection of either translation or splice blocking MOs resulted in the same phenotypic defects including those in the brain, somites, and tail. To ensure that the morpholino was evenly distributed throughout the injected embryo, embryos were co-injected with *chd7* MO and GFP mRNA. As expected, the GFP mRNA was dispersed evenly throughout the entire embryo (Fig. 3D). Results from the WISH analyses performed using embryos co-injected with GFP mRNA and *chd7* MO were indistinguishable from those using embryos injected with *chd7* MO alone. These results, in addition to our dosage-dependence and RT-PCR assays, suggest that both the translation and splice blocking MOs result in truncated or defective Chd7 protein production. Moreover, the anatomical regions affected by *chd7* MO injection correspond to areas in which we have shown *chd7* to be expressed in zebrafish, namely the brain and the somites, consistent with a primary role for *chd7* in zebrafish long-axis formation.

### ***Chd7*** **functions in directing bilaterally symmetric expression of somitogenesis genes**

Since injection of 6 ng/nl *chd7* translation-blocking MO had the most dramatic effect on 48 hpf morphants, this MO was used for all ensuing experiments. To identify genetic defects resulting from Chd7 knockdown, *chd7* MO injected zebrafish embryos were collected and fixed at the 13 somite stage of development (Kimmel et al. 1995). Injected embryos were then analyzed by WISH to visualize the expression patterns of selected axial patterning genes including, *fgf8a* (Reifers et al., 1998), an anterior-posterior polarity gene, *cdx1a* (Davidson and Zon, 2006), a gene necessary for proper posterior polarity, *dlc* and *her7* (Oates et al., 2005), segmentation clock genes, *mespa* (Sawada et al., 2000), and *ripply1* (Kawamura et al., 2005; Zhang et al., 2008), genes that play a role in the determination of anterior-posterior polarity of the individual somites, among other important functions. The most prominent defect was an asymmetrical display of gene expression in the somites and/or tailbud (Fig. 4A-B, D-E, G-H, J-K, M-N). This was significant for *cdx1a* ($t=4.08$, $p=0.015$), *dlc* ($t=4.22$, $p=0.013$), *her7* ($t=4.76$, $p=0.009$), *mespa* ($t=2.86$, $p=0.046$), and *ripply1* ($t=10.46$, $p=0.0005$) (Fig. 4C, F, I, L,O). Asymmetric expression of *fgf8a* was just above significance at the 0.05-level ($t=2.58$, $p=0.061$). Only 3 of 77 embryos (3.9%) injected with GFP mRNA showed bilaterally asymmetric GFP expression, which suggests that asymmetric distribution of *chd7* MO is not the cause of this trend. To ensure that the results presented here were not due to off-target effects of the relatively high dose of translation blocking MO, we repeated the experiments with *chd7* splice blocking morphant embryos using a small subset of probes and obtained identical results – i.e., the same frequency of asymmetric gene expression (data not shown). In all, these data suggest important roles for *chd7* downstream of A-P specification during zebrafish somitogenesis.

To determine whether the asymmetric expression of these genes is associated with broader laterality defects or if this asymmetry is specific to the somites, expression of *cmlc2*, a heart marker, and *spaw,* a gene important for the determination of visceral and diencephalic left-right asymmetry (Long et al., 2003) were analyzed. Defects in early heart development precluded an accurate assessment of heart laterality (data not shown), however *spaw* expression was found to be bilateral in 36 of 51 (>70%) *chd7* morphants (Supplementary Fig. 2) indicating that laterality defects in *chd7* morphants may be wide spread. A more thorough assessment of the linkage between organ and somite laterality via Chd7 activity would be an interesting area of further research.

## DISCUSSION

### Roles for Chd7 in somitogenesis

Somitogenesis is a complex and vital process in vertebrate development that involves many known genes distributed across several families of signaling proteins, and a vast amount of work has been done to characterize this process (see reviews: Stickney et al., 2000; Pourquié, 2001; Aulehla and Herrmann, 2004; Sewell and Kusumi, 2007; Geetha-Loganathan et al., 2008; Dunwoodie, 2009). To our knowledge, there are currently no chromatin remodelers reported to play a role in somitogenesis. Chd7 is a member of the Chromodomain Helicase DNA-binding protein family. It is a large protein, over 3000 amino acids long and containing a predicted 37 exons in zebrafish (Ensembl Zv9). It uses the energy provided from the breakdown of ATP to modulate the links between histones and DNA (Hall and Georgel, 2007; Marfella and Imbalzano, 2007; Ho and Crabtree, 2010). Members of the CHD family have the abilities to catalyze structural changes in chromatin that allow access to DNA bound to nucleosomes, repositioning of nucleosomes, transfer of histone octamers to donor DNA, and replacement of histones with histone variants (Längst and Becker, 2004; Workman, 2006; Gangaraju et al., 2007; Thompson et al., 2008) These activities work *in vivo* to modulate proper transcription, replication, and repair of the eukaryotic genome (Eberharter and Becker, 2004; Sif, 2004; Altaf et al., 2007; Osley et al., 2007; Thompson et al., 2008). It is therefore highly likely that CHD proteins will have multiple functions in vertebrate development.

We investigated the role of Chd7 during zebrafish somitogenesis. Using morpholino antisense technology and WISH we demonstrated that Chd7 is necessary for proper symmetric expression of key somitogenesis genes located downstream of Wnt

signaling, including *cdx1a*, *dlc*, *her7*, *mespa*, and *ripply1* whereas A-P specification and segment polarity appear to be largely unaffected (Fig. 4). This suggests that Chd7 is critical for the junction between A-P specification and segmentation clock activity. Additional work is required to flesh out the specific points along the somitogenesis pathway where Chd7 is acting.

Recently, Chd7 was found to interact with its paralog Chd8 *in vitro*, possibly forming one component of a protein complex (Batsukh et al., 2010). This complex is predicted to have functions similar to *kismet*, the only *Drosophila melanogaster* gene related to members of the third CHD subfamily (Batsukh et al., 2010). *Kismet*, a member of the *Drosophila* trithorax group, is known to play a role in segmentation and segment identity during *Drosophila* development (Daubresse et al., 1999). In addition, there is evidence that Chd8 binds directly to β-catenin *in vivo*, as well as the promoters and 5' coding regions of some β-catenin target genes (Thompson et al., 2008), suggesting an association between the Chd7/Chd8 complex and the Canonical Wnt signaling pathway. Short hairpin RNA against Chd8 has also been shown to result in the activation of several β-catenin target genes, implying that Chd8 may negatively regulate β-catenin-targeted gene expression (Thompson et al., 2008). Notably, we found that two Wnt target genes, *cdx4* and *ntla*, exhibit upregulated expression upon Chd7 knockdown (Supplementary Fig. 3). We did not observe an obvious, qualitative upregulation in the Wnt target gene *cdx1a* (unlike *cdx4* and *ntla*), but we did observe asymmetric expression in the tailbud (Fig. 4A-C). More work is necessary to determine the exact mechanism behind the differences in these expression patterns. One possibility is that *cdx1a* cannot be expanded anteriorly due to the presence of other negative regulators, and is instead exhibiting a loss

of symmetric expression due to a failure of proper direction. The putative link between CHDs and Wnt signaling is consistent with our results, and offers a hypothesis that the specific mechanism by which Chd7 modulates zebrafish somitogenesis may be associated with the Wnt signaling pathway. Clearly, this would be a fruitful area of future research.

Our results, which demonstrate roles for Chd7 in PSM segmentation, are similar to those that have revealed a link between chromatin remodeling and segmental identity during craniofacial development. The zebrafish *moz* mutant is lacking the histone acetlytransferase, Moz, which modulates chromatin structure via post-translational histone modification. A conspicuous phenotypic result of this deficiency is an anterior homeotic transformation of pharyngeal arch segments (Miller et al., 2004). Collectively, these studies demonstrate that chromatin remodelers are critical for segmental specification, and A-P patterning during vertebrate development.

**Loss of Chd7 function and the onset of spinal deformity**

Loss of CHD7 function in humans is known to cause CHARGE syndrome (Vissers et al., 2004), in which over 60% of those affected develop later onset scoliosis (Doyle and Blake, 2005). Polymorphisms in the non-coding regions of *CHD7* have also been associated with susceptibility to Idiopathic Scoliosis (Gao et al., 2007). Moreover, CHD7 has recently been implicated as the first known chromatin remodeling protein to play a critical role in initiating normal human puberty (Kim et al., 2008), the life-history stage in which scoliosis most often manifests itself in humans. Other somitogenesis genes have also been implicated in the development of spinal deformities. For example, mutations in *DLL3,* an ortholog of zebrafish *dlc* and member of the Notch signaling pathway, have

been shown to lead to Spondylocostal dysostosis (SD), a human disease marked by several different spinal deformities including vertebral disgenesis, vertebral compression, as well as curvature of the spine (e.g., hemivertebrae and kyphoscoliosis) (Bulman et al., 2000). When allowed to grow to 15 days post fertilization (dpf), low dose (i.e., 2ng/ul) *chd7* MO injected fish exhibit a decrease in ossification and bone mineralization in the spine (Kessen Patten, personal communication). This is consistent with reports linking human scoliosis with osteopenia (Cheng et al., 2001; Hung et al., 2005) and raises the possibility that a combination of decreased bone density (as revealed by low dose injection) and asymmetric PSM segmentation (as revealed by high dose injections) caused by Chd7 deficiency may lead to spinal curvatures. While this hypothesis has yet to be tested, our results, in addition to the works described above, provide abundant evidence suggesting that Chd7 is necessary for proper spinal development, and implicate Chd7 deficiency as a contributor to spinal deformities, specifically scoliosis.

Based on our expression analyses, *chd7* exhibits patterns of strong expression in the brain, tail bud and somite borders beginning at mid-segmentation stages and continuing until just after the process of somitogenesis is complete in zebrafish. This *chd7* expression pattern is conserved across several vertebrate taxa (Bosman et al., 2005; Lalani et al., 2006; Aramaki et al., 2007; Hurd et al., 2007; Kulkarni et al., 2008), suggesting a broad role for *chd7* in proper spinal development and growth coordination, based on the anatomical structures and developmental timing in which it is expressed. The Neuro-Osseus Timing Of Maturation (NOTOM) hypothesis describes a possible model for the onset of Adolescent Idiopathic Scoliosis (AIS) in humans. It states that communication between the central nervous system (the brain) and the axial skeleton

(which is derived from the somites) is essential for the proper growth of the spine, especially throughout human adolescence (Burwell et al., 2008). In AIS patients, it is thought that asynchrony between the brain and the skeleton may lead to improper, asynchronous growth of the spine, and that puberty is the most sensitive time for this asynchrony because growth is occurring so quickly it accentuates and amplifies this miscommunication. Without proper cues from the nervous system, the timing and rate of skeletal development may vary bilaterally, creating odd pressure points during growth and resulting in an asymmetric adult morphology. The expression of *chd7* in the brain and somites across vertebrate taxa, as well as the phenotypes resulting from Chd7 knockdown in zebrafish, lend support for the NOTOM hypothesis for AIS, and may implicate human *CHD7* in this phenomenon. Specifically, it posits a role for *chd7* in normal growth along the anterior-posterior axis in vertebrates via coordinating communication between the central nervous system and the skeleton.

**Widespread laterality defects in *chd7* morphants**

The majority of our *chd7* morphants exhibited bilateral expression of *spaw,* which could be due to a variety of factors including disrupted midline integrity (e.g., Amack et al., 2007; Liu et al., 2011), aberrant monocilia function (e.g., Huang et al., 2011), or Na/K pump defects (e.g., Ellertsdottir et al., 2006). We show here that *ntl* is upregulated in *chd7* morphants, which suggests that the midline is intact. Thus, another mechanism is likely behind the bilateral expression of *spaw* observed here. Whether this defect can be traced to aberrant Kupffer's vesicle (KV) formation and/or function (Huang et al., 2011), or to Na/K pump defects, which may act in parallel to KV function (Ellertsdottir et al.,

2006), remains to be determined. Given chromatin remodelers have not previously been implicated in left-right (LR) axis formation, continued research along these lines is warranted.

**Chromatin remodelers and human diseases**

With increasing interest in the field of epigenetics, we are gaining a better understanding of how gene expression is controlled beyond the DNA sequence. There are several known types of epigenetic factors including DNA methylation, post-translational modifications of histones and chromatin remodelers (Peterson and Laniel, 2004; Shilatifard, 2006; Clapier and Cairns, 2009; Lee et al., 2010). Our work focuses on an ATP-dependent chromatin remodeler that is a member of the chromodomain helicase DNA binding protein family. Mutations in *CHD7* have already been implicated in CHARGE Syndrome (Vissers et al., 2004), although multiple different mutations have been discovered and these mutations do not explain all cases of this disease (Bosman et al., 2005; Lalani et al., 2005; Sanlaville et al., 2006). Our ongoing work is seeking to establish a zebrafish model for human CHARGE Syndrome via *chd7* MO injection (Patten et al., 2012). Here we extend the utility of this system by offering zebrafish *chd7* morphants as a model with which to study normal spinal development as well as the pathology of spinal deformities such as scoliosis. To date, the genetic etiologies of most human spinal deformities remain unknown, which is likely due to the fact that these malformations represent complex diseases that depend on the interaction between genetic background and the environment.

Because they can have multiple functions, can be found in protein complexes, and can affect the expression of multiple genes, chromatin remodelers are good candidates for complex human diseases. In support of this assertion, many human developmental diseases are known to be the consequences of mutations in chromatin modifying genes, including Rubinstein-Taybi, X-linked Alpha Thalassemia, Rett Syndrome, Coffin-Lowry Syndrome, and Schimke immuno-osseous dysplasia (Jiang et al., 2004; Martin, 2010). Moreover, the screening of *Drosophila* models for Huntington disease, spino-cerebellar ataxia, and certain other Mendelian disorders have identified modifications in genes responsible for chromatin remodeling (Fernandez-Funez et al., 2000).

In conclusion, our work provides evidence that chromatin remodelers play a role in zebrafish spinal development and the control of left-right symmetry of the long axis of the body. Based on this work and that of previous investigations (e.g., Gao et al., 2007), we suggest that Chd7 may provide a molecular inroad to the pathophysiology of scoliosis and other human spinal deformities.

## EXPERIMENTAL PROCEDURES

### Zebrafish maintenance

Wild-type AB zebrafish (*Danio rerio*) embryos were raised at 28.5°C on a 14 hour light, 10 hour dark cycle. Embryos and larvae were collected and staged as previously described (Kimmel et al., 1995). Embryos were fixed in 4% paraformaldehyde and stored in 100% methanol for whole mount *in situ* hybridization (WISH). Images were captured using a Zeiss Axiocam digital camera connected to an Antec PC and processed with Adobe Photoshop 7.0. All protocols were carried out in compliance with the Institutional Animal Care and Use Committee (IACUC) at Syracuse University.

### Sectioning of zebrafish embryos

After the completion of WISH, embryos were placed in 900 μl albumin solution (0.4% gelatin, 27% egg albumin, 18% sucrose in PBS) in a small embedding dish (Fisher Scientific, Pittsburg, PA). 100 μl of 25% gluteraldehyde was added to the albumin solution, causing it to harden around the embryos. The embedding dish was wrapped in plastic wrap and allowed to set overnight at 4°C. The next day, using a scalpel, excess albumin was cut away from embedded zebrafish embryos to form a block. The block was fixed in 4% paraformaldehyde for 30 minutes while rocking, and then washed twice for 10 minutes in PBS while rocking. When ready to section, the block was removed from the PBS, dried gently, and glued to the vibratome plate. Using a vibrating microtome (Vibratome 1500, Leica), the block was cut into 35 μm sections. Sections were placed on a glass microscope slide and covered with 80% glycerol and a cover slip, which was sealed with nail polish. Slides were observed using a Zeiss M2 Bio Stereomicroscope.

Images were captured using a Zeiss Axiocam digital camera connected to an Antec PC and processed with Adobe Photoshop 7.0.

**Design of *chd7* morpholinos**

Translation blocking, 5'-TGCAGCCAAGCTTAGAAGCAGGAC-3', and splice blocking, 5′-TTATTTTCTGGCACTAACCATGTCC-3′, *chd7* morpholinos were used to inhibit proper translation of *chd7.* All morpholinos were synthesized by Gene Tools, LLC (Philomath, OR). Standard control MO, 5′-CCTCTTACCTCAGTTACAATTTATA-3′, (Gene Tools, LLC, Philomath, OR) was used in all experiments described and is comparable to *chd7* 5bp mismatch control MO, 5′-TGgAcCCAAcCTTAcAAcCAGGAC-3′ (see *Results*, Gene Tools, LLC, Philomath, OR). Approximately 1 nl of the desired morpholino at a concentration of 2 ng/nl, 4 ng/nl, or 6 ng/nl was injected into each zebrafish embryo at the 1 or 2 cell stage. Injected embryos were incubated at 28.5°C in embryo media until they reached the desired developmental stage. To validate the function of the *chd7* splice blocking morpholino, RT-PCR was used to check for improper splicing using the following primer set: forward- 5′-AGGTGGACTCCGAAGGAAAC-3′, reverse- 5′-CCGTCATCACCACATTTGAG-3′. Amplified cDNA was visualized using gel electrophoresis.

**Whole mount *in situ* hybridization (WISH)**

DIG-labeled RNA probe design and WISH analyses were performed as described (Jacobs et al., 2011). Defects were statistically analyzed using StatPlus:mac (AnalystSoft) t-test for comparing means.

**ACKNOWLEDGEMENTS**

We would like to thank Dr. Jeff Amack for the eGFP plasmid, as well as for the use of his microinjection equipment. We would also like to thank Drs. Jeff Amack, Michael Cosgrove, Eleanor Maine, and Melissa Pepling for helpful comments pertaining to this work, and Fiona Foley for help with zebrafish breeding and microinjections. Finally, thanks to Dr. Katherine Lewis for lending equipment and materials.

**FIGURES**

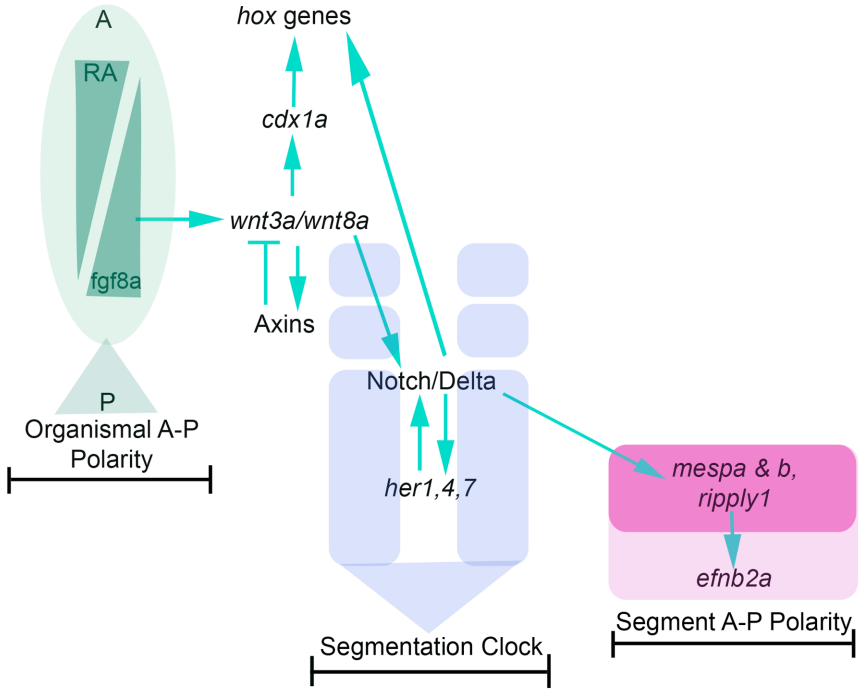


**Figure 1. Somitogenesis is a complex genetic pathway divided into three main patterning events.** Schematic of a simplified version of the somitogenesis signaling pathway based on information from several different vertebrate systems. In the first part of the pathway, the anterior-posterior polarity of the organism is defined by Retinoic Acid and Fgf8. Wnt proteins also play a role in this process and in the activation of the segmentation clock. Next, segmentation clock genes are expressed in an oscillating fashion beginning in the tailbud and moving up the presomitic mesoderm, forming bilateral somite pairs. Finally, the anterior-posterior polarity of each individual somite is defined. Abbreviations: RA, Retinoic Acid; A, anterior; P, posterior.

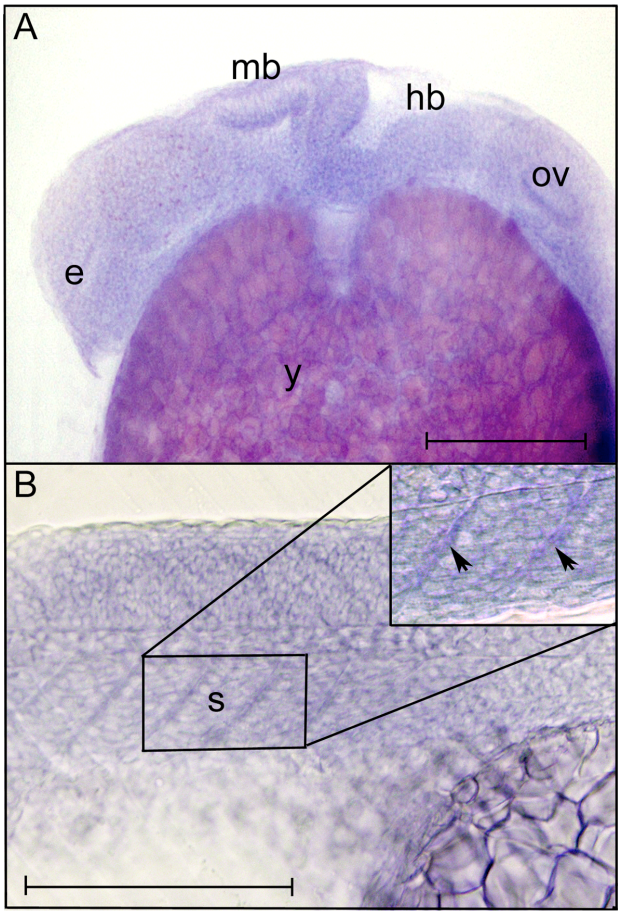


**Figure 2. *Chd7* is expressed in the zebrafish brain, eye, otic vesicle, and somites.** Sagittal sections of 24 hours post fertilization (hpf) zebrafish embryos showing *chd7* expression patterns in **(A)** the brain and **(B)** the somites. Inset in **(B)** shows *chd7* expression along somite borders (arrowheads) at high magnification. Abbreviations: e, eye; hb, hindbrain; mb, midbrain; ov, otic vesicle; s, somite; y, yolk. Scale bar: 200μm.

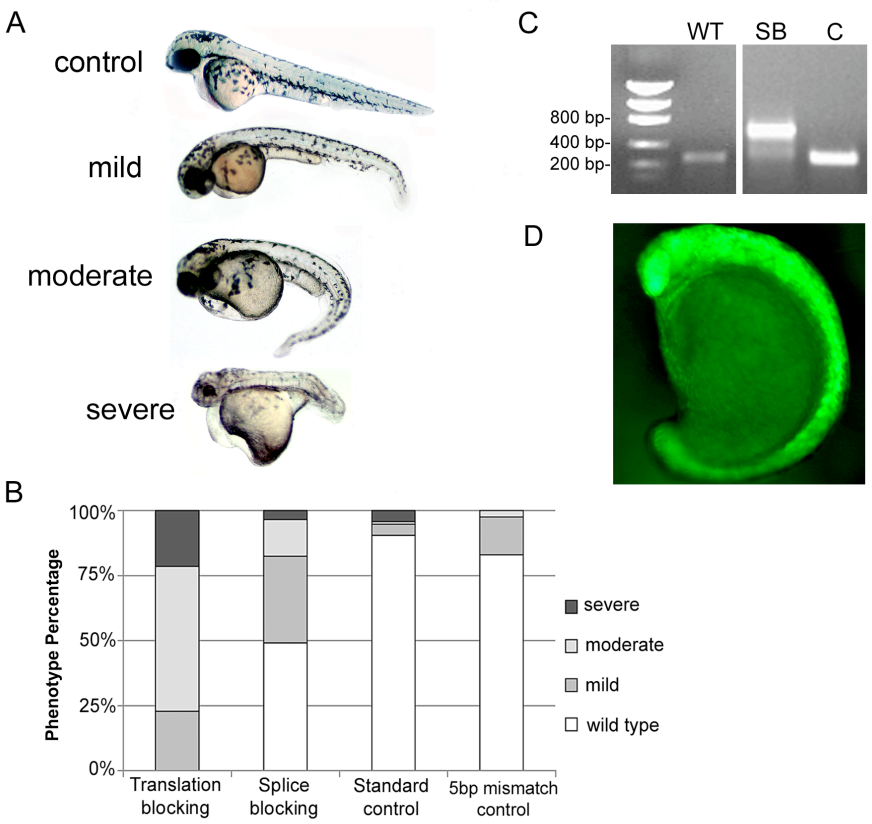


**Figure 3. *Chd7* morpholino injection results in a gradient of phenotypic defects in developing zebrafish. (A)** Representatives of the classes of *chd7* morphant phenotypes at 48 hpf. The top embryo is a control MO injected embryo. The remaining embryos represent the mild, moderate, and severe classes of *chd7* morphants. **(B)** Graph showing the percentage of embryos in each morphant phenotype category upon injection with 6 ng/nl of *chd7* translation blocking, *chd7* splice blocking, standard control, or *chd7* 5 base pair mismatch control morpholino. **(C)** RT-PCR exhibiting the loss of proper splicing of *chd7* mRNA in *chd7* splice blocking morphants. The increased band size is an indicator of the retention of *chd7* intron 2 following mRNA processing. **(D)** A GFP mRNA injected embryo illustrating the even distribution of the injected material throughout the animal. Abbreviations: C, control morpholino; SB, splice blocking morpholino; WT, wild type.

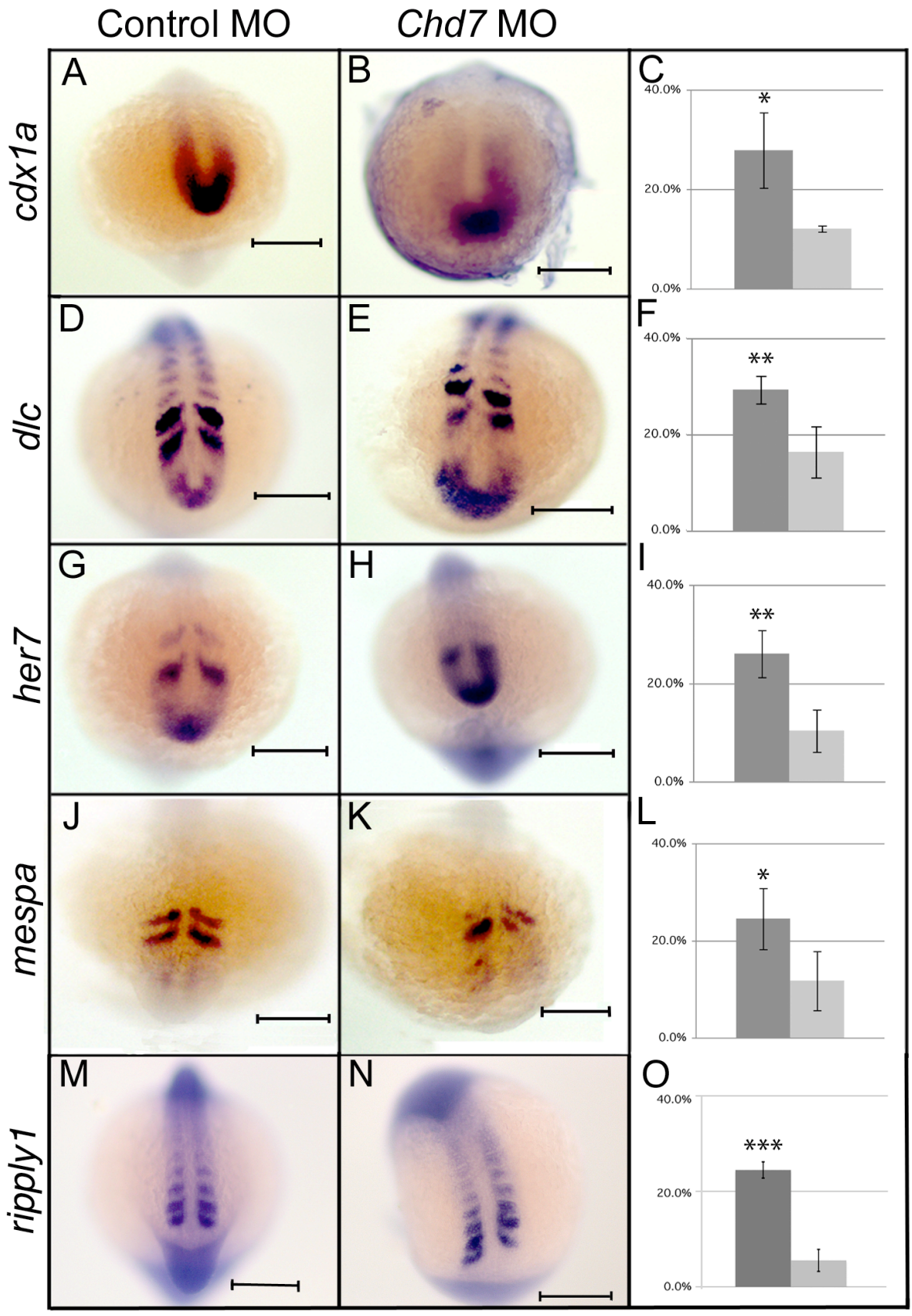
Control MO
Chd7 MO
cdx1a
dlc
her7
mespa
ripply1
A
B
C
D
E
F
G
H
I
J
K
L
M
N
O
40.0%
20.0%
0.0%
*
**
**
*
***

**Figure 4. Loss of Chd7 results in asymmetric expression of somitogenesis patterning genes.** Expression of *cdx1a*, *dlc*, *her7*, *mespa*, and *ripply1* in control morpholino injected zebrafish embryos **(A, D, G, J, M)** is largely symmetric in the somites, presomitic mesoderm, and tailbud at the 13-somite stage of development. Knockdown of Chd7 by *chd7* translation blocking morpholino injection results in a loss of symmetric expression of *cdx1a*, *dlc*, *her7*, *mespa*, and *ripply1* **(B, E, H, K, N)** in zebrafish at the 13 somite stage. Graphs **(C, F, I, L, O)** represent the percentage of animals exhibiting asymmetric gene expression in *chd7* morphants (dark gray bar) and control morphants (light gray bar). Scale bar: 200μm. * equals significance at the $\alpha$=0.05 level, ** equals significance at $\alpha$=0.01, *** equals significance at $\alpha > 0.001$.

**SUPPLEMENTARY FIGURES**

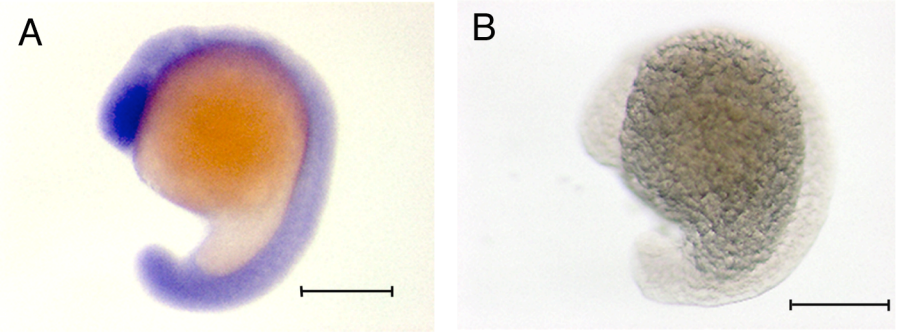


**Supplementary Figure 1. Specificity of the *chd7* riboprobe.** WISH performed using **(A)** antisense and **(B)** sense riboprobes for *chd7* confirms the specificity of the antisense riboprobe. Zebrafish are at the 18 somite stage of development. Lateral view, anterior to the top. Scale bar: 200μm.

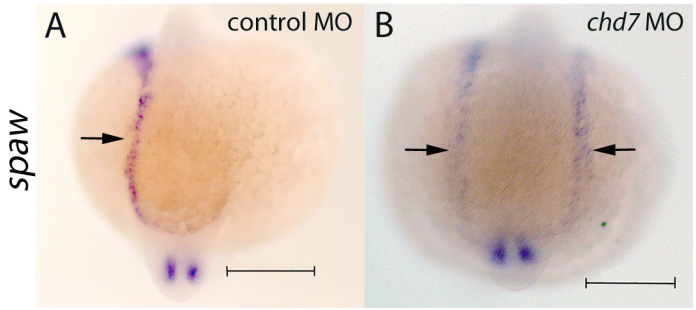


**Supplementary Figure 2. Expression of *spaw* is bilateral in *chd7* morphants.**

**(A)** *Spaw* expression is limited to the left lateral plate mesoderm of the developing zebrafish in most control morphants. **(B)** *Spaw* exhibits bilateral expression in most *chd7* morphants indicating widespread laterality defects. Arrows denote *spaw* expression pattern. Dorsal view, posterior to the bottom. Scale bar: 200μm.

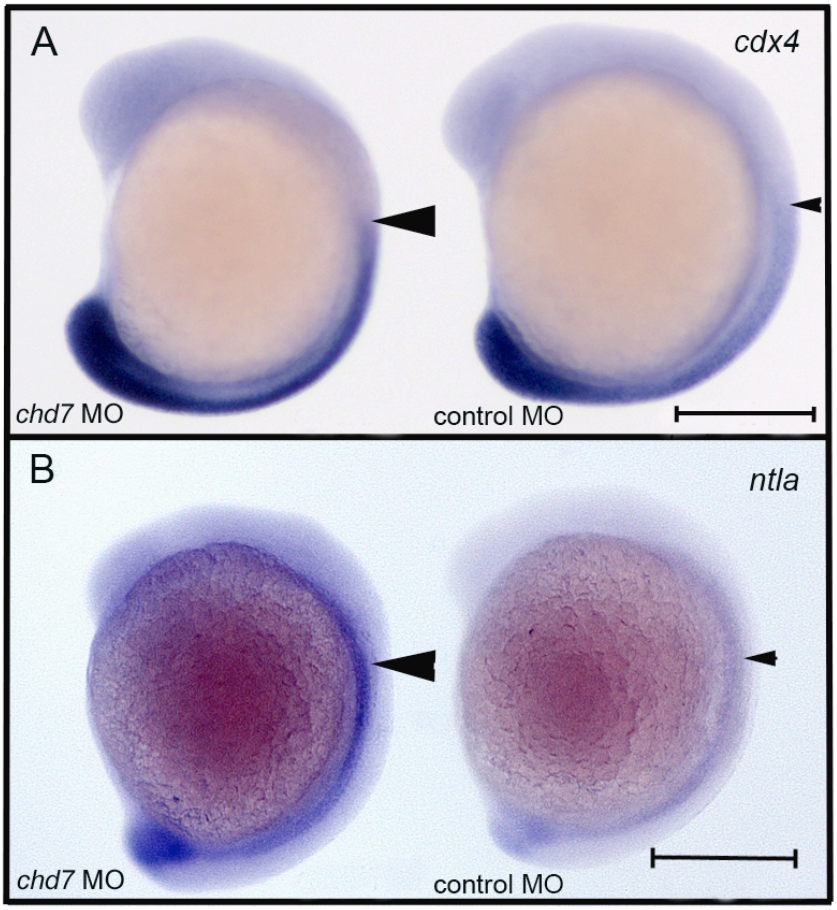


**Supplementary Figure 3. Some Wnt target genes are upregulated upon knockdown of Chd7.** *Cdx4* **(A)** and *ntla* **(B)** are upregulated in *chd7* morphants compared to control embryos. Large arrowheads denote upregulation in *chd7* morphants compared to controls. Both control and *chd7* morphant embryos are captured in one image for each gene for proper comparison purposes. Lateral view, anterior to the top. Scale bar: 200μm.

# Role of Chd7 in Zebrafish: A model for CHARGE syndrome

**Shunmoogum A. Patten* [1,2], Nicole L. Jacobs-McDaniels* [3], Charlotte Zaouter[1], P Drapeau[4], R Craig Albertson[3,5] and Florina Moldovan[1,2]**

Affiliation: [1]Sainte-Justine Hospital Research Center

[2]Faculty of Dentistry, University of Montreal

[3]Department of Biology, Syracuse University

[4]Department of Pathology and Cell Biology, Faculty of Medicine, University of Montreal

[5]Department of Biology, University of Massachusetts

*Both authors contributed equally to this work

**ABSTRACT**

CHARGE Syndrome is caused by mutations in the *CHD7* gene. Several organ systems including the retina, cranial nerves, inner ear and heart are affected in CHARGE Syndrome. However, the mechanistic link between mutations in *CHD7* and many of the organ systems dysfunction remains elusive. Here, we show that Chd7 is required for the organization of the neural retina in zebrafish. We observe an abnormal expression or a complete absence of molecular markers for the retinal ganglion cells and photoreceptors, indicating that Chd7 regulates the differentiation of retinal cells and plays an essential role in retinal cell development. In addition, zebrafish with reduced Chd7 display an abnormal organization and clustering of cranial motor neurons. We also note a pronounced reduction in the facial branchiomotor neurons and the vagal motor neurons display aberrant positioning. Further, these fish exhibit a severe loss of the facial nerves. Knock-down of *Chd7* results in a curvature of the long body axis and these fish develop irregular shaped vertebrae and have a reduction in bone mineralization. *Chd7* knockdown also results in a loss of proper segment polarity illustrated by flawed *efnb2a* and *ttna* expression, which is associated with later vascular segmentation defects. These critical roles for Chd7 in retinal and vertebral development were previously unrecognized and our results provide new insights into the role of Chd7 during development and in CHARGE Syndrome pathogenesis.

## INTRODUCTION

Mutations in the *CHD7* gene (NM_017780) in 8q12.1 were identified as causative for CHARGE (Coloboma, Heart defects, Atresia of the choanae, Retarded growth and development, Genital hypoplasia, Ear anomalies; OMIM # 214800)) Syndrome (Vissers et al., 2004; Aramaki et al., 2006; Jongmans et al., 2006; Lalani et al., 2006; Sanlaville et al., 2006). Heterozygosity for nonsense, deletion or missense *CHD7* mutations is estimated to occur in 60–80% of patients with CHARGE Syndrome; these mutations are distributed throughout the coding sequence and do not appear to be correlated with specific aspects of the clinical phenotype (Lalani et al., 2005; Vuorela et al., 2007; Wincent et al., 2009). The majority of *CHD7* mutations identified thus far are *de novo*; however, evidence for germline mosaicism has been suggested for families with multiple affected siblings (Wessels et al., 2010). Children affected by CHARGE Syndrome have a variable association of features including ocular deficits, heart malfunctioning, olfactory dysfunction, retarded growth, vestibular dysfunction, cranial nerve anomalies and intellectual disability (Carey, 2005; Aramaki et al., 2006; Sanlaville et al., 2006). All of these characteristics have variable degrees of penetrance, with some being present in virtually all CHARGE patients, whereas others are less frequently observed (Blake and Prasad, 2006). Although there is clear evidence that mutations in the *CHD7* gene are causative in CHARGE Syndrome, the pathogenic mechanisms elicited by these mutations that lead to organs and systems dysfunction are not fully understood.

Chd7 is one of nine members of the Chromodomain Helicase DNA- Binding (CHD) domain family of ATP-dependent chromatin remodeling enzymes (Marfella and Imbalzano, 2007). It consists of functional domains such as a chromatin organization

modifier, SNF2-related helicase/ATPase and BRK domain (Allen et al., 2007; Marfella and Imbalzano, 2007). Recently, DNA-binding sites on chromatin have shown that chd7 binding is correlated to areas of mono- and dimethylated lysine 4 of histone H3 (Srinivasan et al., 2008; Schnetz et al., 2009). The *Chd7 Drosophila* ortholog, *kismet* down-regulates transcriptional elongation by RNA polymerase II through the recruitment of ASH1 and TRX and may be involved in the maintenance of stem cell pluripotency by regulating methylation of histone H3 lysine 27. Chd7 is also implicated in cell fate specification of mesenchymal stem cells (Takada et al., 2007). During osteoblast and adipocyte differentiation, Chd7 forms a complex with NLK, SETDB1 and PPAR-γ, then binds to histone H3 at PPAR-γ target promoters and suppresses ligand-induced transactivation of PPAR-γ target genes, which leads to a change in cell fate (Takada et al., 2007). Recently, Chd7 has been shown act synergistically with PBAF to promote neural crest gene expression and cell migration (Bajpai et al., 2010). Thus, Chd7 is thought to play a variety of essential roles during development in many species.

The understanding of cause and pathogenesis of many complex human diseases has been improved through the study of model organisms. Zebrafish are a well-established model used to study developmental biology because of their accessibility, optical transparency and rapid development. Over the past decade, the utility of this model organism in investigations of human health and disease has become more explicit. Major advantages of this vertebrate model include a high degree of homology to human genes, as well as conservation of developmental pathways. The zebrafish *chd7* gene is located on chromosome 2 and alignment of the zebrafish genomic sequence with mouse *Chd7* and human *CHD7* shows the gene structure is conserved across species (Bosman et

al., 2005). Given that the zebrafish *chd7* gene is highly similar to the human *CHD7* gene, elucidating roles for Chd7 in zebrafish development could significantly contribute to our understanding of the function of Chd7 in CHARGE Syndrome pathogenesis. Therefore, we sought to utilize zebrafish to assess the pathogenic effect of the loss of function of Chd7 and understand the role of the zebrafish homolog of the mammalian *Chd7* during development. We show that *chd7* is robustly expressed in developing zebrafish embryos, particularly in the retina, hindbrain and tail bud. Loss of function of Chd7 results in several defects including abnormal neural development, curvature of the long axis of the body, abnormal cranial neural crest (CNC) development, otolith anomalies, smaller eye and pericardial edema. These defects are similar to the major congenital anomalies associated with human *CHD7* mutations in CHARGE Syndrome. Finally, we reveal for the first time a critical role of Chd7 in retinal organization and bone mineralization.

## RESULTS

### *Chd7* transcript is broadly expressed in developing zebrafish

To begin to explore the role of Chd7 in developing zebrafish, we first analyzed the developmental expression of *chd7* mRNA. *In situ* hybridization results showed that *chd7* was expressed relatively ubiquitously throughout early zebrafish embryogenesis (Fig. 1 A-C) until around the 13 somite stage of development when more discrete expression in the eye primordium, and the perimeter of the somites was observed (Fig. 1 D). As somitogenesis continued, *chd7* became highly expressed in the retina as well as in the brain, somites, and tailbud of the embryo (Fig. 1 E-F). Finally at 48 hpf, *chd7* expression in the tail began to diminish, however expression in the brain and in the eye remained strong (Fig. 1 G). The sense probe did not show any *in situ* staining suggesting that there was no non-specific hybridization (Fig. 1 E').

### Loss of function of Chd7 leads to several and widespread morphological abnormalities

Next, we depleted zebrafish embryos of Chd7 protein using an antisense morpholino oligonucleotide (MO) designed against the translation initiation sites of *chd7* mRNA. Embryos injected with *chd7*-MO exhibited phenotypes marked by curvature of the long axis of the body, a flattening of the head, abnormal tail fins, smaller eyes and heart defects (498 embryos from 12 experiments; Fig. 2, 3 A-C). These defects were observed in a dosage-dependent manner (Supplementary Fig. 1). As embryos were injected with increasing concentrations of *chd7*-MO, the resulting defects became more severe (Supplementary Fig. 1 C-D).

To exclude the possibility that this phenotype may have resulted from non-specific or mistargeting effects of the MO, we also designed and injected zebrafish embryos with a *chd7* splice-blocking morpholino (SBMO) and control 5-bp mismatch MO. We recently showed by RT-PCR analysis that the morpholino-targeted region exhibited abnormal splicing of *chd7* in embryos injected with *chd7* SBMO and normal splicing in uninjected and control-MO injected embryos (Jacobs-McDaniels and Albertson, 2011). Embryos injected with the *chd7* SBMO exhibited morphological defects similar to those observed in the *chd7* morphants (Fig, 2 D). On the other hand, all control MO-injected larvae developed normally (436 embryos from 12 experiments; Fig. 2 E and Fig. 3) and no apparent phenotype was observed when compared to untreated wild-type embryos (510 embryos from 12 experiments; Fig. 2 A). To further confirm that the lack of Chd7 underlies all the phenotypic alterations observed in *chd7*-MO zebrafish, a rescue experiment was performed. We found that expression of *chd7* mRNA which had no complementary sequence to *chd7*-MO can correct all the developmental defects (249 embryos from 6 experiments; Fig.2 E) and no apparent phenotype was observed when compared to control-MO fish (Fig. 2). Thus, the amount of newly-synthesized Chd7 coded by the rescuing mRNA in the initial stages was sufficient to prevent the developmental anomalies imparted by the *chd7*-MO. Altogether these findings were consistent with a reduction in Chd7 expression and they suggest that the phenotype observed with *chd7*-MO-injected embryos was specific and due to a direct result of Chd7 protein depletion.

We focused the analysis of the loss of function of Chd7 in embryos injected with 2 ng/nl of *chd7*-MO. At 48 hpf, we found that chd7-MO-injected (2 ng/nl) embryos

exhibited a small eye phenotype (Fig. 3B,E) compared to control-MO (Fig. 3A,E) and wild-type fish (Fig. 3 E). We observed that the hearts of *chd7*-MO-injected embryos were developmentally impaired and have signs of severe pericardial edema compared to controls and wild-type fish (Fig. 3 F). The atrial and ventricular chambers in these fish can be distinguished (Fig. 3 D), but these compartments were dysmorphic and more tube-like (inset, Fig. 3 D) than the well-defined and tightly looped chambers of control-MO injected fish and wild-type fish (Fig. 3 C). Injection of *chd7* mRNA significantly rescued the morpholino eye and heart phenotypes (Fig. 3 E-F).

At 48 hpf, *chd7*-MO-injected (2 ng/nl) embryos also displayed a very specific defect in otolith formation (214 embryos from 12 experiments; Fig. 4 B-D). We observed that 63 % of the morphants exhibited otoliths that were asymmetric in size (135/214; p=0.006, ANOVA; Fig. 4 B,D), and 15 % possessed only one otolith (32/214; p=0.008, ANOVA; Fig. 4 C-D). The enlarged or single remaining otolith was often shaped irregularly as opposed to the round and smooth otoliths in control-MO (249 embryos from 6 experiments; Fig. 4 C), wild-type embryos or mRNA rescue embryos (Fig. 4 D). In addition, the general size and morphology of the ear and the formation of semicircular canals were affected in morphants with a single otolith. Fish with defective otoliths also had a pronounced curvature of the body axis, usually remained on their sides at the bottom of their dish, and exhibited a circling swimming behavior upon a touch (tail tap) or acoustic (dish tap) stimulation (data not shown).

**Chd7 plays critical roles in primary axis development and vertebral mineralization**

Loss of function of Chd7 led to a pronounced curvature of the body axis in 25 % of the morphants (12 experiments; $p<0.001$, ANOVA; Fig. 5 A-C) compared to control-MO (12 experiments; Fig. 5 A,C) and wild-type embryos (12 experiments; Fig. 5 C). This phenotype was completely rescued by co-injection of *chd7* mRNA (6 experiments; Fig 5 C). Recently, *CHD7* gene polymorphisms were associated with susceptibility to idiopathic scoliosis in human populations (Gao et al., 2007). We therefore sought to examine vertebral phenotypes at various developmental stages (Fig. 5 D-F). Chemical staining of the vertebrae at later stages revealed that the spine of zebrafish injected with 2 ng/nl of *chd7*-MO had several skeletal anomalies but exhibited no scoliotic curves (242 fish from 6 experiments; Fig. 5 E,F). Notably, *chd7*-MO-injected (2 ng/nl) fish had smaller, irregular vertebral segments (6 experiments; Fig. 5 F), wider intervertebral disc space (6 experiments; Fig. 5 F) and smaller neural and hemal spines (Arrows; 6 experiments; Fig. 5 F). The pedicles of the neural spines were in some cases missing or fused. Mineralization can be assessed by the intensity and localization of the alizarin red S stain (Gregory et al., 2007) .We observed a marked decrease in the alizarin red S staining of the vertebral segments of chd7-MO-injected fish (242 fish from 6 experiments; Fig. 5 D-F) compared to control-MO, suggesting a reduction in vertebral mineralization in *chd7* morphants. These data suggest *chd7* could play a critical role in vertebral development.

***Chd7* is required for proper somite polarity and segmental vascularization**

Morpholino effects on protein abundance typically last for <7 days (Nasevicius and Ekker, 2000) and surprisingly, we observed post-embryonic vertebral defects in chd7-

MO zebrafish. However, the skeletal malformation observed in chd7-MO injected fish (in Fig. 5) resembles the phenotype observed when somite segmentation is disrupted (Takahashi et al., 2000; Koizumi et al., 2001). To determine whether the abnormality in segmentation of the vertebral axis was due to developmental somite malformation, we analyzed the somite segmentation phenotype. To do so, we examined expression of the segment-polarity gene, *ephrin B2a* (*efnb2a*). *In situ* hybridization expression data for *efnb2a* revealed defects in the delineation of somite borders. To verify this defect in somite borders, a segment boundary marker, *titin a* (*ttna*), was used. Specifically, zebrafish *chd7* morphant embryos showed a loss of distinct borders between individual somites at the 13 somite stage, as exhibited by *efnb2a* expression (146 embryos; $p=0.008$, t-test; Fig. 6 A-C) and *ttna* expression (112 embryos; $p=0.006$, t-test; Fig. 6 D-F). Stage matched control MO injected embryos exhibited distinct expression of *efnb2a* within each somite (149 embryos, Fig. 6 A-B), and *ttna* expression marked clear boundaries between adjacent somites (143 embryos, Fig. 6 D-E). Sectioning of *efnb2a* stained embryos revealed that this defect occurs throughout the somitic tissue in *chd7* morphants (inset, Fig. 6 A-B). Therefore, *chd7* appears to be important for proper segment boundary formation. These results also suggest that the skeletal malformation observed later on during development in *chd7* morphants was likely caused by defective somite segmentation.

Furthermore, since *efnb2a* is involved in arterial-venous differentiation (Shaw et al., 2006) and the development of intersegmental vasculature is dependent on proper segmentation of the presomitic mesoderm (PSM), we utilized a *Fli1*-GFP transgenic zebrafish line to test for defects in vascular development caused by Chd7 knockdown.

With this resource, we observed aberrant vascular organization. After 48 hours, *chd7* MO injected embryos displayed improper patterning of the intersegmental vasculature along the long axis of the body (56 embryos; p=0.001,t-test; Fig. 6 G-I). Since these vessels form at the boundaries between somites (Childs et al., 2002), this phenotype is likely due to a lack of intersomite specification in *chd7* morphants, and is similar to defects observed in other mutants defined by aberrant PSM segmentation (Shaw et al., 2006).

**Chd7 function is required for retinal organization**

We next thought to further analyze the eye morphology of the *chd7* morphants. To permit a detailed assessment of the *chd7*-MO small eye phenotype, histological analysis was performed on embryos at 72 hpf (Fig. 7). Histology revealed that retinal organization was severely disrupted in *chd7*-MO–injected embryos (120 embryos, Fig. 7 B). Specifically, the retinas lacked the characteristic laminated structure of both control-MO (142 embryos, Fig. 7 A) and wild-type embryos at 72 hpf. Immunostaining further confirmed disruption of retina formation. Retinal ganglion cells appear to be reduced and disorganized in the *chd7*-MO–injected embryos based on staining for the retinal ganglion marker Zn-8 (5 experiments; Fig. 7 C, D). Staining with 3A10, a neurofilament marker was abnormal in that the normally recognizable stripe of expression of the photoreceptor layer was not present in the *chd7*-MO–injected embryos (8 experiments; Fig. 7 E, F). Similarly, cone photoreceptor staining with Zpr-1 antibody was absent in *chd7* morphants (Supplementary Fig. 2). These findings suggest a novel role of Chd7 in retinal organization and the development of photoreceptors.

**Chd7 is essential for correct positioning of cranial motor neurons and proper projection of facial and trigeminal motor axons**

Previous studies have demonstrated a role for Chd7 in neuronal development (Aramaki et al., 2007; Hurd et al, 2010; Melicharek et al., 2010) and patients with CHARGE Syndrome often display several neurological disorders. We found that *chd7* is expressed in the developing zebrafish hindbrain and loss of function of chd7 leads to flattening of the head. To determine if these molecules are required for proper neural development in this area, we examined the cranial motor neurons of *chd7*-MO-injected embryos using *Isl1*-GFP transgenic zebrafish embryos. These embryos express GFP under the control of a motor neuron-specific *Isl1* promoter. Interestingly, we observed a disrupted organization of the cranial motor neurons in the *chd7*-MO-injected embryos (9 experiments; Fig. 8 B) when compared to control-MO-injected embryos (9 experiments; Fig. 8 A). *Chd7*-MO-injected embryos demonstrated a severe disorganization and clustering of both Va and Vp clusters of the trigeminal (nV) neurons (Fig. 8 B). In addition, loss of Chd7 resulted in a reduction of facial (nVII) branchiomotor neuron populations (9 experiments; Fig. 8 B). Furthermore, the vagal (nX) motor neurons in *chd7*-MO-injected embryos exhibited aberrant medio-lateral positioning and cell-to-cell spacing (9 experiments; Fig. 8 B). *Chd7*-MO-injected embryos also exhibited extremely low levels of staining of the peripherally extending axons from nV neurons when compared to control-MO-injected embryos (9 experiments; Fig. 8 C, D). Furthermore, *chd7*-MO injected embryos exhibited severe loss of the facial sensory ganglion and the axonal extensions from nVII neurons (9 experiments; Fig. 8 C, D).

**Chd7 plays a key role in cranial neural crest development**

CHARGE Syndrome is thought to result from the abnormal development of the neural crest. Recently, CHD7 and PBAF have been shown to cooperate during embryonic development to promote proper neural crest specification and cell migration (Bajpai et al., 2010). We sought to examine the relationship between Chd7 and CNC development in zebrafish using a *Fli1*-GFP transgenic zebrafish line. We injected *Fli1*-GFP embryos with *chd7*-MO at the single cell stage and then assayed for CNC defects between 34-36 hpf by counting the number of CNC segments, which should approximate pharyngeal arch number, within each embryo. We observed CNC defects in over 90 % of *chd7*-MO-injected embryos (63 embryos, Fig.9 D). About one third of these had a reduction in the number of CNC segments, whereas the remaining animals showed more severe phenotypes characterized by the gross disorganization or absence of obvious CNC populations (Fig. 9 B, C). Disorganized CNC segments tended to possess fewer cells and lacked sharp borders between adjacent segments (Fig. 9 C). The phenotype of control-MO-injected zebrafish embryos mimicked that of wild type animals including well-defined segments and appropriate segment numbers (71 embryos, Fig. 9 A). These data lend support for the function of Chd7 in proper CNC development and patterning. Whether the defects reported here are due to aberrant CNC migration or improper pharyngeal arch patterning remains to be investigated.

**DISCUSSION**

The present results show a novel and essential role of Chd7 in retinal organization, axial patterning and bone development and mineralization. Furthermore, knockdown of zebrafish *chd7* results in abnormalities similar to those described in CHARGE Syndrome, as we observed inner ear, heart, eye, cranial ganglia, neural crest and skeletal defects in *chd7* morphants. Collectively, our findings demonstrate that Chd7 function is essential for proper neural and cranial neural crest development. In addition, to our knowledge, this is the first study to report the requirement of *chd7* in retinal and vertebral development.

Chd7 has been implicated in spinal deformities (Gao et al., 2007) and scoliosis is one of the minor clinical features in some CHARGE patients (Blake and Prasad, 2006). Here, loss of function of Chd7 resulted in the curvature of the body axis, irregular vertebral segments and smaller neural and hemal spines. The *chd7* morphants did not exhibit any skeletal defects reminiscent of a scoliotic adult phenotype, however, suggesting that either scoliosis in CHARGE patients is secondary to the effects of attenuated Chd7 levels, or due to primary effects that occur later in development. Our findings also showed that zebrafish embryos deficient in Chd7 mineralize vertebrae more slowly than control siblings, indicating a critical role for Chd7 in promoting mineralization during normal development. Delays in vertebral mineralization may result from a general retardation in growth and development; however, we did not detect any distinguishable differences in length between the *chd7* morphants and controls at all developmental stages examined (Supplementary Table 1). Interestingly, a similar delay of mineralization in zebrafish has been reported after knockdown of *collagen XXVII*

(Christiansen et al., 2009). Furthermore, in the absence of BMP signaling, zebrafish bone mineralization was delayed (Smith et al., 2006). Chd7 has been shown to regulate BMP signaling (Hurd et al., 2010; Laymen et al., 2009). Thus, it is possible that disruption of Chd7 affected the transcription of genes that are crucial for bone mineralization. We also show that a loss of somite border identity during somitogenesis, as exhibited by *efnb2a* and *ttna* expression, is linked to a loss of organized segmental vasculature following *chd7* MO injection and skeletal defects. We hypothesize that early defects in *efnb2a* expression lead to improper segmental patterning later in development, affecting structures such as segmental vasculature and bone mineralization. The link between the process of somitogenesis and the defects in border specification will require further investigation. For example, since *efnb2a* expression persists after somite epithelialization, the irregular *efnb2a* expression observed here could be the result of an accumulation of upstream defects occurring early in the somitogenesis signaling pathway (i.e., indirect effects). Alternatively, it is also possible that Chd7 modulates *efnb2a* expression in a manner that is independent of the process of somite formation (i.e., direct effects).

CHARGE Syndrome patients often have microphthalmia (Ben Becher et al., 1994; Van Meter and Weaver 1996; Akisu et al., 1998) and here we found that loss of function of Chd7 in zebrafish resulted in a small eye phenotype. The retinas in zebrafish develop rapidly and begin differentiation by 36 hpf (Larison and Bremiller, 1990; Link et al., 2000). The differentiating retinal neurons undergo terminal differentiation by 52 hpf and become functional at around 3 dpf (Link et al., 2000; Erdmann et al., 2003; Masai et al, 2003). A functional retina consists of a laminated neuronal tissue with the ganglion cell layer on the inside, inner nuclear layer in the middle, and the outer nuclear layer on

the outside. In between these layers are the synaptic layers: the inner and outer plexiform layer (Larison and Bremiller, 1990; Schmitt and Dowling, 1999). Notably, the retinas in *chd7* morphants fail to laminate, which suggests a novel function for Chd7 in retinal patterning. Furthermore, our findings are similar to disruptions in retinal lamination as observed in the young zebrafish mutant that carries a mutation in *brg1*, a gene that encodes for a subunit of the Swi/Snf of ATP-dependent chromatin remodeling complexes (Link et al., 2000). Moreover, retinal ganglion cells were reduced and the photoreceptor layer were absent in the *chd7*-MO-injected embryos. These data suggest that Chd7 is required for the development of retinal cells. In *Drosophila*, the *chd7* ortholog *kismet* is essential for transcription of the pro-neural factor *atonal* (*Atoh1*) and regulation of retinal photoreceptor cell development (Melicharek et al., 2008). *Drosophila ato* mutants produce no photoreceptors in the eye (Jarman et al., 1995). Chd7 has also been recently shown to control the expression of *sox9* (Bajpai et al., 2010). Zebrafish *sox9* mutants reveal that Sox9 is required for retinal differentiation and it also helps with retinal organization and regulates the number of photoreceptor cells (Yokoi et al., 2009). Thus, it is likely that that loss of function of Chd7 disrupts the gene network that is crucial for retinal cellular development and organization.

Several ganglionic defects have been reported in CHARGE patients, including defects in the facial and vestibulo-acoustic ganglia (Byerly and Pauli, 1993; Lacombe, 1994). *Chd7* knockdown resulted in important phenotypes relevant to cranial ganglia development, branchiomotor development, and vagal motor neuron positioning. Anomaly in facial nerves has also been demonstrated in CHARGE Syndrome (Jongmans et al., 2006). Loss of function of Chd7 resulted in a severe loss of facial nerves in the

morphants. Altogether, these results suggest that Chd7 and downstream targets are important for neuronal development and proper axonal projections.

Neural crest cells are multipotent cell populations with the ability to migrate, leading to the formation of several key developmental structures including bones, cartilages, nerves, and connective tissues (Huang and Saint-Jeannet, 2004). CNC, specifically, migrate into the pharyngeal arches where they play a role in the formation of facial bone, muscle, and cartilage (Grenier et al., 2009). In addition, CNC migrate into the optic vesicle and otic placode, where they play key roles in the development of muscular and skeletal elements in the eye and the inner ear, respectively (Knight and Schilling, 2006; Lwigale and Bronner-Fraser, 2009). Some key developmental defects in CHARGE patients can be traced to aberrant CNC development, including coloboma of the eye, external ear malformations, inner ear defects and a spectrum of facial defects (Blake et al., 1998; Amiel et al., 2001; Lalani et al., 2005). Our *chd7* morphant zebrafish embryos displayed obvious defects in CNC migration, based on observations of pharyngeal arch development and number. We did not fully characterize CNC activity in the optic nerve or otic placode of our *chd7* morphants, however, we did observe and quantify significant defects in eye and otic vesicle development. CHD7 is essential for the formation of multipotent migratory neural crest in humans and *Xenopus* (Bajpai et al., 2010) and recently, CHD7 was found to play a role in proper neurogenesis of the inner ear in mice (Hurd et al, 2010). Our results support a role for Chd7 in proper CNC migration and differentiation, and substantiate the use of *chd7* morphant zebrafish as an *in vivo* animal model for CHARGE Syndrome.

The *chd7* –MO-injected embryos displayed a very specific defect in otolith and semicircular canal formation and they also exhibited a circling swimming behavior consistent with vestibular dysfunction. Such inner ear malformations are very similar to those reported in CHARGE Syndrome patients (Morgan et al., 1993; Tellier et al., 1998; Abadie et al., 2000; Satar et al., 2003). In addition, CHARGE patients have been reported to have vestibular problems and hyperactivity (Souriau et al., 2005), and this may be due to inner ear defects. CHD7 is necessary for proliferation of inner ear neuroblasts and inner ear morphogenesis by the maintenance of *Fgf10*, *Otx2* and *Ngn1* expression (Hurd et al., 2010). Fgf signaling and *Otx* genes have also been shown to be important for inner ear development in zebrafish (Alvarez et al., 2003; Chang et al., 2004; Hammond and Whitfield, 2006; Schimmang, 2007). Thus, our zebrafish model for CHARGE Syndrome can be useful to further explore the mechanisms underlying inner ear anomalies in CHARGE pathogenesis. For instance, it will be interesting to investigate whether loss of function of *chd7* in zebrafish results in a downregulation of *Fgf10* and *Otx2* and whether overexpression of one or more of these genes could rescue *chd7*-MO phenotypes.

Heart defects have been reported to be associated with CHARGE Syndrome (Thomas and Frias, 1987; Aramaki et al., 2006; Jongmans et al., 2006; Lalani et al., 2006; Jyonouchi et al., 2009). Here we report that the hearts of *chd7*-MO-injected embryos are developmentally impaired and have signs of severe pericardial edema. Heart anomalies described in CHARGE Syndrome patients include ventricular and atrial septal defects and conotruncal defects (Thomas and Frias, 1987; Devriendt et al., 1998). In this study, we did not fully characterize the observed heart defects in the *chd7* morphants. The atrial and ventricular chambers in these fish can be distinguished, but these compartments were

dysmorphic and more tube-like than the well-defined and tightly looped chambers of wild-type fish. Future studies using *chd7* zebrafish morphants could help to identify components in the Chd7 regulatory network that are essential for heart development and further our understanding of one of the major anomalies reported in CHARGE patients.

In conclusion, we have examined the role of zebrafish Chd7. We provide evidence that zebrafish highly express *chd7* in the retina, brain and somite boundaries. Loss of function of Chd7 resulted in several morphological defects similar to those observed in patients with CHARGE Syndrome. We then performed a detailed analysis of uncharacterized defects of CHARGE Syndrome and show that the presence of Chd7 is crucial for proper neural, retinal and vertebral development in zebrafish. These data provide new insights on the role of Chd7 and the mechanistic link between defects in the *chd7* gene and the organs and systems dysfunction associated with CHARGE Syndrome. Furthermore, on the basis of the overlap in clinical features between zebrafish *chd7* morphants and CHARGE Syndrome, we suggest zebrafish can be a valuable *in vivo* tool to further understand the pathophysiological mechanisms underlying the abnormalities associated with CHARGE Syndrome.

## EXPERIMENTAL PROCEDURES

### Animals

Wild-type AB, *Isl1*-GFP WIK transgenic and *Fli1*-GFP transgenic zebrafish (*Danio rerio*) embryos were raised at 28.5 °C, and collected and staged using standard methods (Kimmel et al., 1995). Wild-type AB fish and *Fli1*-GFP transgenic zebrafish were purchased from the Zebrafish International Resource Center (ZIRC; University of Oregon, Eugene, OR). *Isl1*-GFP WIK transgenic line was kindly provided by Dr. Hitoshi Okamoto (RIKEN Brain Science Institute, Wako, Japan) (Uemura et al., 2005). Embryos and larvae were anaesthetized in 0.02% tricaine (MS-222; Sigma Chemical, St. Louis, MO) in phosphate-buffered saline (PBS) prior to all procedures.

### Ethics Statement

All protocols were carried out in compliance with the guidelines stipulated by the Canadian Council for Animal Care (CCAC), the CHU Sainte-Justine Research Center, as well as the Institutional Animal Care and Use Committee (IACUC) at Syracuse University and at the University of Montreal. This study was approved by the CHU Sainte-Justine Research Center ,University of Montreal (ZF-09-60/Category B) and the Syracuse University (IACUC # 07-010) ethics committees.

### Design and synthesis of DIG-labeled RNA probes for *chd7, efnb2a* and *ttna*

Total RNA was isolated from blastula stage zebrafish embryos using the RNeasy Mini Kit (Quiagen, Valencia, CA). Reverse transcription was performed to make cDNA using the QuantiTect Reverse Transcription Kit (Quiagen, Valencia, CA). *Chd7* fragments were

amplified by PCR using 5'-GCTATTGACCGCTTCTCTCG-3' and 5'-TGCTCCTTTACGCAGGAGAT-3' primers (resulting in a 362bp amplicon from about halfway through the cDNA sequence) and cloned into the pGEM-T Easy vector (Promega, Madison, WI) following the manufacturer's protocol. Zebrafish *efnb2a* (Barrios et al., 2003) and *ttna* (Oates et al., 2005) plasmids were kind gifts from Dr. Steven Wilson and Dr. Andrew Oates respectively. To synthesize the antisense probe, the previously constructed plasmid was linearized using the restriction enzyme SpeI (New England BioLabs, Inc., Ipswich, MA) for 2 hours at 37 °C. Linearization was confirmed by gel electrophoresis using a 1% agarose gel. Linearized plasmid was incubated with T7 RNA Polymerase (Roche Diagnostics, Indianapolis, IN) in the presence of digoxigenin (DIG) label (Roche Diagnostics, Indianapolis, IN) and RNase Inhibitor (Roche Diagnostics, Indianapolis, IN) for 2 hours at 37 °C. To synthesize the sense strand, the restriction enzyme ApaI (New England Biolabs, Inc., Ipswich, MA) and SP6 RNA Polymerase (Roche Diagnostics, Indianapolis, IN) were used. Plasmid DNA was eliminated with DNase (Roche Diagnostics, Indianapolis, IN) by incubation at 37 °C for 20 minutes. DIG-labeled RNA was precipitated in 0.2M EDTA, 4M LiCl, and 100% ethanol overnight at -20 °C, and then resuspended in DEPC water. Agarose gel electrophoresis was used to confirm the presence of a purified probe and any unused probe was stored at -20 °C.

**Whole mount *in situ* hybridization analysis**

Whole mount *in situ* hybridization was performed on staged zebrafish embryos using both sense and antisense *chd7*, *efnb2a* and *ttna* riboprobes. Methods for *in situ*

hydridization analysis followed (Albertson and Yelick, 2005; Jacobs et al., 2011). Briefly, staged embryos were fixed overnight in 4% paraformaldehyde, and then dehydrated in methanol. When ready to use, embryos were rehydrated in phosphate buffered saline with 0.1% Tween-20 (PBSt). Embryos were permeabilized by proteinase K digestion and then hybridized with the riboprobes overnight at 70 °C. The next day, embryos were put through graded solutions of 75%, 50%, and 25% prehybridized solution in 2X saline-sodium citrate (SSC) followed by a wash in 0.2X SSC for 30 minutes at 68°C. They were then placed in blocking solution for several hours, and incubated in α-DIG antibody overnight. Finally, embryos were washed again and incubated in staining solution in the dark until sufficient staining appeared on the embryos. Embryos were dehydrated in methanol to facilitate clearing of background staining and then rehydrated in PBSt. Embryos were stored in glycerol.

Embryos in glycerol were visualized using a Zeiss M2 Bio Stereomicroscope, with motorized focus drive and X-Cite UV light source with GFP filter. Images were captured using a Zeiss Axiocam digital camera connected to an Antec PC and processed with Adobe Photoshop 7.0.

**Generation of zebrafish *chd7* morpholino and mRNA rescue experiments**

To eliminate Chd7 function, two types of antisense morpholino oligonucleotide were used to disrupt the translation of *chd7* transcripts. The translation-blocking morpholino, 5'-TGCAGCCAAGCTTAGAAGCAGGAC-3' and the splice blocking, 5′-TTATTTTCTGGCACTAACCATGTCC-3′ were synthesized by Gene Tools (Philomath, OR). The morpholino was injected into single-cell stage zebrafish embryos at doses of 2

ng/embryo, 4ng/embryo and 6 ng/embryo. To validate the function of the *chd7* splice blocking morpholino, RT-PCR was used to check for improper splicing using the following primer set: forward- 5′-AGGTGGACTCCGAAGGAAAC-3′, reverse- 5′-CCGTCATCACCACATTTGAG-3′. Amplified cDNA was visualized using gel electrophoresis.

To confirm the specificity of the *chd7* morpholinos, a mismatch morpholino (lower case) was used: TGgAcCCAAcCTTAcAAcCAGGAC (Gene Tools. OR). Furthermore, rescue experiments were performed. Full-length wild type zebrafish *chd7* gene was subcloned into pcs2+ vector and capped mRNA was synthesized using the Sp6 promoter and the mMessage mMachine Kit (Ambion). Three hundred picograms of the synthetic mRNA was then injected into embryos at the one-cell stage. Rescued embryos were visualized and counted using the Olympus SZX12 stereoscope.

Injected and uninjected embryos were then incubated in embryo media at 28.5 °C for 24 h, after which they were assessed for viability. Wild type, *Isl1*-GFP WIK and *Fli1*-GFP transgenic zebrafish embryos injected with *chd7* morpholino were assessed for morphological differences from control morpholino injected or uninjected embryos under an Olympus SZX12 stereoscope at 24, 48 and 72 hpf. *Isl1*-GFP transgenic zebrafish were stage matched to 48 hpf and fixed in 4% paraformaldehyde for 4 h and then analyzed for differences in branchiomotor neuron development and migration from uninjected controls using a Zeiss AxioImager Z1 compound microscope. Images were photographed using a Zeiss LSM 510 confocal microscope at 488 nm under a 20× objective, and were compiled using Zeiss LSM Image Browser software. *Fli1*-GPF zebrafish were staged to

34-36 hpf and screened for CNC segmentation defects using an X-Cite UV light source with GFP filter mounted to a Zeiss M2 Bio Stereomicroscope.

**Immunohistological procedures**

Zebrafish specimens were fixed in 4% paraformaldehyde and were either used for whole-mount immunostaining or embedded in paraffin. Transverse sections (1.5-3 μm) of paraffin-embedded specimens were deparaffinized in xylene and were rehydrated in a graded series of ethanol. Serial sections were collected from the central retina.

For immunofluorescence microscopy, whole embryos and eye sections were washed several times in PBS and permeabilized for 30 min in 4% Triton-X 100 containing 2% bovine serum albumin (BSA) and 10% goat serum. Following permeabilization, tissues and retinal sections were incubated in the primary antibody 3A10 (Developmental Studies Hybridoma Bank; 1:500) for 48 h at 4 °C on a shaker. Tissues and eye sections were washed several times in PBS over a 24 h period, and then incubated in the secondary antibody conjugated with Alexa Fluor 488 (Molecular Probes, Carlsbad, CA, 1:2000) for 4–6 h at room temperature. Animals were washed in PBS several times, de-yolked, cleared in 70% glycerol and mounted. Z-stack images were photographed using a Zeiss LSM 510 confocal microscope under a 20x objective, and were compiled using Zeiss LSM Image Browser software.

For immunoperoxidase methods, slides were incubated with a blocking serum (Vectastain; Vector Laboratories, Burlingame, CA) for 45 minutes, after which they were blotted and then overlaid with the primary antibodies Chd7 (Santa Cruz Biotechnology, Santa Cruz, CA ; 1/600) and zn-8 (Developmental Studies Hybridoma Bank; 1/200) for

18 hours at 4°C. The slides were washed 3 times in PBS, pH 7.4, and incubated with secondary antibodies (anti- mouse (1:1000) or anti- rabbit (1:1000), Vectastain) for 1 hour at room temperature, followed by staining according to the avidin-biotin-peroxidase complex method (Vectastain ABC assay). Color was developed with 3,3-diaminobenzidine (Dako Diagnostics Inc., Mississauga, ON, Canada) containing hydrogen peroxide. Slides were counterstained with Harris modified hematoxylin (Fisher Scientific, Ottawa, ON, Canada). Eye sections were also stained with 1% Toluidine Blue. Images were captured using a Leica DMR microscope mounted with a Qimaging Retiga 1300 camera.

**Skeletal staining**

Juvenile zebrafish were fixed in 4% paraformaldehyde in PBS for 48 hr at 4 °C and dehydrated to 100% ethanol over 2 days. Fish were then cleared in a 1% KOH solution containing approximately 4.5 ml of 3% $H_2O_2$ per 100 ml 1% KOH for 2 h, followed by 2 h in half this concentration (2.25 ml $H_2O_2$ per 100 ml 1% KOH). This latter step ensures a stepwise progression from $H_2O_2$ to water, which helps reduce tissue expansion. Zebrafish were then rinsed twice in distilled water, and transferred to a 30% saturated sodium tetraborate solution (Borax; Acros Organics) in water, overnight. Any remaining soft tissues were digested in a solution containing 1.0% trypsin and 2.0% Borax in water for 2–4 h. Digestion was deemed complete when the primary axis of the axial skeleton became visible. The fish were subsequently rinsed three times in distilled water to remove all residual trypsin, prior to staining for 12 h or more in a solution of 75% ethanol and Alizarin red S. Vertebral mineralization was assessed after Alizarin red S staining.

Fish were examined using a Leica M205FA stereomicroscope. Digital images were collected with Leica DFC490 camera.

Calcein staining was performed as described (Du et al., 2001). Briefly, fish were anesthetized in 0.6 mM MS-222 buffered to pH 7.0 and immersed in 0.2% calcein in 10% Hank's solution buffered to pH 7.2 for 10 min. followed by three 10 min. washes in Hank's solution. Vertebral mineralization was assessed after calcein staining using a Leica DMR microscope. Digital images were collected with a Qimaging Retiga 1300 camera.

**Sample number and statistical analysis**

Each batch number consisted of at least 40 fish. For each data set, we provided the total number of fish used followed by the batch number. The sample number for wild-type fish consisted of 12 batches with a total of 510 fish used (510 fish from 12 experiments); 12 batches with a total of 436 fish for *chd7* morphants (436 fish from 12 experiments); 12 batches with a total of 498 fish for control-MO injected embryos (498 fish from 12 experiments) and 6 batches with a total of 249 mRNA rescue experiments (249 fish from 6 experiments). Immunohistochemistry were performed on at least 6 batches for both control-MO and *chd7*-MO fish. Statistical analyses were performed and data were plotted in SigmaPlot 11.0 (Systat Software Inc., San Jose, CA, USA). Significance was determined using paired Student's *t*-tests, one-way ANOVAs and Fisher's least significant difference tests for normally distributed, equal variance data. Kruskal–Wallis ANOVA and Dunn's method of comparison were used for non-normal distributions.

**ACKNOWLEDGEMENTS**

FM was supported by Yves Cotrel Foundation and SP was supported by CHU Sainte-Justine and Foundation of the Stars scholarship. We are grateful to G. Laliberté and R. Milette for animal care. We would also like to thank Jeff Amack for the use of microinjection equipment and for *Fli1*-GFP transgenic fish. Thanks to Fiona Foley for help with the microinjections. The monoclonal antibodies 3A10 and zn-8 developed by Thomas M. Jessell and Jane Dodd were obtained from the Developmental Studies Hybridoma Bank, developed under the auspices of the National Institute of Child Health and Human Development, and maintained by the University of Iowa, Department of Biological Sciences (Iowa City, IA).

**FIGURES**

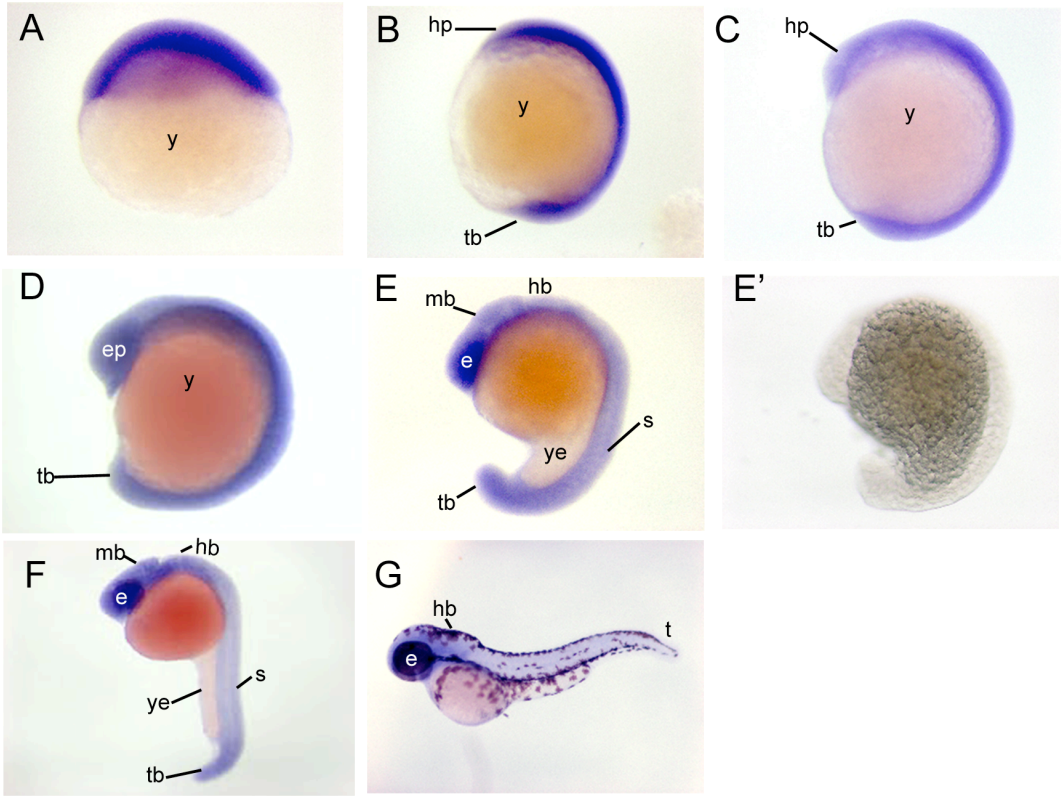


**Figure 1. *Chd7* expression patterns during zebrafish embryogenesis.** *Chd7* was expressed ubiquitously throughout the embryo during epiboly (**A**), at the 4 somite stage (**B**), and at the 8 somite stage (**C**). (**D**) At the 13 somite stage, expression remained relatively ubiquitous, but with stronger expression noted within the retina and at the perimeters of developed somites. (**E**) At the 18 somite stage, tissue-specific expression was observed in the eyes, brain, somites, and tailbud. This expression pattern remained through 24 hours post fertilization (**F**). (**E'**) No staining occurred when hybridized with a *chd7* sense probe. (**G**) At 48 hours post fertilization, *chd7* expression began to diminish from the body of the zebrafish but remained in the eye and in the brain. e, eye; ep, eye primordium; mb, midbrain; hp, head primordium; s, somite; t, tail; tb, tailbud; y, yolk; ye, yolk extension.

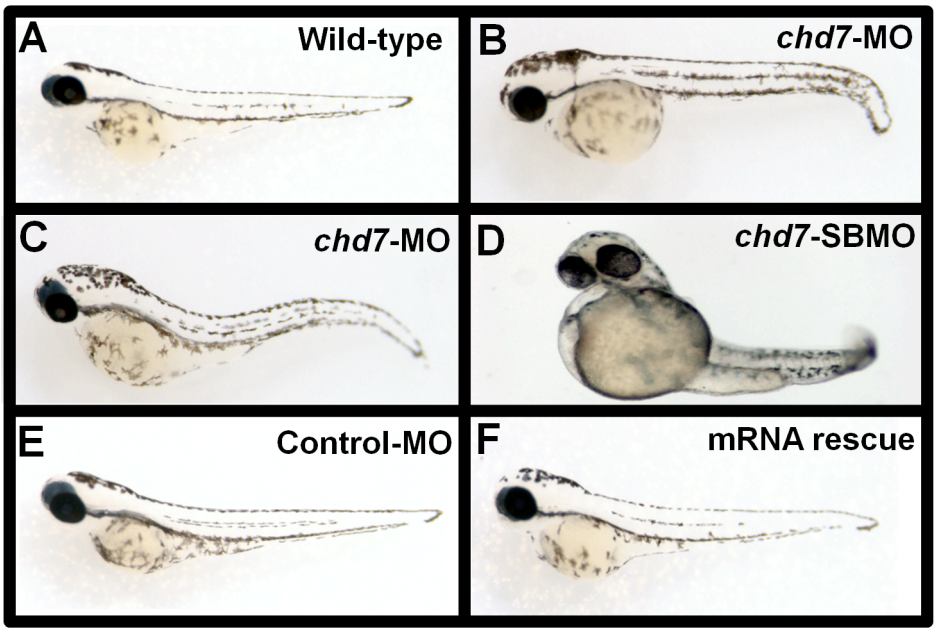


**Figure 2. *Chd7*- MO injections and mRNA rescue experiments.** Control-MO injected (**E**) *chd7*-MO + *chd7*-mRNA co-injected (**F**) zebrafish showed no phenotypic defects at 48 hpf and were comparable to wild type zebrafish (**A**) at the same age. Embryos injected with 2 ng/nl *chd7*-MO (**B**-**C**), or 2ng/nl (**D**) *chd7*-SBMO showed several developmental defects.

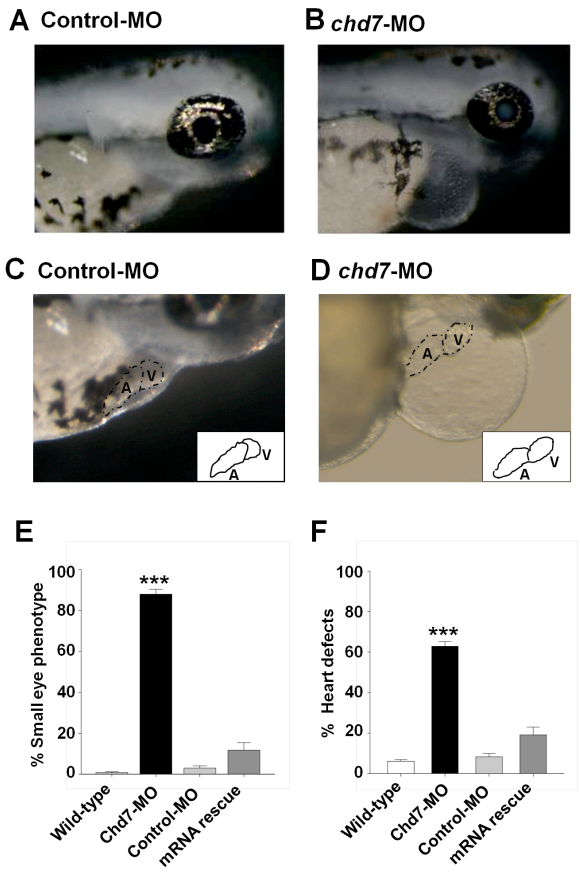


**Figure 3. Knockdown of *chd7* affects eye and heart development.** (**A-B**) Representative images of eye phenotypes induced by injection of *chd7*-MO in zebrafish embryos (**B**) compared with control embryos (**A**) at 72 hpf. Lateral view with anterior to right. *Chd7* morphants had a reduced ocular size. *Chd7*-MO-injected zebrafish exhibited cardiac anomalies such as dysmorphic heart and tube-like heart shape (**D**) compared with control embryos (**C**). Insets in **(C)** and **(D)** represent an illustration of the heart phenotype in control or *chd7* morphant embryos, respectively. (**E-F**) Bar graphs illustrating the prevalence of eye (**E**) and heart (**F**) phenotypes in wild-type (white bar), *chd7*-MO (black bar), control-MO-injected embryos (grey bar) and mRNA rescue (dark grey bar). *** <0.001, * <0.01

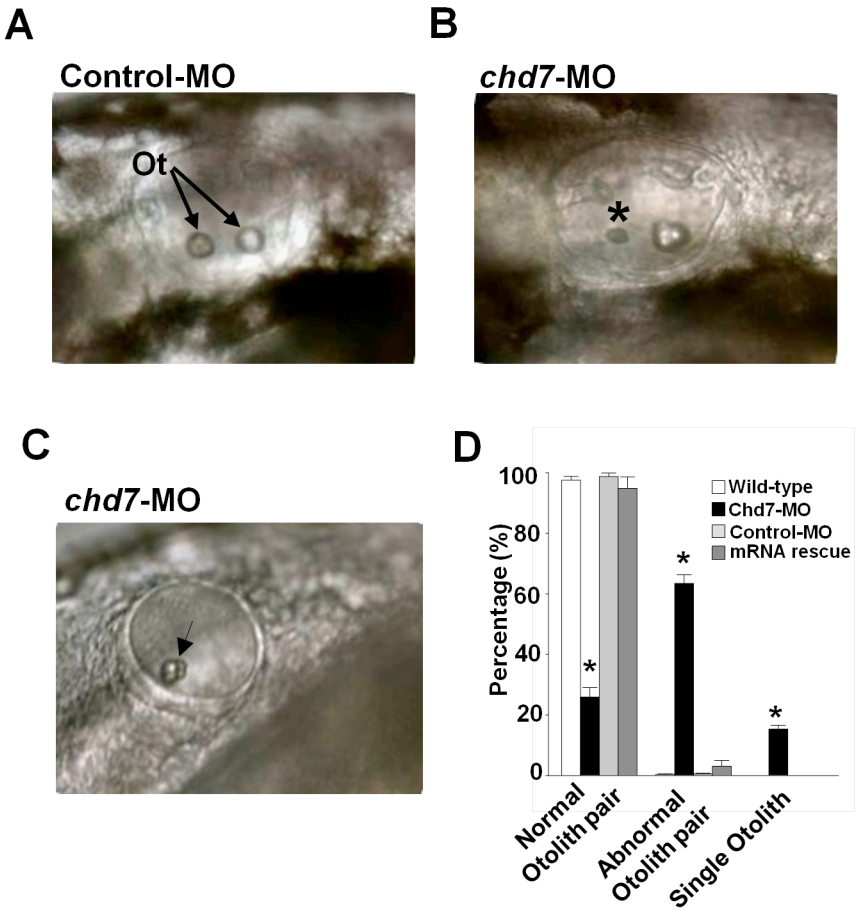


**Figure 4. Knockdown of *chd7* affects otolith development.** (**A**) The otic vesicle of control-MO-injected fish contains two otoliths, by contrast, larva treated with a morpholino against *chd7* (**B,C**) had smaller otoliths (*) or only a single otolith (Arrow). Lateral views with anterior to the left. Ot, otoliths (**D**) Bar graphs illustrating the prevalence of otolith phenotypes in wild-type (white bar), *chd7*-MO (black bar), control-MO-injected embryos (grey bar) and mRNA rescue (dark grey bar). *** <0.001, * <0.01

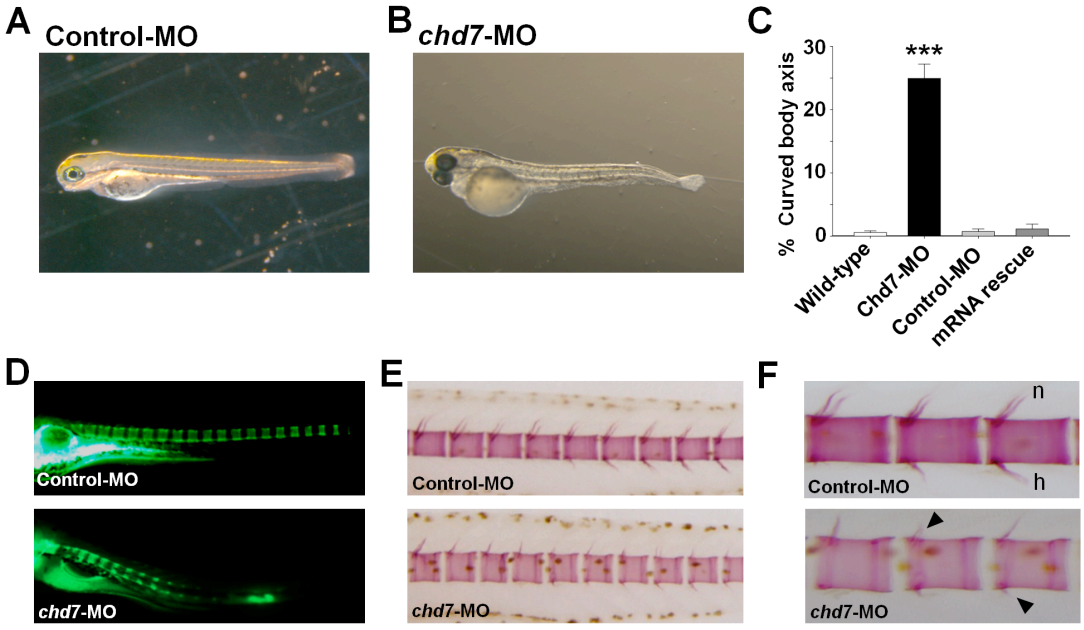


**Figure 5. Chd7 deficiency affects vertebral mineralization.** Lateral view of control-MO (**A**) and *chd7*-MO-injected (**B**) fish at 3 dpf. *Chd7* morphants exhibited a slight curvature of the long body axis (**B**). A significant percentage of the *chd7*-MO-injected (2ng/nl) fish had deformed body axis shape (**C**). Lateral views of *chd7* morphants (lower panel) and control siblings (upper panel) at 8 dpf (**D**) and 14 dpf (**E**) showed a reduced bone mineralization. Vertebrae with reduced or no hemal or neural spines were also observed in the *chd7*-MO-injected fish (**F**; black arrow). h, hemal spine; n, neural spine. *** <0.001

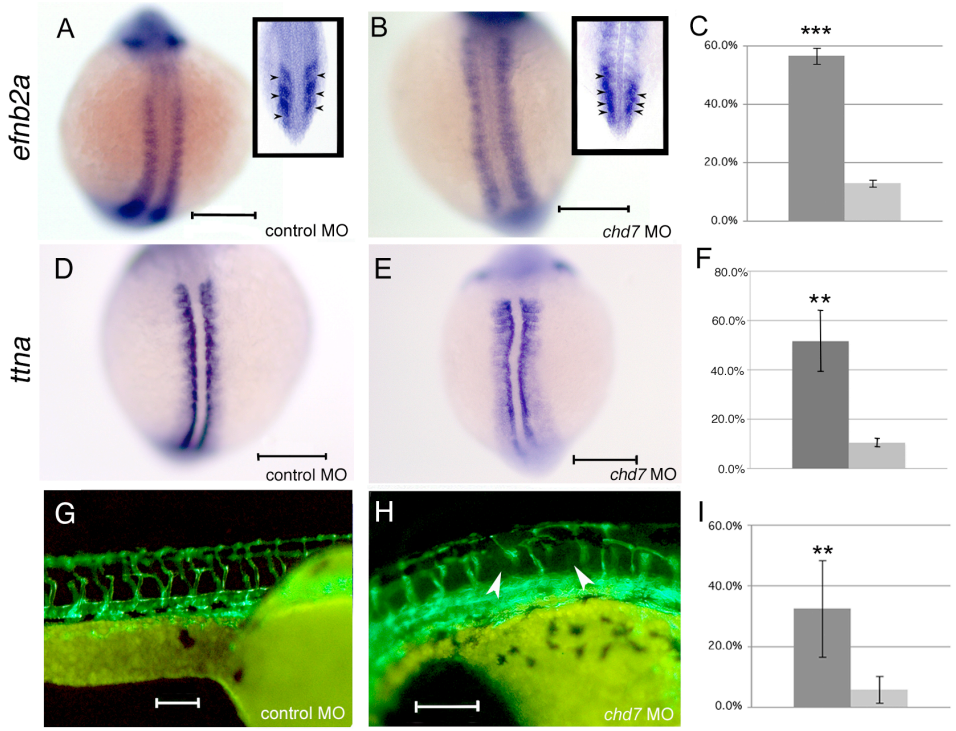


**Figure 6. Chd7 knockdown leads to somite boundary and segmental vasculature defects.** *Efnb2a* expression in control morphant **(A)** and *chd7* morphant **(B)** zebrafish embryos at the 13-somite stage of development. Top is anterior. Insets in **(A)** and **(B)** represent coronal sections through control or *chd7* morphant embryos, respectively, at the 13 somite stage. Posterior views with dorsal towards the top. Expression of *ttna*, a segment boundary marker reiterates the defects in segment boundary formation in *chd7* morphants **(E)** compared to controls **(D)**. Dorsal views with anterior to the top. Segmental vasculature patterning is defective (arrowheads) in *chd7* morphants **(H)** compared to control morphants **(G)** as visualized using *Fli1*-GFP transgenic zebrafish at 48 hpf. Sagittal views with anterior to the right. Graphs show percentages of animals exhibiting *efnb2a* expression defects **(C)**, *ttna* defects **(F)**, or segmental vasculature patterning defects **(I)**. The dark gray bar represents *chd7* morphants and the light gray bar represents control morphants. Scale bar: 200μm. *** <0.001, ** <0.01

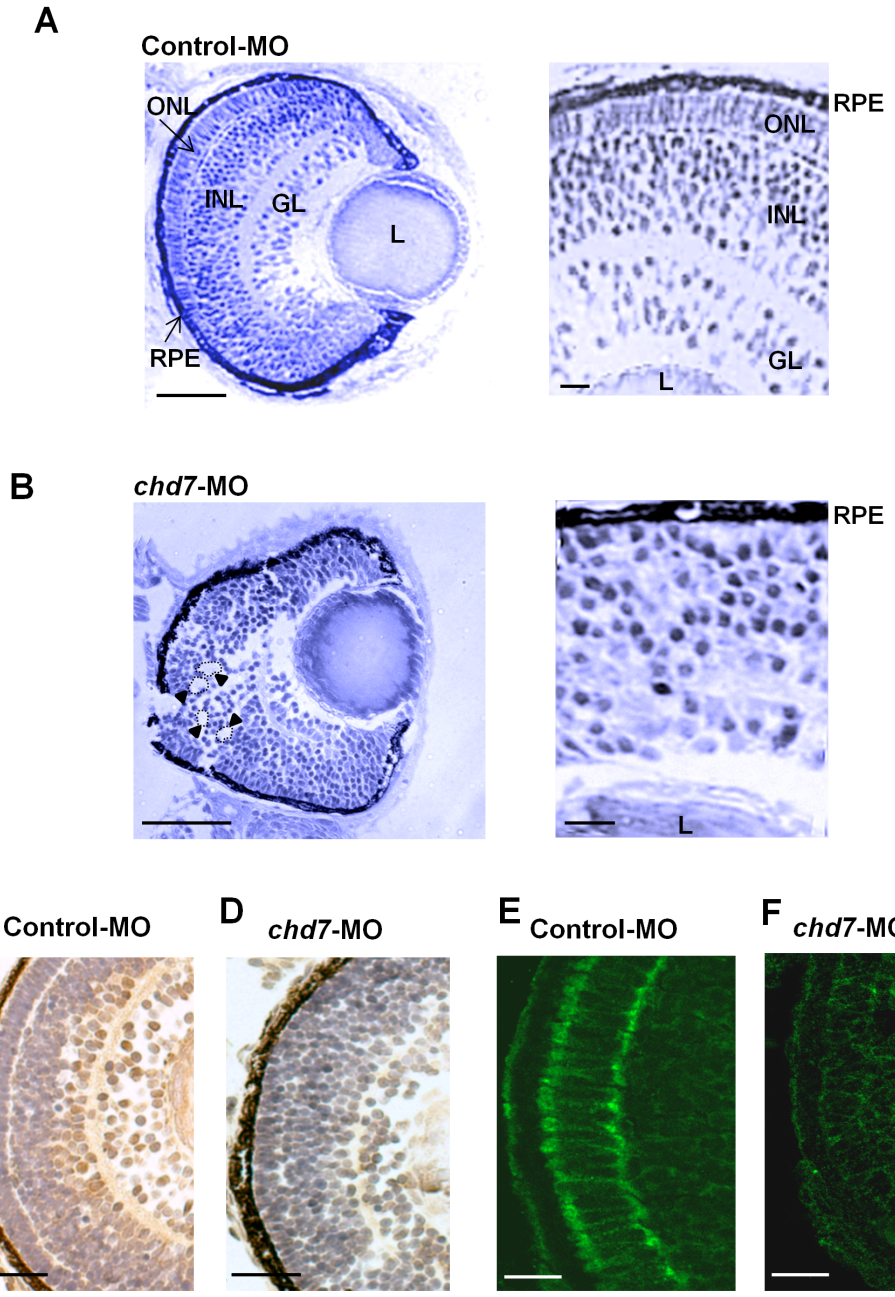
A
Control-MO
ONL
INL
GL
L
RPE
RPE
ONL
INL
GL
L
B
chd7-MO
RPE
L
C Control-MO
D chd7-MO
E Control-MO
F chd7-MO

**Figure 7**. **Chd7 plays an essential role in retinal development**. Retinal organization of control-MO embryos (**A**) and *chd7* morphants (**B**) was revealed by toludiene blue staining. Compared with the highly organized cells and laminated retinal structure in control-MO fish, *chd7*-MO retinal cells are disorganized (**A-B**: *Left panels*). Retinal lamination defect, including rosette formation, is clearly visible in the *chd7* morphants (examples of rosettes are indicated by dotted lines and arrow heads). GL, ganglion cell layer; INL, inner nuclear layer; L, lens; ONL, outer nuclear layer; R, retina; RPE, retinal pigment epithelium. Scale bar: 50 μm. Zn-8 immunoreactivity was performed to label (brown) retinal gangion cells in control-MO (**C**) and *chd7*-MO embryos (**D**). Scale bar: 30 μm. The expression of retinal ganglion cell-specific marker zn-8 is greatly reduced in *chd7* morphants. The photoreceptor layer of control-MO (**E**) and *chd7*-MO-injected (**F**) embryos were stained with 3A10. Chd7 morphants lacked the photoreceptor layer. Scale bar: 5 μm.

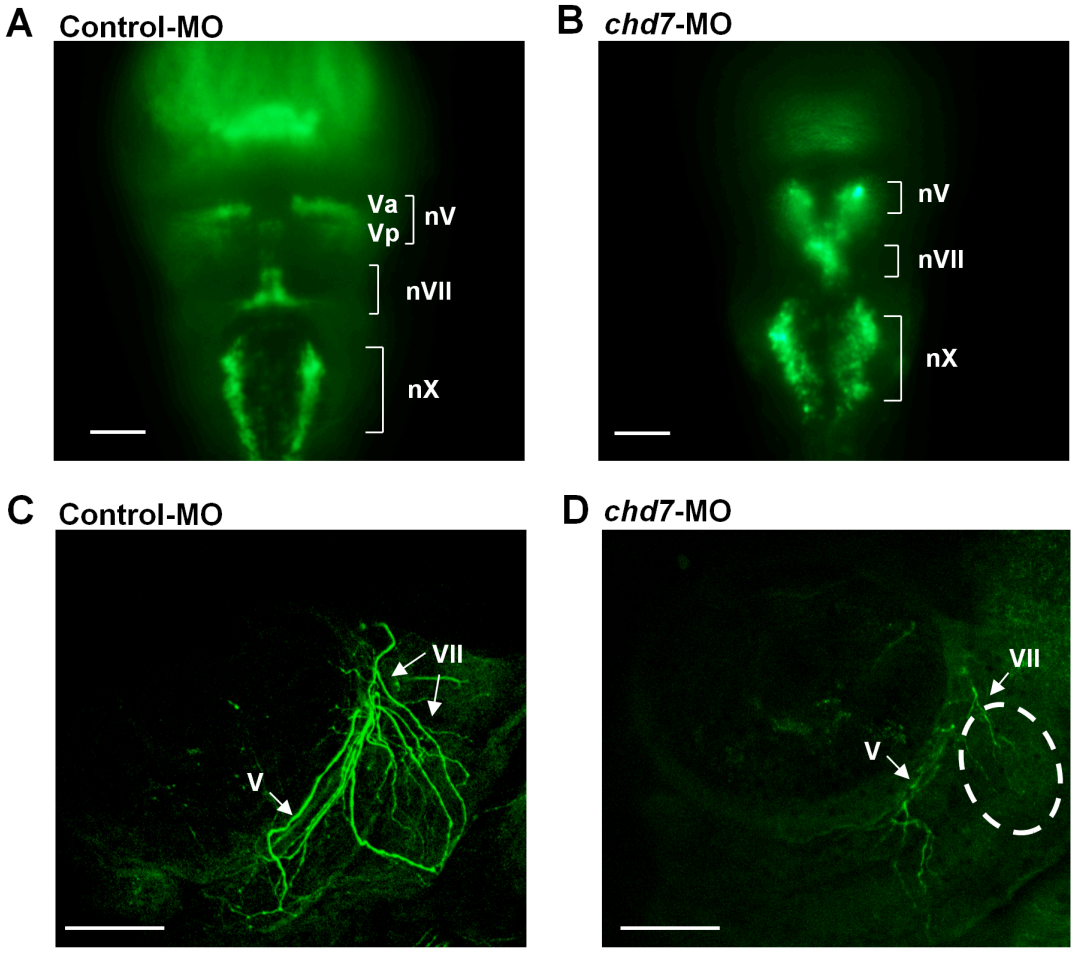


**Figure 8. Chd7 is important for cranial ganglia development and proper projection of facial nerves.** Dorsal view (rostal towards the top) of confocal fluorescent composite images of hindbrain branchiomotor neurons in control-MO injected (**A**) and *chd7*-MO-injected (**B**) 48 hpf *Isl1*-GFP transgenic embryos. (**C, D**) Confocal fluorescent composite images showing anti-3A10 antibody-stained axons of 48 hpf embryos. The broken lines indicate the area of significant loss of VII nerves in *chd7* morphants. nV, trigeminal motoneurons; Va, anterior trigeminal motoneurons; Vp, posterior trigeminal motoneurons; nVII, facial motoneurons; nX, Vagal motoneurons; V, trigeminal nerve; VII, facial nerve. Scale bar: 50 μm

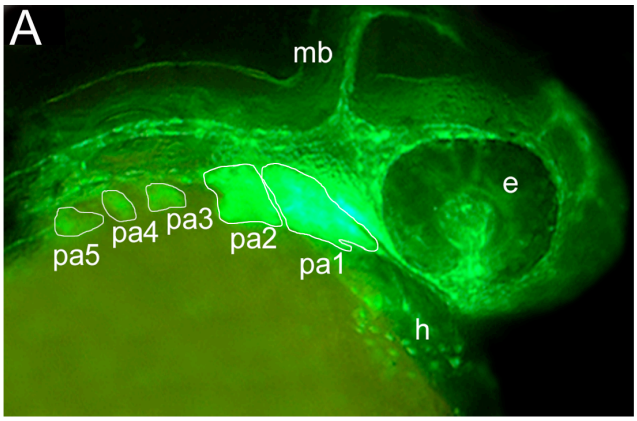
A
mb
e
pa5
pa4
pa3
pa2
pa1
h

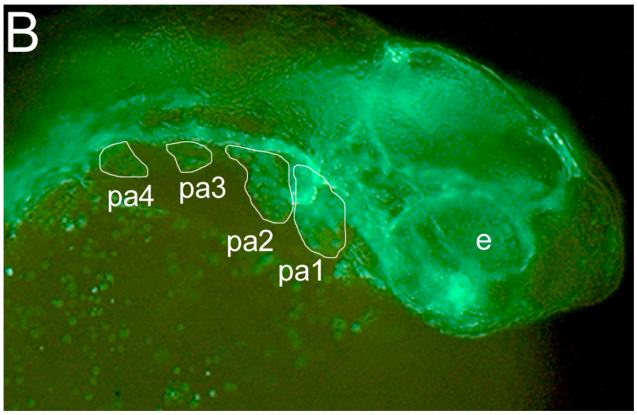
B
pa4
pa3
pa2
pa1
e

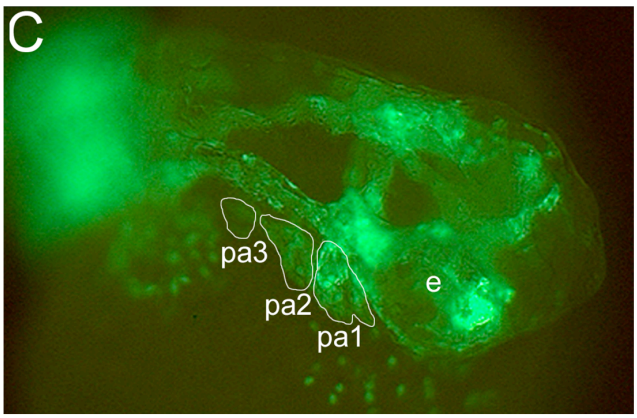
C
pa3
pa2
pa1
e

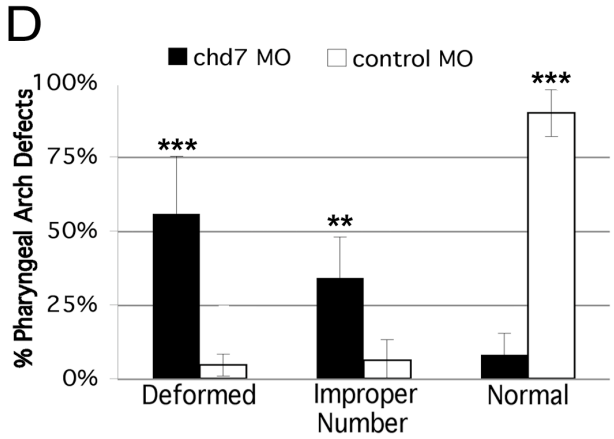
D
chd7 MO
control MO
% Pharyngeal Arch Defects
100%
75%
50%
25%
0%
***
**
***
Deformed
Improper Number
Normal

**Figure 9. Knockdown of *chd7* results in defects in CNC development.** *Fli1*-GFP transgenic embryos were used for MO injections to determine whether Chd7 depletion had an effect on CNC development. Embryos were injected at the 1 cell stage and examined for effects at 34-36 hpf. (**A**) Control-MO injected zebrafish embryos did not exhibit defects in CNC segment shape or number. Alternatively, the majority of *chd7*-MO-injected embryos exhibited aberrant CNC development including an improper number of CNC segments (**B**), as well as severely disorganized (**C**) or missing CNC populations. (**D**) Based on the t-test comparing means, there was a significant difference in CNC defects between *chd7*-MO and control-MO-injected zebrafish embryos. More than half of the *chd7*-MO-injected fish had deformed or missing CNC segments and about one third developed an improper number of segments. **=0.01; *** <0.001; e, eye; mb, midbrain; pa1-5, pharyngeal arches 1-5.

## SUPPLEMENTARY FIGURES AND TABLE

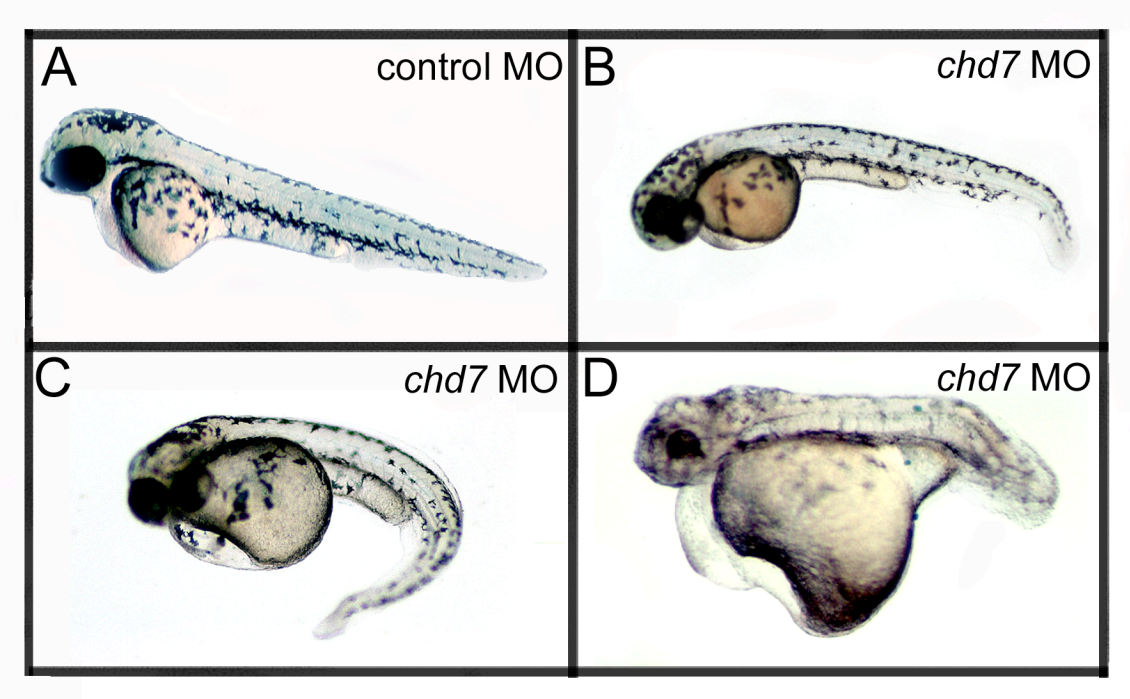


**Supplementary Figure 1. *Chd7*- MO injections are dosage dependent.** As the concentration of the *chd7*-MO injection increased, the phenotypic defects became more severe. (**A**) Control-MO injected zebrafish showed no phenotypic defects 48 hpf and were comparable to wild type zebrafish at the same age. Embryos injected with 2 ng/nl (**B**), 4 ng/nl (**C**), or 6 ng/nl (**D**) *chd7*-MO showed increasing severity of developmental defects with increasing MO concentration.

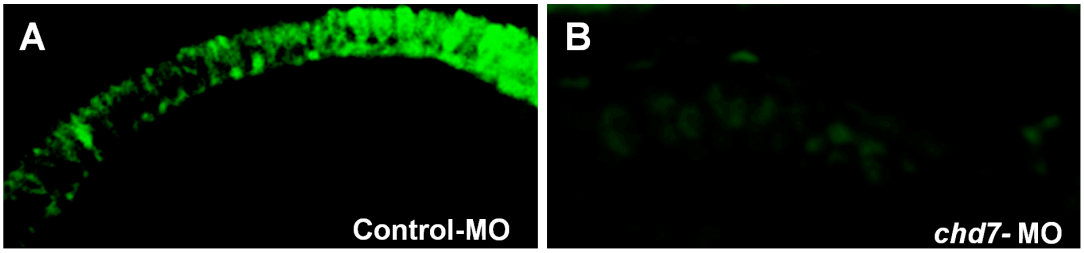


**Supplementary Figure 2. Chd7 plays an essential role in photoreceptor development**. The photoreceptor layer of control-MO (**A**) and *chd7*-MO-injected (**B**) embryos were stained with Zpr-1. Chd7 morphants lacked the photoreceptor layer.

**Table 1. Measurement of zebrafish size at different ages**

| Days post-fertilization (dpf) | Standard length[a] (mm) | |
|---|---|---|
| | Control-MO | chd7-MO |
| 3 dpf | 3.2 ± 0.1 | 3.1 ± 0.2 |
| 5 dpf | 4.1 ± 0.2 | 4.3 ± 0.1 |
| 8 dpf | 5.0 ± 0.1 | 4.8 ± 0.3 |
| 14 dpf | 6.4 ± 0.2 | 6.4 ± 0.1 |

[a] Standard length is the distant from the snout to the caudal peduncle or to the posterior tip of the notochord in pre-flexion larvae, as described by Parichy et al. 2009

# RNA-Seq as a method to evaluate changes in the zebrafish transcriptome in response to Chd7 knockdown

**Nicole L. Jacobs-McDaniels[1] and R. Craig Albertson[1,2]**

Affiliation: [1]Department of Biology, Syracuse University

[2]Department of Biology, University of Massachusetts

**ABSTRACT**

RNA-Seq is a novel, high throughput sequencing method using next generation sequencing technology to examine transcriptome dynamics. Chd7 is a chromatin remodeler associated with human scoliosis and CHARGE Syndrome and is known to play critical roles in zebrafish development. To determine direct or indirect targets of Chd7, we combined morpholino antisense technology with RNA-Seq to determine genes that were differentially expressed in response to Chd7 knockdown. Our results identified more than 2000 genes significantly up- or downregulated in response to Chd7 knockdown including several patterning genes, Wnt receptors, an Fgf receptor, and members of the Notch signaling pathway. Additionally, we found genes involved in heart, eye, otolith, and neural crest cell development to be differentially expressed in *chd7* morphant zebrafish. These data are consistent with previously described *chd7* morphant zebrafish phenotypes (Jacobs-McDaniels and Albertson, 2011; Patten et al., 2012), and with implicated roles for this factor in human disease. More broadly, we have accumulated a plethora of data for further analysis to help us gain a better understanding of the functions of a relatively uncharacterized chromatin remodeler.

## INTRODUCTION

The Chromodomain Helicase DNA-binding Protein (CHD) family of ATP- dependent chromatin remodelers is a group of nine known proteins, categorized into three subfamilies. CHD proteins regulate transcription by using the energy from ATP to disrupt interactions between nucleosomes and DNA, thereby altering the structure of the chromatin (Tran et al., 2000; Wang and Zhang, 2001; Stockdale et al., 2006). The CHD family is both evolutionarily conserved and of critical importance to animal development (Marfella and Imbalzano, 2007), however the biological function of many of these proteins remains unknown or poorly characterized.

CHDs are also implicated in human health and disease. Defects in members of the CHD family have been associated with several diseases including neuroblastomas (Thompson et al., 2003; White et al., 2005), Dermatomyositis (Ge et al., 1995), CHARGE (*coloboma* of the eye, *h*eart defects, *a*tresia of the choanae, *r*etardation of growth, *g*enital abnormalities, *e*ar abnormalities and deafness) Syndrome (Vissers et al., 2004), cancer (Mulero-Navarro and Esteller, 2008), and scoliosis (Gao et al., 2007). We became interested in one specific member of the CHD family, *chromodomain helicase DNA binding protein 7* (*chd7*) because of its association with two human diseases. Specifically, a scoliosis-associated haplotype is centered over exons 2-4 in human *CHD7* (Gao et al., 2007), and mutations in *CHD7* are implicated in about 60% of patients diagnosed with CHARGE Syndrome (Jongmans et al., 2006; Lalani et al., 2006). Congruent with the association of *CHD7* with scoliosis, we have previously shown that Chd7 plays a role in controlling left-right symmetry during zebrafish (*Danio rerio*) somitogenesis (Jacobs-McDaniels and Albertson, 2011). Moreover, we recently offered

Chd7-deficient zebrafish as an experimentally tractable animal model for human CHARGE Syndrome (Patten et al., 2012). In both studies we (1) examined endogenous expression of *chd7* mRNA, and (2) assessed the effects of Chd7 knockdown through the use of *chd7* translation and splice blocking morpholinos in zebrafish. These studies provided compelling evidence that Chd7 function is conserved from fish to humans, making zebrafish an excellent model for the study of these diseases.

*Chd7* may have several important roles in development, as this gene exhibits conserved expression across several vertebrate taxa in the nervous system, heart, somites, eyes, extremities, auditory system, and numerous other vital anatomical structures (Sanlaville et al., 2006; Aramaki et al., 2007; Hurd et al., 2007). As a chromatin remodeler, it is highly likely that Chd7 influences gene networks essential for proper development of multiple organ systems. The experiments performed here sought to identify a more extensive list of networks in which Chd7 functions. Because of its conservation across vertebrate taxa, determination of the roles and molecular interactions of zebrafish Chd7 in development and homeostasis may provide inroads into the etiologies and pathophysiologies along a broad spectrum of debilitating human diseases.

To determine the factors that interact with Chd7, a transcriptome-wide approach utilizing next generation sequencing, termed RNA-Seq, was employed. RNA-Seq is a relatively new approach using next generation sequencing technologies to explore transcriptome dynamics. Next generation sequencing is a novel high-throughput sequencing method that provides a rapid and cost-effective means to generate vast amounts of sequence information (Marguerat and Bahler, 2010), and this technology has revolutionized the way we study gene regulation. In addition, RNA-Seq can be used to

compare transcript levels between different cell types or organisms under different treatment conditions. Although this is a relatively new technology, several published works exist in which next generation sequencing technology has been used successfully (Mortazavi et al. 2008; Berger et al., 2010; Hohenlohe et al., 2010; Tang et al., 2010; Twine et al., 2011). Moreover, new advances in the field allow for the sequencing of RNA directly, with no need for amplification (Mamanova et al., 2010), proving how quickly this field is evolving.

In this study, zebrafish embryos injected with *chd7* morpholino (MO) were analyzed to ascertain transcriptome-wide changes when compared to control MO injected embryos. Based on previous work (Vissers et al., 2004; Gao et al., 2007; Jacobs-McDaniels and Albertson, 2011; Patten et al., 2012) and *chd7* expression studies (Sanlaville et al., 2006; Aramaki et al., 2007; Hurd et al., 2007; Jacobs-McDaniels and Albertson, 2011; Patten et al., 2012) we expect that this treatment will perturb the expression of genes involved in the development of the eyes, heart, somites, auditory system, nervous system, and cranial neural crest cells. This approach will allow us to identify transcripts downstream of Chd7 activity in the zebrafish embryo that may be important for the proper development and function of these structures. It is our hope that this information will provide the foundation for future developmental, biomedical, and clinical studies.

## EXPERIMENTAL PROCEDURES

### Zebrafish maintenance and morpholino injection

Wild-type AB zebrafish (*Danio rerio*) were raised at 28.5°C on a 14 hour light, 10 hour dark cycle. The evening prior to MO injection, adult fish were transferred to breeding tanks. Males and females were kept separate by a clear plastic barrier in the center of the tank. The morning of injection, the clear barrier was removed and the fish were allowed to spawn. Embryos were collected immediately following fertilization to assure they were at the earliest stages of development. 1-2 cell stage embryos as previously described (Kimmel et al., 1995) were injected with 6 ng/nl *chd7* translation blocking MO (here after referred to as "*chd7*MOs") or 6 ng/nl control MO (cMO's) (Gene Tools, LLC, Philomath, OR). For information on testing and verification of MO functions, refer to Jacobs-McDaniels and Albertson (2011), and Patten et al. (2012).

### RNA isolation and library sequencing

Two days following MO injection, morphant zebrafish larvae were collected and total RNA from whole embryos was isolated using a Qiagen RNeasy kit (Qiagen, Inc., Valencia, CA). RNA was quantified using an Agilent 2100 Bioanalyzer (Agilent Technologies, Inc., Santa Clara, CA). RNA samples were processed using an Illumina mRNA-Seq Sample Prep kit (Illumina, Inc., San Diego, CA) and sequenced on an Illumina Genome Analyzer II-x at the Genomics Core Facility at the University of Oregon (Eugene, OR). Two sequence files (from two sequencing lanes) were generated in FASTQ format. Nucleotide barcodes were used to sort three biological replicates of *chd7*MO reads (from one lane), and three replicates of cMO reads (from a second lane).

**Processing RNA-Seq reads, quality control and mapping with TopHat**

Using the Barcode Splitter option in the Galaxy platform (Giardine et al., 2005; Blankenberg et al., 2010; Goecks et al., 2010), the two original FASTQ sequence files were separated into six separate files. The median number of sequences for each file was 15,039,103 reads. Next, the Galaxy FASTQ Groomer was used to convert each set of sequences to fastqsanger format. To determine the quality of the reads, we used FastQC, a quality control tool for high throughput sequence data (Babraham Bioinformatics). The FastQC output provides several pieces of important quality information including average sequence length, % GC content, per base sequence quality, per base sequence content, sequence quality scores, and overrepresented sequences. It is important to verify that the data is of high quality before proceeding to map the reads with TopHat (see below).

Our sequencing data was of good quality based on our FastQC analysis. The average sequence length was 101 bases. We used the "per base" data sets to appropriately trim low quality bases from the beginnings or ends of our sequenced reads before proceeding to TopHat. To do this, we used Galaxy's FASTQ Trimmer (Blankenberg et al., 2010). On average, the first 8 bases and the last 38 bases were trimmed from each read. Our sequences for mapping were approximately 55 bases.

Finally, we used TopHat for Illumina in the Galaxy platform. TopHat can quickly map splice junctions for RNA-Seq reads. First, it aligns RNA-Seq reads to a large genome using the ultra high-throughput short read aligner Bowtie, then TopHat analyzes Bowtie's mapping results to identify splice junctions between exons (Trapnell et al.,

2009). Reads were mapped to the Zv9 version of the zebrafish genome. Default parameters for TopHat were used.

**Cufflinks for transcript assembly and estimation of abundance**

Cufflinks is an open-source software program for RNA-Seq data that assembles transcripts, estimates transcript abundances, and tests for differential expression and regulation of transcripts. Cufflinks roughly assembles aligned RNA-Seq data into a transcript set, then estimates the relative abundances of each transcript based on the number of reads in support of that transcript (Trapnell et al., 2010). The unit of measurement Cufflinks uses to measure relative abundance of transcripts is Fragments Per Kilobase of exon per Million fragments mapped (FPKM). We used Cufflinks (version 0.0.5) through the Galaxy platform to process the TopHat output aligned read files. Quartile normalization was performed to improve accuracy of differential expression calls for low abundance transcripts and bias correction was performed to improve the accuracy of transcript abundance estimates.

**Cuffcompare and Cuffdiff to test for differential expression**

After Cufflinks was used on all 6 TopHat outputs, the assembled transcripts were sent to Cuffcompare using the Galaxy platform (Trapnell et al., 2010) for comparison against a reference annotation. We used the annotation file "Danio_rerio.Zv9.65.gtf", which was downloaded from Ensembl as our reference. This allowed Cuffcompare to classify each transcript as known or novel. Additionally, for our purposes of determining differential

expression, combined transcript .gtf files were constructed in Cuffcompare for use with Cuffdiff.

Cuffdiff (Trapnell et al., 2010) is the third part of the Cufflinks software program and is used to determine significant differences in transcript expression, splicing, and promoter usage. First, we pooled all *chd7*MO read data and compared it to all pooled cMO read data for an overall comparison of the above characteristics. Then, we performed pair-wise comparisons between each *chd7*MO dataset and cMO dataset. In this study we focused on the genes that are differentially expressed between morphant and control embryos.

**Using the Cuffdiff output and Ensembl Biomart to infer differentially expressed loci**

The Cuffdiff transcript differential expression outputs in the Galaxy platform included extensive lists of loci determined to be differentially expressed. To determine significant changes in expression, we used an ln(fold change) of ±0.7, which corresponds to about a two-fold increase or decrease in expression, as the cutoff. According to the Cufflinks User Manual (http://cufflinks.cbcb.umd.edu/manual.html), the fold change is determined by dividing FPKM value 1 by FPKM value 2. In all cases *chd7*MO data was used as value 1, and the cMO data was used as value 2. Therefore, a positive ln value would correspond with a downregulation of gene expression in the *chd7*MO zebrafish and a negative ln value would correspond with an upregulation of gene expression in *chd7*MO zebrafish. Loci exhibiting significantly different expression were determined from Cuffdiff, a list of these regions was downloaded and inputted into Ensembl's Biomart query (http://www.ensembl.org/biomart/martview). There are many attributes that can be

selected as Biomart outputs spanning categories such as gene name, ontology, expression, and protein domain information. For this study, we selected gene/transcript names, gene/transcript IDs, and gene ontology (GO) as outputs. For ease of understanding and repetition, we developed a flow chart (Fig. 1) listing each of the steps in the RNA-Seq method described thus far and the resources available for online analysis steps.

**Using CateGOrizer to batch analyze gene ontologies of differentially expressed genes**

CateGOrizer (Hu et al., 2008) is a free web tool that performs a batch analysis of GO terms by counting the number of occurrences of each GO term within a pre-defined set of parent terms. Using the GO terms output from Ensembl's Biomart, we determined the major GO classifications of each group of significantly upregulated or significantly downregulated genes, respectively. This allowed us to gain a broad perspective of the biological changes that were occurring in the zebrafish *chd7*MO as a result of Chd7 knockdown.

## RESULTS/DISCUSSION

### Differential gene expression

Over 2000 genes showed significant differences in expression between *chd7*MO and cMO zebrafish. Of these, 1199 genes were significantly upregulated and 1251 genes were significantly downregulated in response to *chd7* knockdown. The range of differentially expressed genes was 624.76 to -266.20-fold. We determined the top 20 up- and downregulated genes in *chd7*MOs by analyzing the results of an overall comparison as well as all pair-wise comparisons between replicates. A list of the top 20 up- and downregulated genes, as well as select information describing these genes can be found in Tables 1 and 2, respectively. For a gene to be included in these tables, it must have exhibited a significant difference in expression in (1) the overall morphant versus control data comparison, and (2) at least 6 out of the 9 pair-wise comparisons. Beyond the top 20 up- and downregulated sets of genes, there were several differentially expressed genes whose functions correspond with previous work characterizing the functions of *chd7*. These are presented in Table 3 and include genes that play roles in somitogenesis, axial patterning, eye and heart development, as well as neural crest cell development and migration.

### Top 20 upregulated genes upon *chd7* knockdown

Several genes found to be significantly upregulated in *chd7*MOs function in ATP binding, nucleotide binding, and/or DNA binding, all of which are consistent with the roles of Chd7. There are also two notable groups of patterning genes that are highly upregulated in *chd7*MOs: (1) *hox* genes; *hoxc13b*, *hoxc6b*, and *hoxc12b* which play a role

in multicellular organismal development, specifically anterior-posterior patterning (Amores et al., 1998; Holstein et al., 2011; Michaut et al., 2011); and (2) *vox* and *vent*, both of which are implicated in dorsal-ventral pattern formation. Both *hoxc13b* and *hoxc12b* are posteriorly expressed in zebrafish (Thisse, et al., 2004; Fauny et al., 2009), while *hoxc6b* is more anteriorly expressed (Thisse et al., 2004). Interestingly, the anterior expression boundary of *hoxc6* is correlated with the rib bearing vertebrae in zebrafish (the "thoracic" vertebrae in amniotes; Bird and Mabee, 2003). In moderately defective *chd7*MOs, the most posterior part of the tail is kinked (Jacobs-McDaniels and Albertson, 2011; Patten et al., 2012), which may allude to a posterior *hox*-patterning defect. Additionally, *hox* genes are directed by several somitogenesis genes including members of the Notch signaling pathway and *cdx4*, which were also differentially expressed in *chd7*MOs. Cumulatively these losses in proper *hox* gene expression and direction, could contribute to the defects observed along the long axis of the body in zebrafish *chd7*MOs, however more work is necessary to verify this.

*Rargb*, a retinoic acid receptor (Linville et al., 2009), is another gene that is highly upregulated in *chd7*MOs. *Chd7* zebrafish morphants have been shown to exhibit curves and kinks along the long axis of the body (Jacobs-McDaniels and Albertson, 2011). Retinoic acid is important for A-P patterning (Moreno and Kintner, 2004), and in maintaining left-right symmetry during somitogenesis (Kawakami et al., 2005). Loss of Chd7, and therefore an upregulation of *rargb*, is a possible mechanism responsible for upsetting the normal body symmetry in *chd7*MOs, leading to the observed curves and kinks along the long axis of the body. More generally, mis-expression of *hox* genes*, vox,*

*vent* and *rargb* upon *chd7* knockdown, suggest that this gene plays a critical role in establishing the major body axes of the vertebrate embryo.

*Lbh*, a gene that plays a role in angiogenesis and heart development, endochondral bone development (Conen et al., 2009), and early limb bud patterning (Briegel and Joyner, 2011) is also highly upregulated in *chd7*MOs. *Lbh* is expressed in the branchial arches and neural crest-derived sensory neurons in mice (Briegel and Joyner, 2011), which is consistent with a role for Chd7 in zebrafish neural crest cell development (Patten et al., 2012).

**Top 20 downregulated genes upon *chd7* knockdown**

Upon analysis of those genes downregulated in *chd7*MOs we also found several having ATP, nucleotide, and/or DNA binding functions. Unlike the top set of upregulated genes, the 20 most downregulated genes performed relatively disparate functions. For instance, *Kdm6b*, a lysine specific demethlyase, shows high levels of downregulation. Downregulation of this gene can increase methylation of key *kdm6b* target genes, inhibiting transcription. More work is necessary to determine the effects of *kdm6b* loss in *chd7*MO zebrafish. Members of the slow myosin heavy chain group of genes, *smyhc 1*, *2,* and *3*, were also found to be highly downregulated in *chd7*MOs, suggesting a dysfunction in motor activity in these zebrafish. Based on personal observations, *chd7*MOs do exhibit improper myomere formation and deficient swimming capabilities, however it remains to be tested whether these defects are due to abnormal muscle structure/activity, or to other defects including curvature of the long axis of the body. Finally, *greb1*, a gene found to function in hormone-responsive tissues and cancer (Hnatyszyn et al., 2010; Antunes et

al., 2011), is downregulated in *chd7*MOs. Determination of the interactions between Chd7 and *greb1* would be an interesting area of future research and may lead to insights into how chromatin remodelers may function in the onset of cancer.

**Differentially expressed genes have functions in epigenetic gene regulation, left-right symmetry, somitogenesis, and neural crest cell development and migration**

Due to the large number of differentially expressed genes, not all can be discussed here. We chose several key genes that we found to be consistent with our previous work or discussed in the primary literature. Table 3 is a summary of upregulated and downregulated genes of interest in *chd7*MOs that are not among the top 20 in either category.

Among the upregulated genes, several members of the WD-40 Repeat (WDR) family show differential expression. *Wdr3*, *wdr55*, and *wdr63* are all significantly upregulated in *chd7*MOs, as are the DNA methyltransferase genes *dnmt5* and *dnmt3*. Intrestingly, the *chd7* paralog, *chd2*, is also upregulated, perhaps to compensate for the loss of Chd7 expression. All of these genes can function in epigenetic regulation, comparable to the functions of Chd7.

Consistent with previous work illustrating that *chd7* plays a role in controlling zebrafish somitogenesis (Jacobs-McDaniels and Albertson, 2011), the Wnt target, *cdx4*, is significantly upregulated in *chd7*MOs. Previously, this was observed using whole mount *in situ* hybridization. Several Wnt receptors and an Fgf receptor were also differentially expressed in *chd7*MOs. Members of both the Wnt and Fgf families are known to play important roles in somitogenesis (Dubrulle et al., 2001; Aulehla and

Herrmann, 2004; Shimizu et al., 2005; Geetha-Loganathan et al., 2008). Also consistent with previous work examining zebrafish somitogenesis (Stickney et al., 2000; Holley, 2007), several regulators of Notch signaling, *gmds*, *ptb1a*, and *psen1* are significantly upregulated. *Lft1* and *smo*, genes important in maintaining proper left-right asymmetry were also shown to be upregulated in *chd7*MOs. Whether the asymmetric pattern of expression of these genes is also disrupted by Chd7 knockdown remains to be tested.

Mutations in *chd7* have been associated with human CHARGE Syndrome (Vissers et al., 2004) and zebrafish *chd7*MOs have been offered as a model organism to study CHARGE Syndrome based on their phenotypic defects (Patten et al., 2012). Humans with CHARGE Syndrome can have many developmental abnormalities including defects in the eyes, ears, heart, and genitalia. We found differentially expressed genes important for neural crest cell development and migration, axon guidance, vascular development, angiogenesis, retina development, otolith and otic vesicle development, and heart tube and cardiac cell development in *chd7*MO zebrafish. Among the genes found to be downregulated in *chd7*MOs were the WDR members *wdr33* and *wdr43*, which are epigenetic modulators of gene expression. Downregulation of *gnl3*, involved in retina development (Schmitt et al., 2009), and *atp1a1*, which functions in heart tube, cardiac cell (Shu et al., 2003; Langenbacher et al., 2011), otolith, and otic vesicle development (Blasiole et al., 2006), may be responsible for these CHARGE Syndrome-like symptoms in *chd7* zebrafish morphants. Interestingly, *atp1a1* is also known to play a role in maintaining left-right symmetry, as well as in heart morphogenesis (Shu et al., 2003; Ellertsdottir et al., 2006; Cibrian-Uhalte et al., 2007). Loss of this gene's expression may contribute to the previously described left-right symmetry, and other key morphogenic

defects in *chd7* zebrafish morphants (Jacobs-McDaniels and Albertson, 2011; Patten et al., 2012). It should be noted that over 60% of humans afflicted with CHARGE Syndrome develop later onset scoliosis (Doyle and Blake, 2005), potentially linking *atp1a1* to both spinal deformities and CHARGE Syndrome.

We have also previously showed evidence of defects in cranial ganglia development, in proper projection of facial nerves, and in segmental vasculature in *chd7*MO zebrafish (Patten et al., 2012). We found *nrp1a*, a gene involved in axon guidance (Feldner et al., 2005), vascular development, and angiogenesis (Lee et al., 2002) to be downregulated upon Chd7 loss, consistent with the previously described *chd7*MO phenotypes. Taken together, many of the genes that exhibit changes in expression in response to Chd7 knockdown exhibit functions that have been associated with Chd7 and human CHARGE Syndrome symptoms. These genes may be the mechanisms behind the defects described in both *chd7*MO zebrafish and human CHARGE Syndrome patients. More work is necessary to verify these connections.

In concordance with previous findings that Chd7 knockdown causes defects in cranial neural crest cell development and migration (Patten et al., 2012), we found several differentially expressed genes in our analysis that are important in neural crest cell migration, development, and cell fate specification. Genes that function in neural crest and cartilage development that we found to be upregulated in *chd7*MOs include, *tfap2a* (Arduini et al., 2009), *pbx4* (Yu and Moens, 2005), *smo* (Eberhart et al., 2006) and *nusap1* (Nie et al., 2010). *Nrp1a*, which is downregulated, functions in neural crest cell migration (Sato et al., 2006) and *sec23a*, also downregulated, is important in cartilage development (Lang et al., 2006). It is interesting to note that there are more upregulated

genes that function to control neural crest cell lineages than downregulated genes in *chd7*MO zebrafish.

**Using CateGOrizer to understand major gene ontologies affected by Chd7 knockdown**

To get a broad overview of the major gene ontologies affected by Chd7 knockdown in zebrafish embryos, we performed a gene ontology analysis using CateGOrizer (Hu et al., 2008). CateGOrizer is a free web tool that performs a batch analysis of GO terms by counting the number of occurrences of each GO term within a pre-defined set of parent terms. The GOA2GO classification method was used for our analysis. Broadly, both up- and downregulated gene classes represented gene ontologies including biological processes (16.93%, 16.29%, respectively), cellular processes (11.17%, 10.31%, respectively), and molecular functions (9.77%, 10.15%, respectively). Development was defined as about 5% of the total gene ontologies for both classes. Binding represented 2-3% of the gene ontologies. A more in depth breakdown of gene ontologies represented by up- and downregulated genes is shown in Fig. 2. Although this approach is very broad, it helps to provide an overview of the physiological and cellular functions affected by Chd7 knockdown.

**RNA-Seq is a straightforward method for the study of transcriptomics**

By capitalizing on next generation sequencing technology, RNA-Seq offers an innovative, rigorous, but relatively economical way to gain a transcriptome-wide view of how one variable can change the genetic program of an organism. In this work, we used

RNA-Seq to examine changes in gene expression upon knockdown of the chromatin remodeling protein, Chd7. Although zebrafish *chd7* function has recently been studied in the contexts of somitogenesis and human CHARGE Syndrome (Jacobs-McDaniels and Albertson, 2011; Patten et al., 2012), there is still much to be learned about this gene within the context of development and disease. Because of its function as a chromatin remodeler, we expected Chd7 to interact with many factors involved in the development of a multitude of traits.

One of the advantages of next generation sequencing technologies is, unlike a gene-by-gene approach, prior knowledge of gene function and/or expression is not necessary and the entire transcriptome can be analyzed simultaneously. We used a combination of morpholino antisense technology and RNA-Seq to gain a more comprehensive understanding of the genes that interact with and are affected by Chd7.

**Conclusion**

This work is the first transcriptome-wide study analyzing genetic changes in response to knockdown of a member of the Chromodomain Helicase DNA Binding protein family. Using RNA-Seq we were able to identify and quantify differentially expressed genes in *chd7*MO zebrafish embryos compared to cMO zebrafish embryos. We have shown several connections between genes with significantly different expression levels and *chd7*MO zebrafish phenotypes, making our data useful in complementing and extending our previous work with Chd7 (Jacobs-McDaniels and Albertson, 2011; Patten et al., 2012). Finally, we have accumulated a plethora of useful data using a relatively new protocol. We realize there is still much work to be done in terms of analyzing this data

set. It is our hope that others will make use of these data for further genetic, developmental, biomedical, and evolutionary research.

## FIGURES AND TABLES

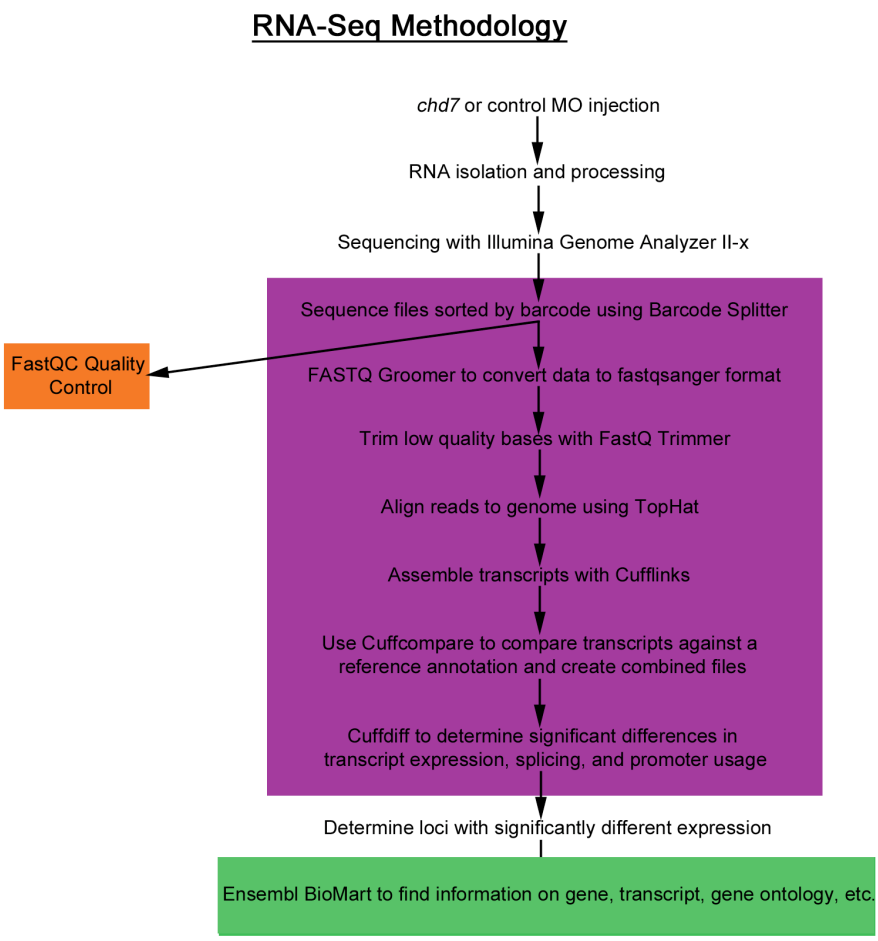


**Figure 1. RNA-Seq Methodology Flow Chart.** This figure represents a condensed series of the methods we used to complete our RNA-Seq analysis. The steps in the purple box were performed using the Galaxy platform (http://main.g2.bx.psu.edu/). FastQC (http://www.bioinformatics.bbsrc.ac.uk/projects/fastqc/) was used as a quality control check and is represented by the orange box. The green box represents the final step in our RNA-Seq analysis in which we used Ensembl's Biomart (http://www.ensembl.org/biomart/martview) to determine genes found at loci determined to have significantly different expression in *chd7*MOs compared to cMOs.

## Upregulated Gene Ontologies

A

| Gene Ontology | Percentage |
|---|---|
| Biological Process | 16.93% |
| Cellular Process | 11.17% |
| Molecular Function | 9.77% |
| Catalytic Activity | 5.83% |
| Metabolism | 5.57% |
| Development | 4.74% |
| Cellular Component | 4.07% |
| Cell | 3.58% |
| Macromolecule Metabolism | 3.34% |
| Intracellular | 3.19% |
| Other | 31.81% |

B

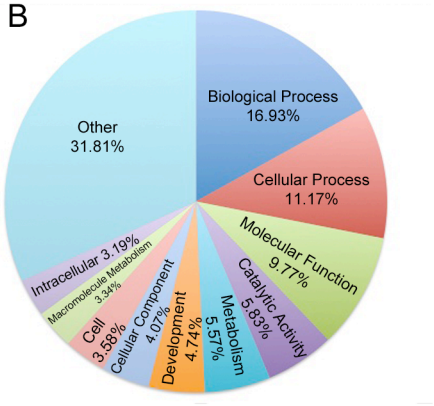


## Downregulated Gene Ontologies

C

| Gene Ontology | Percentage |
|---|---|
| Biological Process | 16.29% |
| Cellular Process | 10.31% |
| Molecular Function | 10.15% |
| Catalytic Activity | 6.25% |
| Metabolism | 5.67% |
| Development | 5.31% |
| Cellular Component | 4.69% |
| Cell | 3.90% |
| Macromolecule Metabolism | 3.28% |
| Intracellular | 2.97% |
| Other | 31.18% |

D

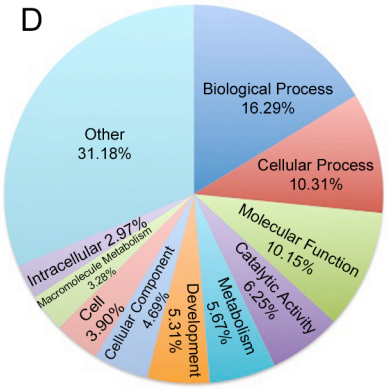


**Figure 2. Genes differentially expressed in *chd7*MOs span a wide range of gene ontologies.** To gain a broad understanding of the functions of differentially expressed genes in *chd7*MOs, we used CateGOrizer to perform a gene ontology analysis. This figure depicts tables and pie charts visually denoting the top 10 gene ontologies represented by genes upregulated (A) and downregulated (B) in *chd7*MOs compared to cMOs. Approximately one third of the characterized GOs in both categories do not fall into one of the listed GOs and is labeled as "other".

## Top 20 Genes Upregulated in *chd7* Morphants

| Gene | Description | Selected Ontologies | Location | FPKM control MO | FPKM *chd7* MO | Fold Change | p-value | Ensembl Gene ID | References |
|---|---|---|---|---|---|---|---|---|---|
| *ppl* | periplakin | cytoskeleton, cellular component | chr3:36708976-36731172 | 0.0202799 | 12.67 | 624.7565323 | 5.96E-07 | ENSDARG00000037898 | |
| *hk1* | hexokinase 1 | carbohydrate metabolic process, phosphorylation, nucleotide binding, ATP binding, transferase activity | chr13:23113100-23148025 | 0.0193914 | 3.21169 | 165.6244521 | <0.001 | ENSDARG00000039452 | |
| *ccdc88a* | coiled-coil domain containing 88Aa | cytoskeleton remodeling and cell migration, enhances akt signaling | chr13:53551-63011 | 0.0760116 | 5.89431 | 77.54487473 | <0.001 | ENSDARG00000063681 | Enomoto et al., 2006 |
| *smek2* | suppressor of mek1 | regulation of hepatic glucose metabolism, histone deacetylation | chr13:68757-78141 | 0.0760116 | 5.89431 | 77.54487473 | <0.001 | ENSDARG00000039619 | Yoon et al., 2010; Lyn et al., 2011 |
| *rtn4b* | reticulon 4b | endoplasmic reticulum, structural constituent of cell wall | chr13:69617-120404 | 0.0760116 | 5.89431 | 77.54487473 | <0.001 | ENSDARG00000059238 | |
| *CABZ01089918.1* | clone based-uncharacterized | protein binding | chr13:53879982-53881126 | 0.247295 | 8.65871 | 35.01368811 | <0.001 | ENSDARG00000086952 | |
| *srf* | serum response factor | DNA binding, protein dimerization activity | chr13:53893508-53909033 | 0.247295 | 8.65871 | 35.01368811 | <0.001 | ENSDARG00000038131 | |
| *lbh* | limb bud and heart development homolog (mouse) | transcription cofactor, regulates angiogenesis, endochondral bone formation | chr13:53936194-53938330 | 0.247295 | 8.65871 | 35.01368811 | <0.001 | ENSDARG00000087377 | Conen et al., 2009 |
| *CABZ01079775.1* | clone based-uncharacterized | uncharacterized | chr13:53945699-53976940 | 0.247295 | 8.65871 | 35.01368811 | <0.001 | ENSDARG00000074585 | |
| *mrpl2* | mitochondrial ribosomal protein L2 | translation, intracellular, structural constituent of ribosome | chr13:53978583-53984792 | 0.247295 | 8.65871 | 35.01368811 | <0.001 | ENSDARG00000062568 | |
| *inpp5a* | inositol polyphosphate-5-phosphatase A | negative regulator of inositol signaling, regulates dendritic morphology, involved in synaptic plasticity | chr13:53994418-54009879 | 0.247295 | 8.65871 | 35.01368811 | <0.001 | ENSDARG00000089915 | Sekulic et al., 2010; Windhorst et al., 2012 |
| *vox* | ventral homeobox | dorsal/ventral pattern formation, regulation of transcription, DNA-dependent, DNA binding | chr13:54046956-54049197 | 0.247295 | 8.65871 | 35.01368811 | <0.001 | ENSDARG00000014277 | |
| *vent* | ventral expressed homeobox | dorsal/ventral pattern formation, regulation of transcription, DNA-dependent, DNA binding | chr13:54056772-54063429 | 0.247295 | 8.65871 | 35.01368811 | <0.001 | ENSDARG00000017164 | |
| *hnrnpc* | heterogeneous nuclear ribonucleoprotein C | nucleic acid binding, ribonucleoprotein complex, nucleotide binding | chr2:37727933-37736951 | 0.103393 | 2.53833 | 24.55030805 | 0.0007739 | ENSDARG00000053810 | |
| *serbp1* | SERPINE1 mRNA binding protein 1 | regulates stability of plasminogen activators | chr2:3397407-3409194 | 1.73153 | 42.1016 | 24.31468124 | <0.001 | ENSDARG00000087421 | Koensgen et al., 2007 |
| *akt2* | akt murine thymoma viral oncogene homolog 2 | protein phosphorylation, protein tyrosine kinase activity, ATP binding, negative regulation of apoptosis, transferase activity | chr18:39007941-39050674 | 0.305211 | 5.32013 | 17.43099036 | 0.0001982 | ENSDARG00000011219 | |
| *rargb* | retinoic acid receptor, gamma b | regulation of transcription, DNA-dependent, sequence-specific DNA binding, steroid hormone receptor activity | chr11:1991815-2049041 | 2.05939 | 34.6944 | 16.8469304 | <0.001 | ENSDARG00000054003 | |
| *hoxc13b* | homeo box C13b | regulation of transcription, DNA-dependent, multicellular organismal development, fin regeneration, DNA binding | chr11:2108753-2111963 | 2.05939 | 34.6944 | 16.8469304 | <0.001 | ENSDARG00000090023 | |
| *hoxc6b* | homeo box C6b | regulation of transcription, DNA-dependent, multicellular organismal development, DNA binding | chr11:2148535-2150246 | 2.05939 | 34.6944 | 16.8469304 | <0.001 | ENSDARG00000046045 | |
| *hoxc12b* | homeo box C12b | regulation of transcription, DNA-dependent, multicellular organismal development, DNA binding | chr11:2178785-2180948 | 2.05939 | 34.6944 | 16.8469304 | <0.001 | ENSDARG00000046043 | |

Table 1. This table lists the top 20 genes upregulated in chd7MO zebrafish. It gives information about the gene, its Ensembl gene ID, the FPKM values determined as a result of our RNA-Seq analysis, the fold change in gene expression and the p-value.

## Top 20 Genes Downregulated in *chd7* Morphants

| Gene | Description | Selected Ontology | Location | FPKM control MO | FPKM *chd7* MO | Fold Change | p-value | Ensembl Gene ID | Reference |
|---|---|---|---|---|---|---|---|---|---|
| *gart* | phosphoribosylglycinamide formyltransferase | ATP binding, biosynthetic process | chr1:989727-1015830 | 12.6122 | 0.0473781 | -266.2031614 | 3.74E-05 | ENSDARG00000051855 | |
| *smyhc1* | slow myosin heavy chain 1 | skeletal muscle thin filament assembly, nucleotide binding, ATP binding, motor activity | chr24:42241037-42252740 | 13.5177 | 0.0760719 | -177.6963636 | 0.000924351 | ENSDARG00000071430 | |
| *smyhc2* | slow myosin heavy chain 2 | response to stress, nucleotide binding, ATP binding, motor activity | chr24:42264601-42285123 | 13.5177 | 0.0760719 | -177.6963636 | 0.000924351 | ENSDARG00000071433 | |
| *kdm6b* | lysine (K)-specific demethylase 6B | demethlyation, protein binding | chr7:22933203-22946812 | 1.56699 | 0.0165055 | -94.93744509 | 1.08E-05 | ENSDARG00000088087 | |
| *abcc2* | ATP-binding cassette, sub-family C (CFTR/MRP), member 2 | nucleotide binding, ATP binding, ATPase activity | chr13:553345-583302 | 1.96555 | 0.03285 | -59.83409437 | 1.07E-07 | ENSDARG00000014031 | |
| *glg1* | golgi glycoprotein 1 | membrane, cellular component | chr25:38348948-38368247 | 1.82252 | 0.0394404 | -46.20947049 | <0.001 | ENSDARG00000061282 | |
| *CU207301.12* | clone based- uncharacterized | protein binding, calcium ion binding | chr25:38368917-38378482 | 1.82252 | 0.0394404 | -46.20947049 | <0.001 | ENSDARG00000091667 | |
| *si:ch211-24n20.3* | ZGS project- uncharacterized | myosin complex, protein binding, ATP binding, motor activity | chr24:42124870-42320176 | 20.9034 | 0.464589 | -44.99331667 | 3.48E-06 | ENSDARG00000093715 | |
| *greb1* | growth regulation by estrogen in breast cancer 1 | early response gene in the estrogen receptor-regulated pathway, function in hormone-responsive tissues and cancer | chr17:30463575-30476115 | 12.2447 | 0.291928 | -41.94424653 | 3.99E-09 | ENSDARG00000070794 | Antunes et al., 2009, Hnatyszyn et al., 2010 |
| *taf15* | TAF15 RNA polymerase II, TATA box binding protein (TBP)-associated factor | nucleotide binding, zinc ion binding, nucleic acid binding | chr15:1814484-1833117 | 24.0941 | 0.705307 | -34.16115252 | 8.88E-16 | ENSDARG00000070019 | |
| *abca1b* | ATP-binding cassette, sub-family A (ABC1), member 1B | ATP binding, nucleotide binding, nucleoside-triphosphatase activity | chr14:6395285-6484954 | 11.8143 | 0.385523 | -30.64486425 | <0.001 | ENSDARG00000079009 | |
| *smyhc3* | slow myosin heavy chain 3 | myosin complex, nucleotide binding, ATP binding, motor activity | chr24:42297325-42310039 | 31.3011 | 1.16877 | -26.78123155 | 9.78E-13 | ENSDARG00000045242 | |
| *paics* | phosphoribosylaminoimidazole carboxylase, phosphoribosylaminoimidazole succinocarboxamide synthetase | embryo development, camera-type eye development, DNA binding, ATP binding | chr20:25647721-25660805 | 5.27397 | 0.197202 | -26.74399854 | 1.36E-07 | ENSDARG00000033539 | |
| *ppat* | phosphoribosyl pyrophosphate amidotransferase | metabolic process, cellular component, metal ion binding, transferase activity | chr20:25655479-25669115 | 5.27397 | 0.197202 | -26.74399854 | 1.36E-07 | ENSDARG00000004517 | |
| *mthfd1* | MTHFD1 methylenetetrahydrofolate dehydrogenase (NADP+ dependent) 1 | oxidation-reduction process, ATP binding, nucleotide binding | chr17:49510284-49563032 | 7.3952 | 0.287552 | -25.71778322 | 4.55E-14 | ENSDARG00000040492 | |
| *hpcal1* | hippocalcin-like 1 | cellular component, calcium ion binding | chr20:31257066-31334713 | 287.647 | 12.6371 | -22.76210523 | 2.26E-06 | ENSDARG00000022763 | |
| *apobl* | apolipoprotein B, like | response to chemical stimulus, lipid transport | chr20:31295686-31310798 | 287.647 | 12.6371 | -22.76210523 | 2.26E-06 | ENSDARG00000022767 | |
| *lama1* | laminin, alpha 1 | cell adhesion, regulation of embryonic development, regulation of cell migration, protein binding | chr24:43450377-43542737 | 20.8128 | 0.920525 | -22.60970642 | <0.001 | ENSDARG00000056043 | |
| *spna2* | spectrin alpha 2 | clustering of voltage-gated sodium channels, protein binding, calcium ion binding | chr21:11352584-11419552 | 1.55111 | 0.0715716 | -21.6721437 | 0.00149506 | ENSDARG00000019231 | |
| *dync2i1* | dynein, cytoplasmic 2, intermediate chain 1 | intraflagellar transport, cellular component, protein binding | chr21:11419543-11427049 | 1.55111 | 0.0715716 | -21.6721437 | 0.00149506 | ENSDARG00000057635 | |

Table 2. This table lists the top 20 genes downregulated in chd7MO zebrafish. It gives information about the gene, its Ensembl gene ID, the FPKM values determined as a result of our RNA-Seq analysis, the fold change in gene expression and the p-value.

# Differentially Expressed Genes Consistent With Previous Studies

| Gene | Description | Selected Ontologies | Location | FPKM control MO | FPKM *chd7* MO | Fold Change | p-value | Ensembl Gene ID |
|---|---|---|---|---|---|---|---|---|
| *ptbp1a* | polypyrimidine tract binding protein 1a | dorsal/ventral pattern formation, negative regulation of Notch signaling pathway | chr2:26436471-26448682 | 0.343442 | 5.38195 | 15.6706227 | 3.98E-06 | ENSDARG00000019362 |
| *wdr63* | WD repeat domain 63 | protein binding | chr23:44996474-45021498 | 0.339137 | 4.38034 | 12.91613714 | 2.15E-11 | ENSDARG00000088049 |
| *chd2* | chromodomain helicase DNA binding protein 2 | DNA binding, ATP binding, nucleic acid binding, helicase activity | chr18:24717169-24772356 | 0.329455 | 3.96008 | 12.02009379 | 2.96E-07 | ENSDARG00000060687 |
| *dnmt5* | DNA (cytosine-5-)-methyltransferase 5 | DNA methylation, DNA binding | chr23:17131889-17152704 | 0.865119 | 7.94388 | 9.182413055 | 8.35E-14 | ENSDARG00000057863 |
| *dnmt3* | DNA (cytosine-5-)-methyltransferase 3 | DNA methylation, DNA binding, neurogenesis | chr23:17154081-17175501 | 0.865119 | 7.94388 | 9.182413055 | 8.35E-14 | ENSDARG00000057830 |
| *nusap1* | nucleolar and spindle associated protein 1 | neural crest cell migration, DNA binding | chr13:33475323-33480269 | 1.02409 | 6.85321 | 6.691999727 | 2.82E-08 | ENSDARG00000002403 |
| *psen1* | presenilin 1 | Notch signaling pathway, somite development, Notch receptor processing | chr17:51731080-51749655 | 1.12237 | 6.1999 | 5.523935957 | 9.05E-07 | ENSDARG00000004870 |
| *lft1* | lefty1 | determination of left/right symmetry, dorsal/ventral pattern formation, embryonic heart tube development | chr20:35098589-35100995 | 1.13307 | 5.14181 | 4.537945581 | 4.52E-05 | ENSDARG00000019920 |
| *cdx4* | caudal type homeo box transcription factor 4 | somitogenesis, retinoic acid receptor signaling pathway, anterior/posterior pattern specification | chr14:33816791-33820242 | 2.12568 | 9.39992 | 4.4220767 | 2.08E-06 | ENSDARG00000036292 |
| *wdr3* | WD repeat domain 3 | protein binding | chr9:21887239-21905910 | 0 | 4.37204 | 4.37204 | 1.03E-06 | ENSDARG00000011079 |
| *smo* | smoothened homolog (*Drosophila*) | determination of left/right symmetry, neural crest cell migration, forebrain dorsal/ventral pattern formation, canonical Wnt receptor signaling pathway | chr4:14036631-14045329 | 0.986768 | 4.06843 | 4.122985342 | 5.31E-06 | ENSDARG00000002952 |
| *gmds* | GDP-mannose 4,6-dehydratase | Notch signaling pathway, retina layer formation, nucleotide binding | chr20:26738616-26852157 | 22.635 | 58.7267 | 2.594508505 | 0.001747 | ENSDARG00000026629 |
| *pbx4* | pre-B-cell leukemia transcription factor 4 | neural crest cell migration, brain development, neuron differentiation, axon guidance, skeletal muscle fiber development | chr3:53638912-53714493 | 10.2667 | 26.0065 | 2.533092425 | 0.0095533 | ENSDARG00000052150 |
| *wdr55* | WD repeat domain 55 | protein binding, eye development | chr21:33780748-33801083 | 0 | 2.46021 | 2.46021 | 1.05E-05 | ENSDARG00000007217 |
| *tfap2a* | transcription factor AP-2 alpha | neural crest cell development, neural crest cell fate specification, skeletal system development | chr24:8521274-8532116 | 12.5074 | 25.5409 | 2.042063099 | 0.0035542 | ENSDARG00000059279 |
| | | | | | | | | |
| *atp1a1* | ATPase, Na+/K+ transporting, alpha 1 polypeptide | nucleotide binding, ATP binding, ATPase activity | chr1:1468926-1550157 | 11.4624 | 0.838468 | -13.6706469 | 4.47E-07 | ENSDARG00000001870 |
| *ctnnb1* | catenin (cadherin-associated protein), beta 1 | dorsal/ventral pattern formation, patterning of blood vessels, canonical Wnt receptor signaling pathway, positive regulation of fibroblast growth factor receptor signaling pathway | chr16:7435502-7458987 | 39.9316 | 3.55134 | -11.2440938 | <0.001 | ENSDARG00000014571 |
| *gnl3* | guanine nucleotide binding protein-like 3 (nucleolar) | neural retina development, regulation of neuron differentiation, nucleotide binding | chr11:4021604-4033144 | 6.54712 | 0.596306 | -10.9794636 | 2.24E-12 | ENSDARG00000006219 |
| *wdr33* | WD repeat domain 33 | protein binding | chr2:5053651-5086066 | 6.59429 | 0.625539 | -10.5417728 | 0.000971 | ENSDARG00000077264 |
| *vangl2* | vang-like 2 (van gogh, *Drosophila*) | Wnt receptor signaling pathway, striated muscle cell development, neuron migration, embryonic eye morphogenesis | chr7:6171587-6218979 | 1.7066 | 0.171456 | -9.95357409 | 1.45E-07 | ENSDARG00000027397 |
| *sec23a* | Sec23 homolog A (*S. cerevisiae*) | cartilage development, pectoral fin morphogenesis | chr17:10455926-10510720 | 6.78189 | 1.12709 | -6.01716811 | 2.77E-09 | ENSDARG00000016636 |
| *nrp1a* | neuropilin 1a | axon guidance, vascular development, angiogenesis | chr24:1172123-1331189 | 63.4108 | 15.5351 | -4.08177611 | 0.0007497 | ENSDARG00000071865 |
| *wdr43* | WD repeat domain 43 | protein binding, vasculogenesis, angiogenesis | chr17:24649784-24663840 | 3.49641 | 0 | -3.49641 | 5.72E-05 | ENSDARG00000018272 |

Table 3. This table lists several genes not among the top 20 up- or downregulated in chd7MOs, but supporting our previous studies or other studies in the primary literature. It gives information about the gene, its Ensembl gene ID, the FPKM values determined as a result of our RNA-Seq analysis, the fold change in gene expression and the p-value.

# Using whole mount *in situ* hybridization to link molecular and organismal biology

**Nicole L. Jacobs[1], R. Craig Albertson[1], Jason R. Wiles[1, 2]**

Affiliation: [1]Department of Biology, Syracuse University

[2]Department of Science Education, Syracuse University

**ABSTRACT**

Whole mount *in situ* hybridization (WISH) is a common technique in molecular biology laboratories used to study gene expression through the localization of specific mRNA transcripts within whole mount specimen. This technique (adapted from Albertson and Yelick, 2005) was used in an upper level undergraduate Comparative Vertebrate Biology laboratory classroom at Syracuse University. The first two thirds of the Comparative Vertebrate Biology lab course gave students the opportunity to study the embryology and gross anatomy of several organisms representing various chordate taxa primarily via traditional dissections and the use of models. The final portion of the course involved an innovative approach to teaching anatomy through observation of vertebrate development employing molecular techniques in which WISH was performed on zebrafish embryos. A heterozygous *fibroblast growth factor 8 a* (*fgf8a*) mutant line, *ace,* was used. Due to Mendelian inheritance, *ace* intercrosses produced wild type, heterozygous, and homozygous *ace/fgf8a* mutants in a 1:2:1 ratio. RNA probes with known expression patterns in the midline and in developing anatomical structures such as the heart, somites, tailbud, myotome, and brain were used. WISH was performed using zebrafish at the 13 somite and prim-6 stages, with students performing the staining reaction in class. The study of zebrafish embryos at different stages of development gave students the ability to observe how these anatomical structures changed over ontogeny. In addition, some *ace/fgf8a* mutants displayed improper heart looping, and defects in somite and brain development. The students in this lab observed the normal development of various organ systems using both external anatomy as well as gene expression patterns. They

also identified and described embryos displaying improper anatomical development and gene expression (i.e., putative mutants).

For instructors at institutions that do not already own the necessary equipment or where funds for lab and curricular innovation are limited, the financial cost of the reagents and apparatus may be a factor to consider, as will the time and effort required on the part of the instructor regardless of the setting. Nevertheless, we contend that the use of WISH in this type of classroom laboratory setting can provide an important link between developmental genetics and anatomy. As technology advances and the ability to study organismal development at the molecular level becomes easier, cheaper, and increasingly popular, many evolutionary biologists, ecologists, and physiologists are turning to research strategies in the field of molecular biology. Using WISH in a Comparative Vertebrate Biology laboratory classroom is one example of how molecules and anatomy can converge within a single course. This gives upper level college students the opportunity to practice modern biological research techniques, leading to a more diversified education and the promotion of future interdisciplinary scientific research.

**PROTOCOL TEXT- Plasmid Transformation of Target cDNA**

Part I: Transformation of Plasmid

(Time Required: 3 hours plus overnight incubation)

1) Warm SOC nutrient broth in a 42°C water bath (500 µl per reaction)
2) Thaw competent cells on ice
3) Add 1 µl plasmid to 25 µl competent cells
4) Place on ice for 20 minutes
5) Heat shock cells in 42°C water bath for 45 seconds
6) Immediately place cells on ice for 2 minutes
7) Add 500 µl of 42°C nutrient broth to each vial of cells
8) Shake at 37°C for 2 hours at 255 rotations per minute (rpm)
9) Plate 75 µl transformation mix on Luria Bertani (LB) agar plates
10) Incubate plates inverted at 37°C overnight

Part II: *E. coli* Culture

(Time Required: 15 minutes plus overnight incubation)

1) For each reaction, aliquot 3 ml LB broth and 3 µl of 50 mg/ml ampicillin into a culture tube
2) Scrape 1 bacteria colony from the agar plate and add to each culture tube
3) Shake culture tubes at 37°C at 255 rpm overnight

Part III: Plasmid Prep

(Time Required: 1.5 hours)

1) Isolate plasmid from overnight cultures using the 5 Prime FastPlasmid Mini Kit (Catalog #2300000)
2) To check for the presence of prepared plasmid, run the DNA eluted from the kit on a 1% Tris-Acetate-EDTA (TAE) gel stained with ethidium bromide

**PROTOCOL TEXT- *In situ* DIG-labeled RNA Probe Synthesis**

Part I: Linearization of Plasmid

(Time Required: 2.5 hours)

1) In a 1.5 ml microfuge tube, combine:

| | |
|---|---|
| Prepared Plasmid | 20 µl |
| Restriction Enzyme* | 2 µl |
| Buffer** | 10 µl |
| 10X Bovine Serum Albumin (BSA) | 10 µl |
| Diethyl Pyrocarbonate (DEPC) Water | 58 µl |
| | 100 µl |

2) Incubate at 37°C for 2 hours

*Varies with plasmid

**Varies with restriction enzyme

Part II: Transcription

(Time Required: 3 hours)

1) In a 1.5 ml microfuge tube, combine:

| | |
|---|---|
| Linear Plasmid | 4 µl |
| 10X Transcription Buffer** | 4 µl |
| Digoxigenin Label Mix | 4 µl |
| Polymerase* | 2 µl |
| RNase Inhibitor | 2 µl |
| DEPC Water | 24 µl |
| | 40 µl |

2) Incubate at 37°C for 1 hour

3) Add 2 µl of polymerase*

4) Incubate at 37°C for 1 hour

5) Add 2 µl of DNase

6) Incubate at 37°C for 20 minutes

*Varies with plasmid

**Varies with polymerase

Part III: Precipitation

(Time Required: 5 minutes plus 2 hour to overnight incubation, 1 hour to centrifuge and re-suspend)

1) Add 4 µl of 0.2M EDTA

2) Add 5 µl of 4M lithium chloride

3) Add 150 µl of ice cold 100% ethanol

4) Incubate at -80°C for 2 hours to overnight

5) Centrifuge at 14,000 rpm for 30 minutes at 4°C, decant away supernatant

6) Dry pellet for 7 minutes

7) Re-suspend in 20 µl DEPC water

8) Incubate at 37°C for 5 minutes

Part IV: Fractionation - Perform only if probe size is greater than 0.6 kb

(Time Required: Varies based on probe size, usually no more than 20 minutes)

1) In a 1.5 ml microfuge tube, combine:

| | |
|---|---|
| RNA Probe | 20 µl |
| DEPC Water | 12 µl |
| Sodium Bicarbonate | 4 µl |
| Sodium Carbonate | 4 µl |
| | 40 µl |

2) Incubate in a 60°C water bath. Base the incubation time on the equation:

Time (min.) = (starting kb – desired kb) / (.11 x starting kb x desired kb)

Average desired size = 0.6 kb

Part V: Final Precipitation

(Time Required: 5 minutes plus 2 hour to overnight incubation, 1 hour to centrifuge and re-suspend, 1 hour for gel electrophoresis)

1) Add 40 µl DEPC water

2) Add 8 µl Sodium Acetate

3) Add 1.04 µl Glacial Acetic Acid

4) Add 240 µl ice cold 100% ethanol

5) Incubate at -80°C for 2 hours to overnight

6) Centrifuge at 14,000 rpm for 30 minutes at 4°C, decant away supernatant
7) Dry pellet for 7 minutes
8) Re-suspend in 20 µl DEPC water
9) Vortex to mix
10) To check for the presence of riboprobe, run the re-suspended solution on a 1% TAE gel stained with ethidium bromide

**PROTOCOL TEXT- Whole Mount *In situ* Hybridization**

Part I: Fixation of Embryos and Proteinase K Digestion

(Time Required: Fix overnight plus 4 hours the next day for storage, 2.5 hours from storage to Part II)

1) Collect staged zebrafish embryos and fix in 4% paraformaldehyde (PFA) overnight at 4°C
2) Wash fixed embryos in phosphate buffered saline containing 0.1% Tween-20 (PBSt) 3 times for 10 minutes each
3) To ensure exposure of the embryos to the experimental reagents, manually dechorionate embryos (if necessary) using fine-tipped forceps
4) Dehydrate embryos by washing in a graded series of 25% and 50% methanol in PBSt for one hour each wash, then store in 100% methanol at -20°C
5) When ready to use, rehydrate embryos in PBSt by washing in 50% (2 times) and 25% (1 time) methanol in PBSt for 10 minutes each. Finally wash 2 times for 10 minutes each in 100% PBSt. Exact timing is not important for PBSt/methanol washes

6) Bleach embryos in a 10% hydrogen peroxide solution in PBSt, if necessary, to remove dark pigments. Embryos should incubate in hydrogen peroxide solution for 10-20 minutes, depending on the age of the embryo, and the cap of the microfuge tube should remain open to prevent build-up of air pressure
7) Digest embryos with 50 mg/ml Proteinase K diluted 1:5000 in PBSt for 3-15 minutes, depending on the age of the embryo
8) Re-fix embryos in 4% PFA for 30 minutes, and then wash 3 times in PBSt for 5 minutes each

Part II: Hybridization of Riboprobes

(Time Required: 3 hours plus overnight for hybridization, 1.5 hours the next day to Part III)

9) Prehybridize embryos with prehybridization solution (PHS) in a preheated 70°C water bath for 2-3 hours
10) Remove PHS, add 0.5 ml hybridization solution and 1.5 µl previously synthesized Digoxigenin labeled riboprobes, incubate at 70°C overnight. Temperature can fluctuate within a few degrees depending on the riboprobe target
11) The next day, wash embryos at 70°C in graded solutions of 75%, 50%, and 25% PHS in 2X saline-sodium citrate (SSC) for 10 minutes each, then wash in 0.2X SSC for 30 minutes at 68°C
12) Wash in Maleic Acid Buffer (MAB) 2 times for 10 minutes each at room temperature

Part III: Anti-Digoxigenin (α-DIG) Antibody Incubation

(Time Required: 3 hours plus overnight to block, 2.5 hours the next day to Part IV)

13) Transfer embryos to a 12 well plate
14) Pre-block embryos in 1-2 ml blocking solution for at least 3 hours at room temperature
15) Simultaneously, pre-block the antibody by preparing a second volume of blocking solution and diluting the anti-digoxigenin antibody 1:2000 in this solution
16) Remove pre-block and add 1-2 ml pre-blocked α-DIG solution, incubate overnight at 4°C
17) The next day, wash embryos in MAB. Allow the embryos to incubate in MAB for 5 minutes first, then perform buffer changes and incubate for two 10 minute, one 30 minute and one 60 minute interval. Exact timing is not necessary
18) Wash embryos 3 times for 5 minutes each in Alkaline Phosphatase (AP) buffer

Part IV: Staining and Final Processing

(Time Required: 1 hour to overnight for staining, depending on the riboprobe used, 4 hours to beginning of glycerol washes, 6-10 hours per glycerol wash, may be stored in glycerol)

19) Add 1-2 ml staining solution to the embryos, wrap the plate in foil, and check staining at regular intervals (about every 20 minutes) until staining is sufficient
20) Wash embryos with PBSt 2 times for 5 minutes each to stop the staining reaction
21) Dehydrate embryos using 10 minute washes in 25% (1 time) and 50% (2 times) methanol in PBSt, then in 100% methanol, to remove background staining

22) Allow embryos to incubate in 100% methanol for at least 2 hours at room temperature
23) Rehydrate in PBSt using 10 minute washes in 50% (2 times) and 25% (1 time) methanol in PBSt, then wash in 100% PBSt 2 times
24) Transfer stained embryos to an 80% glycerol solution in PBSt, using a graded series of washes, and store at 4°C.

**RECIPES**

LB agar plates- 10 g LB agar + 250 ml distilled water, autoclave, when cool to the touch add 250 µl ampicillin, pour 15-20 ml warm solution into each petri dish, allow agar to solidify

LB broth- 12.5 g LB Broth + 200 ml distilled water, autoclave, allow to cool before use

1% TAE gel- 0.4 g agarose, 40 ml 1X TAE, 2 µl ethidium bromide; load 7 µl plasmid (Plasmid Transformation of Target cDNA) or 3 µl riboprobe and 4 µl DEPC water (*In situ* DIG-labeled RNA Probe Synthesis) + 1 µl loading dye, 5 µl DNA ladder

Prehybridization solution- 50% formamide, 5X SSC, 9.2mM citric acid, 1% Tween-20

Hybridization solution- prehybridization solution plus 500 µg/ml tRNA and 50 µg/ml Heparin

MAB- 100mM Maleic Acid, 150mM NaCl, 0.2M NaOH, 0.1% Tween-20, pH to 7.5

Blocking Solution- 3 parts MAB, 1 part 10% Boehringer blocking reagent in MAB, 1 part heat deactivated lamb serum

AP buffer- 60mM Tris-HCl pH to 9.5, 60mM NaCl, 30mM $MgCl_2$, 0.1% Tween-20

Staining Solution- 5-Bromo-4-chloro-3-indolyl phosphate (BCIP) and Nitro blue tetrazolium (NBT) in AP buffer

**REPRESENTATIVE RESULTS**

When performed correctly, the reaction between the NBT, BCIP, and alkaline phosphatase will form a purple precipitate that should appear on the zebrafish embryo as a purple stain. Riboprobes should be previously synthesized from cDNA corresponding to the gene of interest. Therefore, it can be concluded any stain visualized represents areas of the zebrafish in which the gene of interest has been transcribed at that particular developmental stage. For the purposes of this course, riboprobes were synthesized from *aldh1a2* (previously *raldh2*; Begemann et al., 2001; Figure 1); *fgf8a* (Reifers et al., 1998; Figure 2); *deltaC* (Oates et al., 2005); *myod1* (Weinberg et al., 1996); *shha* (Krauss et al., 1993), *pax2a* (Brand et al., 1996; Figure 3) and *myl7* (previously *cmlc2*; Yelon et al., 1999) cDNA. Staining was expected in the midline and in anatomical structures including the somites, tailbud, myotome, brain, and heart. *Ace/fgf8a* mutants were expected to have defects in many of these structures. Staining was easily visualized using a standard dissecting microscope. Additional sources contain more information and troubleshooting on WISH techniques similar to those described here (Clark, 2003; D'Costa et al., 2009; Schmoldt et al., 2009; Schoenwolf, 2009).

**DISCUSSION**

WISH was used in a Comparative Vertebrate Biology laboratory course to help students understand the roles of genetics in anatomical development through the visualization of known gene expression patterns. For the first part of the course, students performed dissections on organisms representing several different chordate taxa, allowing them ample time to study, understand, compare, and contrast vertebrate anatomy.

As an introduction to the second part of the course, students were given a formal lecture describing zebrafish development and anatomy. The methods and expected results of the WISH experiment were also discussed. Students were then given live zebrafish at somitogenesis and prim-6 stages of development, and at 2 and 5 days post fertilization (dpf) to examine under the dissecting microscope. This was to give students a better understanding of what zebrafish embryos look like and the types of morphological changes that occur over ontogeny.

In the next laboratory session, students were given zebrafish embryos in which WISH had been previously performed. They were asked to study and describe the gene expression patterns for each gene of interest (riboprobe used). Embryos used for WISH were derived from matings between members of a heterozygous *ace/fgf8a* line. Based on Mendelian inheritance, 25% of the embryos from the *ace/fgf8a* matings were expected to be homozygous mutants and to exhibit defects in many of the anatomical structures focused on in this course. Based on published reports and unpublished observations in the Albertson lab, defects in the brain and improper heart looping were expected, as well as defects in the somites (Brand et al., 1996; Albertson and Yelick, 2005; personal observations).

Students were asked to examine all specimens, wild type (heterozygous animals are indistinguishable from wild type siblings at early stages of development) and homozygous mutants, for each gene expression pattern presented. They were then asked to write lab reports describing their results, and based on their knowledge of anatomy and genetics, how defective gene expression may have precipitated anatomical malformations.

Students seemed to receive this laboratory exercise with excitement and curiosity. Most had never used WISH before and were extremely interested in this part of the course. Students found the different patterns of gene expression in the zebrafish embryos intriguing, some even described the staining patterns visualized by associating them with well-known designs and symbols, such as a smiley face. The resulting lab reports showed the students had a general understanding of the WISH protocol and the expression of genes in specific anatomical structures. Students were also required to understand the specific functions of the genes studied using WISH during the lab, including genes involved in Wnt signaling and members of the somitogenesis pathway (Stickney et al., 2000; Huelsken et al., 2002; Geetha-Loganathan et al., 2008a; Geetha-Loganathan et al., 2008b). It was evident however, that certain students had limited background knowledge of the signaling pathways and genes of interest. More information about these concepts in the WISH introductory lecture may be a welcome addition to the use of WISH in future Comparative Vertebrate Biology courses.

Since the protocol generally takes four consecutive days, depending on the schedule of the course, students may only be able to complete a part of the experiment in class and the instructor must be responsible for the remainder. In our Comparative

Vertebrate Biology class, students completed the staining reactions in the laboratory, while the Teaching Assistant performed all preceding steps. If it is preferred to have the students perform WISH in class, the protocol may be divided into subunits that can be performed over several laboratory sessions, depending on the time frame of the class. If it is not feasible for students to perform the entire protocol, as it was here due to the lab meeting only once a week, students can add the staining solution at the beginning of class and, depending on the riboprobe used, have the staining complete within an hour. The time it takes for the stain to develop varies greatly with each riboprobe and a variety of experimental conditions, and should be predetermined before class. Notably, if students will only be developing the stain in lab, instructors will be responsible for all preceding steps, which will require significant time and effort outside of the classroom. If desired, a shorter alternative to WISH could be immunohistochemistry, using antibody labels to visualize protein localization, however at this time, zebrafish-specific antibodies for developmental genes are not readily available. Another option would be to perform WISH on different vertebrate species and have the students compare the expression patterns of the same genes in different organisms (Pizard et al., 2004; Aramaki et al., 2007; Emerging Model Organisms, 2008; Emerging Model Organisms, 2010).

The overarching goal of using WISH in a Comparative Vertebrate Biology course was to demonstrate to students how molecular biological techniques are used to study anatomical development. It also provided an opportunity for students to speculate as to how altered gene expression may lead not only to developmental malformations but also to evolutionary change. Formalized as evolutionary developmental biology (often referred to as "evo-devo"), this rapidly growing field of study aims to link genotype and

phenotype through development, and to elucidate potential mechanistic bases of evolutionary change. With the rise of this field, more ecologists, organismal biologists, and physiologists are employing molecular techniques in their research. We contend that the use of WISH in a Comparative Vertebrate Biology course will help to keep the curriculum up to date with current technological and conceptual advances in research, and to facilitate a better horizontal alignment of upper level biology courses by combining biological subfields. Moreover, this integrative approach will provide students the opportunity to learn an assortment of biological research techniques in one course, leading to a more diversified education and the promotion of future interdisciplinary scientific research.

**ACKNOWLEDGEMENTS**

The authors would like to acknowledge the Department of Biology at Syracuse University and Dr. Marilyn Kerr for their roles in the administration of the Comparative Vertebrate Biology course. The Albertson lab is supported by grant R21DE019223 from the National Institutes of Health/National Institute of Dental and Craniofacial Research, as well as grant R01AG031922 from the National Institutes of Health/National Institute on Aging.

**FIGURES**

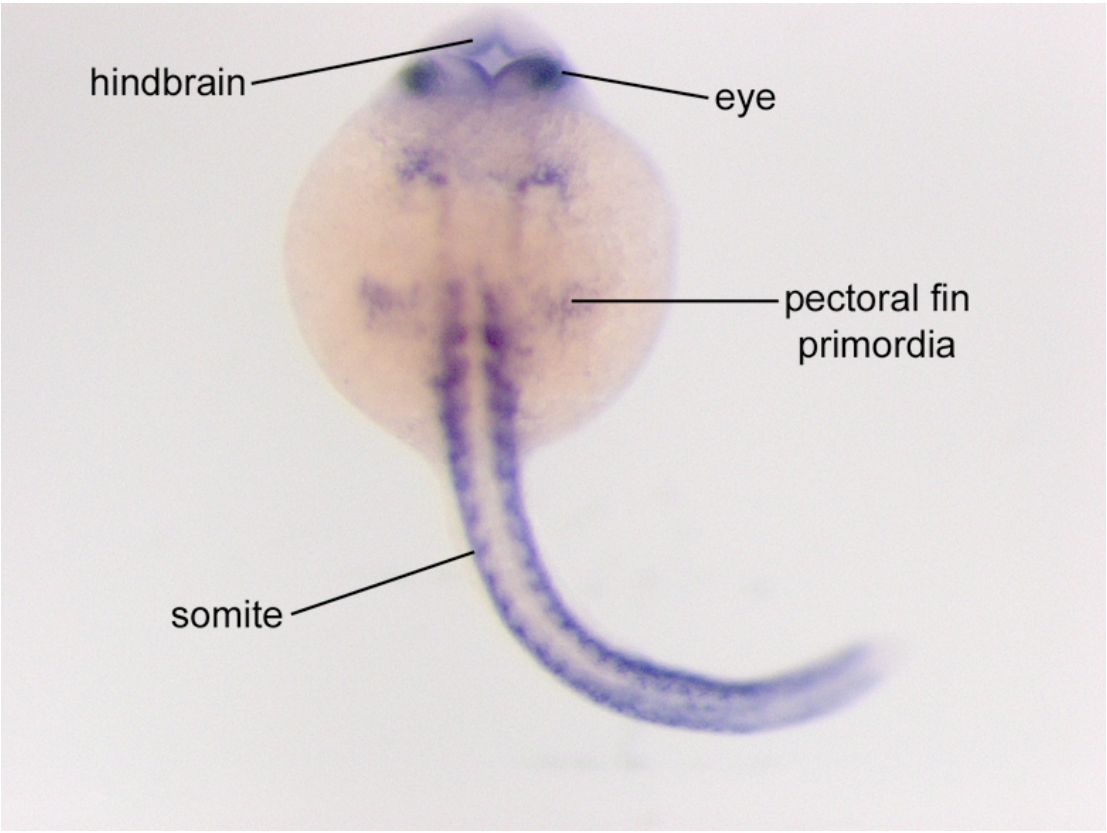


**Figure 1.** A zebrafish embryo 24 hours post fertilization, which has been hybridized with riboprobes specific for *aldh1a2*. Specific staining can be seen in the eyes, hindbrain, pectoral fin primordia, and somites. Anterior is to the top, posterior is to the bottom.

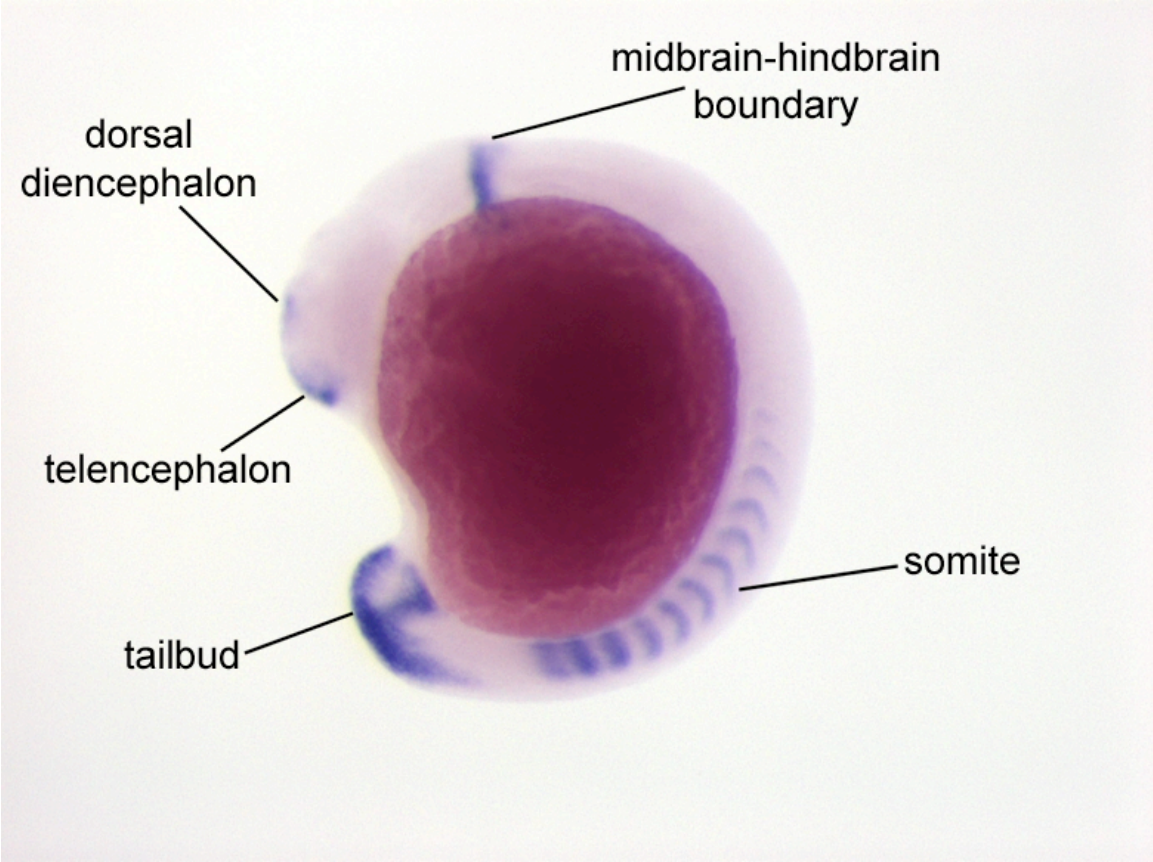


**Figure 2.** A zebrafish embryo at the 13 somite stage of development that has been hybridized with a probe specific for *fgf8a.* Specific staining is seen in the telencephalon, dorsal diencephalon, midbrain-hindbrain boundary, somites, and tailbud. Ventral is to the left, dorsal is to the right.

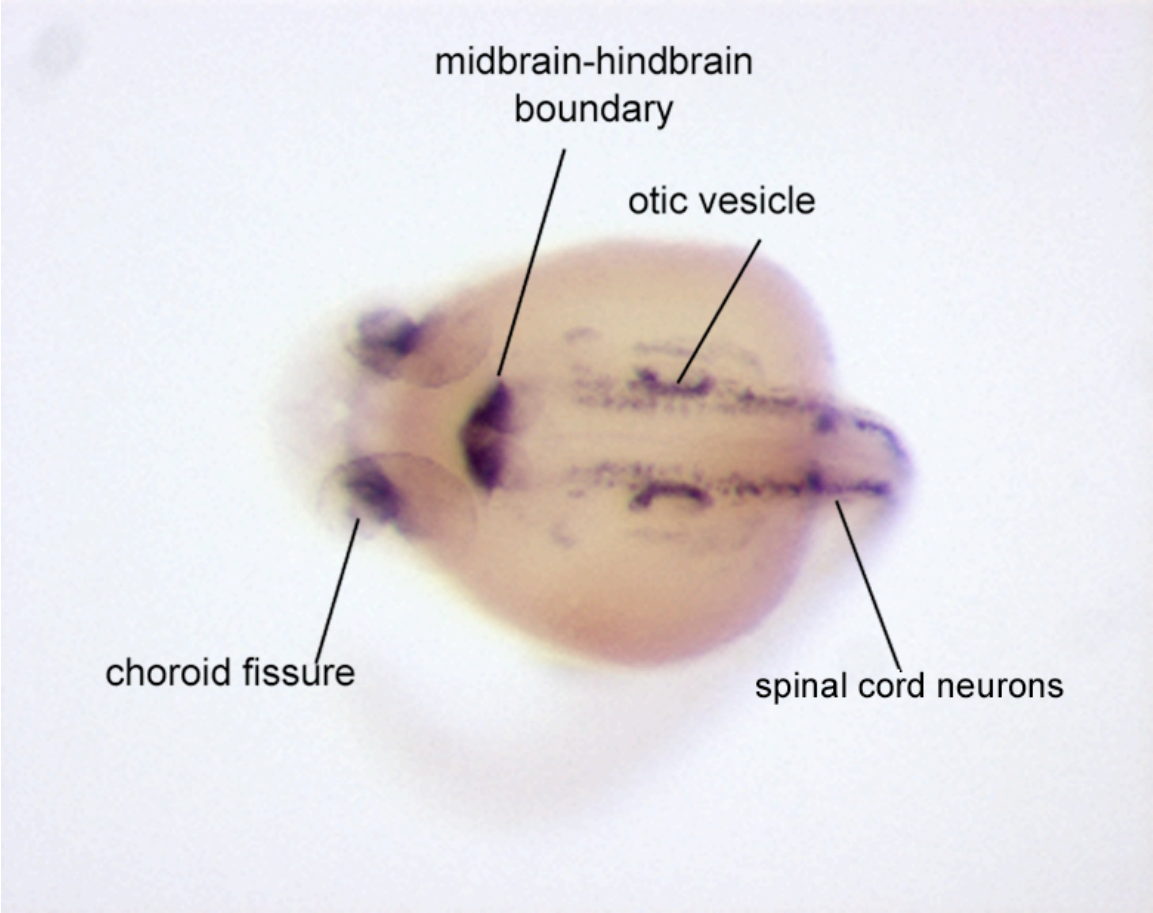


**Figure 3.** A 22 hours post fertilization zebrafish embryo that has been hybridized with a riboprobe specific for *pax2a*, a robust marker useful for visualizing the nervous system. Specific staining can be seen in the choroid fissure, midbrain-hindbrain boundary, otic vesicle, and spinal cord neurons. Dorsal view with anterior to the left.

**TABLE OF REAGENTS**

| Vender | Item # | Description |
|---|---|---|
| Fisher | 2300000 | 5 Prime Fast Plasmid Mini Kit (100 preps) |
| Invitrogen | C404003 | One Shot® TOP10 Chemically Competent *E. coli* with SOC Medium |
| Fisher | BP1425-500 | LB Agar |
| Fisher | BP1426-500 | LB Broth |
| Fisher | BP1760-5 | Ampicillin Sodium Salt |
| Acros | 42383-0010 | Isopropanol |
| Laboratory Products Sales | 430591 | Petri Dish 100 x 20 mm non treated |
| Fisher | 1495911B | 14 ml Culture Tube, Snap Top |
| New England Bio Labs | varies | Restriction Enzymes & Buffers & 10xBSA |
| Sigma | D5758-25mL | Diethyl Pyrocarbonate (DEPC) 25 ml |
| Fisher | s608500 | Sodium Acetate Trihydrate USP/FCC 500g |
| Fisher | 04-355-451 | Gal 200 proof Ethyl alcohol |
| Fisher | bp13321 | Tris-Acetate-EDTA (TAE) 50x Sol 1L |
| Fisher | BP160-100 | Agarose Low EEO 100 g |
| Sigma | 45-E1510 | Ethidium Bromide 10 ml |
| Fisher | BP655-1 | Sucrose Gel Loading Dye 40% Sucrose |
| Fisher | BP2582200 | 1 kb Full Scale DNA Ladder |
| Roche | 11277073910 | DIG RNA Labeling Mix |
| Roche | 1031163 | T3 RNA Polymerase |
| Roche | 10881767001 | T7 RNA Polymerase |
| Roche | 810274 | SP6 RNA Polymerase |
| Roche | 3335399001 | Protector Rnase Inhibitor |
| Roche | 4716728001 | Dnase I, Rnase Free 10,000 units |
| Sigma | e5134-500G | EDTA molecular biology reagent |
| Fisher | L121100 | Lithium Chloride 100 g |
| Fisher | BP357-1 | Sodium Carbonate 1 kg |
| Fisher | BP328-500 | Sodium Bicarbonate, 500 g |
| Fisher | a38500 | Acetic Acid glacial ACS 500 ml |
| Fisher | o4042500 | Paraformaldehyde R 500 g |
| Fisher | bp3991 | PBS Phosphate Buffer Saline 10X |
| Fisher | bp337500 | Tween 20 500 ml |
| Fisher | A4124 | Methanol 5 L |
| Fisher | bp170050 | Proteinase K 50 mg |
| Fisher | F841 | Formamide 1 L |
| Fisher | bp13251 | 20x SSC 1 L |
| Fisher | a940500 | Citric Acid Anhydrous ACS 500 g |
| Sigma | r7876-2.5KU | Ribonucleic acid transfer type V |
| Fisher | bp252450 | Heparin Sodium salt 50 mg |
| Fisher | o3417500 | Maleic acid R 500 g |
| Fisher | s271500 | Sodium Chloride 500 g |
| Fisher | s318500 | Sodium Hydroxide 500 g |
| Roche | 11096176001 | Blocking Reagent |
| Invitrogen | 16070096 | Lamb Serum 500 ml |

| | | |
|---|---|---|
| Roche | 11093274910 | Anti DIG AP fragments |
| Fisher | bp1759500 | 2M Tris Solution 500 ml |
| Fisher | m33500 | Magnesium Chloride 500 g |
| Roche | 11383221001 | BCIP 3 ml |
| Roche | 11383213001 | NBT 3 ml |
| Fisher | AC158920025 | Glycerol 99% 2.5 L |
| VWR | 62406-165 | Plate 12 well PS ST w/Lid |
| Laboratory Products Sales | L262861 | Tube 15 ml screw cap 50/rack 500/cs |
| Laboratory Products Sales | L262890 | Tube 50 ml screw cap 25/rack 500/cs |
| Laboratory Products Sales | L234401 | 1.6 ml microfuge tube |
| Fisher | s37441 | 2 Parafilm 2" x 250 ft |
| USA Scientific | 1020-2520 | Transfer Pipet 7 ml |
| USA Scientific | 1111-3000 | .1-10 µl Pipet Tip, Bulk |
| USA Scientific | 1111-0006 | 1-200 µl Pipet Tip, Bulk |
| USA Scientific | 1111-2021 | 101-1000 µl Pipet Tip, Bulk |
| Grocery Store | | Aluminum Foil |

**EQUIPMENT**

Autoclave
Micro-centrifuge
37°C incubator (with shaker)
4°C micro-centrifuge
Water bath
Vortex
Gel electrophoresis apparatus
-20°C freezer
-80°C freezer
Rocker/shaker
4°C refrigerator
Dissecting microscope (preferably with a teaching screen or camera)

The video based on Chapter 4, *Using whole mount in situ hybridization to link molecular and organismal biology*, can be found at:

http://www.jove.com/video/2533/using-whole-mount-in-situ-hybridization-to-link-molecular-and-organismal-biology

# Using model organisms in an undergraduate laboratory to link genotype, phenotype, and the environment

**Nicole L. Jacobs-McDaniels[1, 2], Eleanor M. Maine[1], R. Craig Albertson[1, 3], Jason R. Wiles[1, 4]**

Affiliation: [1]Syracuse University, Department of Biology

[2]Herkimer County Community College, Science Department

[3]University of Massachusetts Amherst, Biology Department

[4]Syracuse University, Department of Science Education

**ABSTRACT**

We developed laboratory exercises using zebrafish (*Danio rerio*) and nematodes (*Caenorhabditis elegans*) for a sophomore-level Integrative Biology Laboratory course. Students examined live wildtype zebrafish at different stages of development and noted shifts occurring in response to *fgf8a* deficiency. Students were introduced to development in other fish species to demonstrate how variation in developmental systems affects phenotype. Finally, students cultured *glp-1(bn18ts) C. elegans* mutants under different conditions to illustrate how the environment and genetics act concurrently to modulate development. Undergraduate students responded positively to both the fish and *C. elegans* laboratory modules. These novel laboratory exercises are intended to promote an integrative view of biology and to help prepare undergraduate students for independent research with faculty.

**INTRODUCTION**

For decades, model organisms have been used to study a host of biological questions, and these invaluable living crucibles will likely continue to be staple tools of research in the life sciences for years to come (Fields and Johnston, 2005). Historically speaking, model organisms tend to be small, inexpensive, short-lived, and easy to maintain in the lab. More recently, well-established laboratory methods have been developed to facilitate the manipulation and study of their genomes. For these reasons, model organisms are also quite well suited for teaching biological concepts and laboratory skills to undergraduate students.

The list of important and extensively studied model organisms is growing, and now includes such familiar species as the fruit fly, *Drosophila melanogaster*, probably the most popular model organism and a symbol for scientific study; various types of bacteria including the commonly recognized *Escherichia coli*; the budding yeast, *Saccharomyces cerevisiae*; *Arabidopsis thaliana,* a member of the mustard plant family; the nematode, *Caenorhabditis elegans*; the zebrafish, *Danio rerio;* the African clawed frog, *Xenopus laevis*; and the house mouse, *Mus musculus*. Many teaching laboratory activities have been described using model organisms as specimen (see Table I).

It is true, of course, that due to timing and budgetary constraints, it can be difficult to use more complex model organisms, such as mice, in the classroom, especially if facilities are not readily available. Moreover at most colleges and universities it is necessary to obtain permission for the use of live organisms in the classroom, particularly mammals and other vertebrates, and all students may be required to complete training prior to working with animals. These requirements will vary depending on the institution

and the type of organism, but they should be taken into consideration when planning laboratory activities. Nevertheless, many model organisms can be employed quite readily, and for undergraduate students, learning techniques involving such organisms may help prepare them to conduct independent research under faculty supervision.

**A "two model" approach to teaching about genes vs. environment**

Here we describe several laboratory activities designed to target sophomore level undergraduates, focusing on two model species, zebrafish (*Danio rerio*) and a nematode (*Caenorhabditis elegans*). Along with fostering student acquisition of laboratory skills as well as data organization and analysis, we designed exercises with the aim of helping students to better understand and appreciate how the genome and environment interact to influence organismal development. These exercises were a part of a one semester Integrative Biology Laboratory course at Syracuse University.

Prior to using model organisms in the classroom, it is important that students are first familiarized with a basic understanding of (1) animal development, (2) gene logic, (3) molecular and cytochemical techniques, and (4) animal husbandry. This will help to facilitate proper understanding of underlying concepts and execution of laboratory procedures.

## METHODOLOGY

### Model organism 1: zebrafish

Before working with zebrafish in the lab, our students were introduced to general embryology. This included how development is orchestrated by organizers such as Hensen's Node, the Zone of Polarizing Activity and the Apical Ectodermal Ridge; morphogens such as Bone Morphogenic Proteins; and morphogenic fields. Then students were introduced specifically to the zebrafish life cycle and stages of embryonic development (Kimmel et al., 1995). This information was conveyed during weekly lectures, which were meant to provide a basic background and conceptual framework for each week's laboratory.

During the lecture sessions, students were presented with the idea that animals share a related set of developmental genes known as the developmental "toolkit" (Carroll et al., 2005). Toolkit genes are usually transcription factors, or members of signal transduction pathways, which regulate the expression of other genes, thereby controlling many important developmental processes. Key toolkit genes discussed in class were members of the *hox* gene family, *bicoid*, *nanos*, *pax6*, and *fgf24*. During lectures and in-class discussions, students built their pre-lab understanding of the roles of the developmental toolkit in regulating both animal development as well as the evolution of animal form. The aims of these presentations and discussions were to (1) discuss how development produces a complex, multi-cellular organism from a single-cell zygote, and (2) working within this framework, to explain how the developmental program has been shaped via natural selection to produce diversity in animal form.

At the beginning of each lab, another short lecture was given to reinforce the

information that had been previously presented about the study organism, provide additional background information (e.g., on a specific protein or signal transduction pathway), and describe salient methods and techniques. During the zebrafish module, lab activity introductions included the techniques used and how to handle and care for zebrafish both during experiments and as a part of an animal facility.

The first zebrafish laboratory activity focused on guided observations wherein students examined wildtype zebrafish (Fig. 1 A) at different stages of embryonic development. Using copies of a staging chart presented during the lecture, students were asked to determine which stage of development was represented by the embryos they observed. Students were required to draw and describe the embryos in their notebooks for later reference and to annotate their illustrations to indicate specific tissues, organs and structures present at each stage of development.

Next, to prepare for the lab activity, students were introduced to fibroblast growth factor (FGF) signaling. Of particular focus for our activity was the zebrafish line containing an *fgf8* mutation, named *acerebellar,* or "*ace*" because mutants show a loss of the cerebellum (Reifers et al., 1998). To demonstrate the genetic regulation of development in zebrafish, we presented students with embryos resulting from a cross between zebrafish heterozygous for the *fgf8a* mutation. Another major phenotype that results from the loss of *fgf8a* activity in zebrafish is the reduction and often asymmetric development of bones and cartilages that are normally found to be symmetric (Albertson and Yelick, 2005). Based on the Mendelian inheritance of the mutation, approximately one fourth of the resulting offspring were wildtype, one half were heterozygous mutants, and one fourth were homozygous mutants. These embryos were allowed to grow for 6

days, and then bone was stained with Alizarin Red (Sigma-Aldrich) and cartilage was stained with Alcian Blue (Sigma-Aldrich; Fig. 1 B). These are relatively short, simple, and straightforward procedures requiring minimal materials (see [Walker and Kimmel, 2007] for a full description of materials and methods).

With cartilage stained blue and bone stained red in their larval specimens, students could easily visualize developing skeletal structures and differentiate cartilage from bone. Students were encouraged to discriminate between bone and cartilage development in mutant versus wildtype larvae. *Fgf8a* homozygous mutants are also characterized by pericardial edema, a swelling around the heart. Although this phenotype is most likely due to circulation problems and is an indirect effect of the *fgf8a* mutation, it is dramatic, obvious, and easily captures the students' attention. Other potential phenotypes that are easy to observe and quantify by undergraduates include heart rate and the frequency of spontaneous twitching by embryos (both lower in mutant animals).

Students recorded their observations in their notebooks and were then asked to speculate probable functions of *fgf8a* during zebrafish development based on their observations. This exercise was used to help students link genotype to phenotype by demonstrating that changes in the genetic sequence of an individual organism can result in aberrant development of specific tissues, providing students with a foundation upon which the rest of the course was built.

Expanding on our explorations in the zebrafish model, we next wanted to show our students how shifts in development precede and predict changes in adult morphology. Because many of the laboratory tools and techniques developed for use with zebrafish can be applied to other fish systems, we completed the 'fish' component of the course by

introducing students to two evolutionary models: African cichlid fishes and Antarctic notothenioids. These systems were chosen because they exhibit striking natural variation in bone development, providing a logical connection to the bone phenotypes observed in mutant zebrafish. Whereas cichlid species spectrum the levels of bone mineralization (Albertson and Kocher, 2006), certain notothenioids lack nearly all bone (Voskoboynikova, 1993; Voskoboynikova, 1994; Voskoboynikova et al., 1994; Albertson et al., 2010).

Using molecular biological methods developed for the study of zebrafish, students were able to perform a comparative study of gene expression and bone development in cichlids and notothenioids. Students were presented with various species stained for bone and cartilage in the same manner as the zebrafish larvae described previously. Over the course of their evolutionary history, notothenioids have lost their ability to make bone (Albertson et al., 2010). Therefore, only the Alizarin Blue stained cartilage was visible in these samples. In contrast, equivalently staged cichlid larvae exhibited a range of Alizarin Red stained bone, reflecting variation in levels and rates of bone development.

To further illustrate variation in bone development, students compared notothenioid and cichlid specimens that had been probed for expression of *collagen 1a1,* a gene necessary for osteoblast differentiation in vertebrates (Karsenty and Park, 1995), using whole mount *in situ* hybridization (WISH). Cichlids exhibited a range of *collagen 1a1* expression, visualized as a purple staining on the embryo, while notothenioids did not express *collagen 1a1* because they were not making bone. These comparative analyses using non-model organisms were designed to allow students to gain an appreciation for the diversity of animal development, as well as an understanding of how

biodiversity has evolved.

**Model organism 2: *Caenorhabditis elegans***

In order to explore the combined effects of genetics and environment, a second model organism, the nematode worm *C. elegans*, was introduced and employed in an activity to help emphasize the general importance of environmental factors in development. Again, students spent one laboratory session learning about the *C. elegans* life cycle and observing the nematodes at different stages of development under a dissecting microscope. Students also practiced properly transferring the animals to fresh culture plates.

Once students were comfortable handling the nematodes, they were assigned a laboratory activity that demonstrated the combined genetic and environmental influences in the production of phenotypic output. The Notch signaling pathway is a conserved cell signaling mechanism in animal species that controls the specification of cell fate, cell proliferation, and cell differentiation (Schwanbeck et al., 2011). Given its broad and well-studied implications, knowledge of the Notch pathway should be a key objective in an undergraduate biology curriculum.

We focused on a temperature-sensitive mutation in a Notch-type receptor, GLP-1 (**g**erm**l**ine **p**roliferation), known as *glp-1(bn18ts)*, to analyze the effects of environmental changes on Notch signaling. Students were asked to set up parallel *C. elegans* cultures of wildtype and *glp-1(ts)* mutant strains under different temperature and salt regimens. Initially, cultures were maintained on normal and high salt (NaCl) media at 15°C. After adult nematodes produced embryos for 2-3 days, half of the cultures were upshifted to

25°C.

During the next lab session, students were asked to examine their cultures and quantify the phenotypes of animals cultured under different conditions. Wildtype animals were fertile regardless of culture temperature, as were >99% of *glp-1(bn18ts)* mutants raised at 15°C. In contrast, typically 100% of *glp-1(bn18ts)* mutants are sterile when raised at 25°C (Kodoyianni et al., 1992). In addition, embryos that were present at the time of upshift developed abnormally. Students were asked to record the number of sterile and fertile adults in each culture, as well as the presence/absence of embryos and larvae. Loss of fertility was visualized in adult nematodes using a dissecting microscope (Motic). Sterile adults contained no embryos in the uterus and instead had a small transparent patch close to the vulva (Fig. 1 C-D). Students were asked to record in their notebooks any additional observations of phenotypic or behavioral anomalies.

Based on intriguing observations from the lab of Anne Hart at Brown University (personal communication), sterility and embryonic lethality can be rescued by culturing *glp-1(ts)* mutants on medium with an elevated NaCl concentration. Thus, students were asked to compare the percent sterility of *glp-1(bn18)* mutants cultured on high and low NaCl at 25°C. In addition, they were asked to evaluate whether other phenotypic differences were visible in wildtype animals grown on high vs. low NaCl at 25°C. The wildtype animals showed signs of stress under high salt conditions, but did not become sterile, as eggs were easily recognizable in the gonad and embryos/larvae were present on the culture plates. When nematodes from the *glp-1(bn18)* strain were raised under high salt conditions at a high temperature, the sterile phenotype was rescued. In these samples, adult hermaphrodites were observed to contain eggs and embryos, and developing larvae

were observed on the culture plates.

After each group completed their counts of sterile and fertile organisms, the class data were pooled and an obvious trend was noted. Mutants raised on low NaCl plates at 25°C were sterile, whereas the vast majority of mutants raised on high NaCl plates at 25°C were fertile. In addition, wildtype and mutant animals were thin and pale when grown on high NaCl, and the population as a whole grew more slowly than on low NaCl.

Next, as a critical thinking component, students were asked to hypothesize possible biological mechanisms, both at the molecular level and at the organismal level, which may have caused the sterility and rescued the fertility in the *glp-1(bn18)* strain of *C. elegans*. Although the exact mechanism of this phenomenon is unknown, some student hypotheses included changes in the GLP-1 protein structure due to high salt conditions, increasing protein performance and restoring fertility; or at the organismal level, secondary effects of stress in *C. elegans* due to the high salt conditions triggering increased production of chaperone proteins, in turn restoring protein structure and fertility. In addition, students were asked to hypothesize possible mechanisms by which elevated salt might influence population growth. Finally, there was a short class discussion elaborating on different student hypotheses and, based on the data collected, debating their validity.

**RESULTS**

Immediately following the completion of zebrafish exercises, students were asked to complete anonymous evaluations of the zebrafish course content and activities. The general consensus among students was that they very much enjoyed working with live zebrafish specimen compared to prepared slides or pictures, and they enjoyed the laboratory activities. Typical student evaluation responses described the use of zebrafish in the classroom as "interesting," "different," "fascinating," and "a rare experience." According to one respondent, the activity "really helps with the understanding of mutations and gene expression." Based on opinions expressed by the students, they perceived the use of zebrafish in the classroom to be both novel and enlightening.

Following the *C. elegans* exercises, students were asked to evaluate the *C. elegans* module. Students overwhelmingly reported that they enjoyed working with the live organisms and that they perceived their understanding of genetics and development to have improved as a consequence of the laboratory activities. In particular, students appreciated the opportunity to observe and compare the different nematode cultures for themselves, as these activities allowed them to directly witness the effects of mutation and environmental conditions on live organisms. Representative student comments included "I think working with live animals in labs really helps [my] understanding [of] materials from lectures" and "documenting and evaluating the effects ourselves before knowing what was supposed to happen was educational." In addition, students typically enjoyed handling the nematodes, setting up cultures, and following their growth, using such term as "fun," "interesting," "challenging," and "fascinating" to describe the work.

**DISCUSSION**

Overall, the results of the zebrafish and *C. elegans* exercises demonstrated (1) how development produces an organism, (2) the evolutionary significance of development in producing variation in animal form, and (3) how environmental conditions can differentially affect organismal development based on genetic background. These experiments show that genetics and the environment work in tandem to produce the phenotype of an organism.

For this course we chose to use two model systems because each has its own technical advantages, and so that students may have exposure to both systems. If it is not possible to use two model systems, activities using either organism can illustrate genetic and environmental effects on phenotype. Examples of additional activities in each model system include the study of different allelic variations of *glp-1* mutants in *C. elegans* or the heat shock of zebrafish embryos which has been shown to result in changes in gene expression and phenotype (Connolly and Hall, 2008).

The experiments described here are designed to help students appreciate how individuals of the same species can exhibit many different phenotypes - most commonly changes in size, morphology, color, or patterning – depending on specific environmental conditions. Other examples of this include the migratory locust *Schistocerca gregaria*, which can develop as a green short-winged morph or a multi-colored long-winged morph, depending on nymph population density (Rogers et al., 2003; Rogers et al., 2004); the formation of a "Queen" in hymenopteran insects such as bees and ants, which is based on nutrition induced levels of juvenile hormone (Wirtz, 1973; Rachinsky and Hartfelder, 1990; Abouheif and Wray, 2002); and the increased head growth of the water

flea, *Daphnia cucullata*, as a response to the proximity of a predator (Agrawal et al., 1999).

As the study of biology becomes more integrated, it is important to expose undergraduate students to an integrated understanding of the subject, as to better prepare them for scientific research experiences. Pursuing interdisciplinary instruction using model organisms also allows students to become better acquainted with the use of live organisms and, based on our experiences, is both interesting and exciting to students. The laboratory activities described here are significant because they allow undergraduate students to learn about and gain experience working directly with model organisms while simultaneously being introduced to the interdisciplinary idea that both genes and the environment contribute to the development and phenotypic output of any particular organism. Gilbert and Epel (2009) describe these types of interactions in their book *Ecological Developmental Biology* (Gilbert and Epel, 2009). Indeed, the combination of ecological and developmental studies is gaining popularity as a field of investigation. This approach, often termed "Eco-Devo", combines the subfields of ecology and development in an attempt to describe how the integration of genes and environmental conditions influence developmental trajectories. Eco-Devo took its name after evolutionary developmental biology, or "Evo-Devo", the quickly expanding field of study aimed toward understanding ancestral relationships between different taxa via the study of their developmental processes.

**Have model activities? Share them, by JoVE!**

One important resource that can support the inclusion of model organisms in the

undergraduate classroom is the Journal of Visualized Experiments (JoVE). As JoVE is a video journal, it is well suited for sharing effective laboratory classroom procedures that might seem overly tedious or challenging unless you have seen them performed. A good example of a protocol we have employed in our undergraduate teaching laboratories at Syracuse University is our use of WISH in zebrafish embryos to link molecular and organismal biology (Jacobs et al., 2011). It is our hope that such communications will lead to greater adoption of widely used techniques involving model organisms in undergraduate classrooms and that this practice will serve to prepare our budding biologists to participate in independent research, and to deepen an appreciation for and retention of key biological concepts by all students.

**ACKNOWLEDGEMENTS**

The authors would like to acknowledge the Department of Biology at Syracuse University, Dr. Mark Ritchie, and Andrew Siefert for their roles in the administration of the Integrative Biology Laboratory course. They would also like to thank the lab of Dr. Anne Hart for providing information regarding the influence of NaCl on the the *glp-1(ts)* phenotype.

**FIGURE AND TABLE**

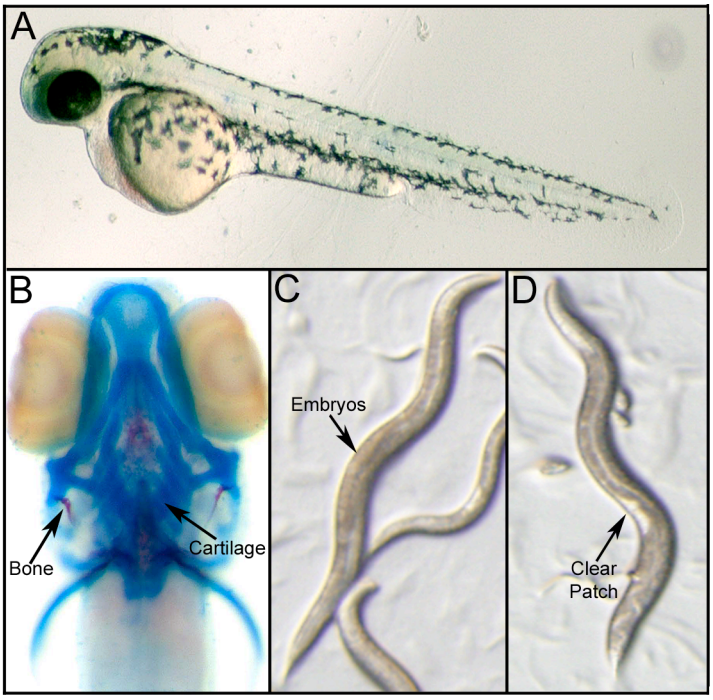


**Figure 1. Examples of zebrafish and *C. elegans* laboratory specimens. (A)** A wild type zebrafish larva 2 days post fertilization. **(B)** A zebrafish larva 5 days post fertilization that has been cleared and stained with Alizarin Red and Alcian Blue. Notice the red bone stain and the blue cartilage stain. Ventral view with anterior to the top. Fertile **(C)** and sterile **(D)** *C. elegans* adult hermaphrodites. Note the presence of embryos in the fertile animals and a clear patch in the sterile animals. Smaller animal in **(C)** is an L4 stage larva.

**Table 1**. Published activities for teaching biological concepts and skills using model organisms.

| Model Organism | Biology Teaching Concepts | Published Activities |
|---|---|---|
| *Arabidopsis thaliana*<br>thale cress | Plant ecotypes; Natural selection | Wyatt and Ballard, 2007 |
| | Patterns of inheritance; linkage of genetic loci | Zheng, 2006 |
| *Caenorhabditis elegans*<br>soil nematode | Population growth; natural selection | Mueller, 2007 |
| | Chemosensory adaptation | Lindblom, 2006 |
| *Danio rerio*<br>zebrafish | Linking molecular and organismal biology; *in situ* hybridization; development | Jacobs et al., 2011 |
| | Development; genetics | D'Costa and Shepherd, 2009 |
| | Tissue regeneration | Hassoun et al., 2008 |
| *Drosophila melanogaster*<br>fruit fly | Population genetics | Johnson and Kennon, 2009 |
| | Bioinformatics; genetics | Calie et al., 2007 |
| *Escherichia coli*<br>gram-negative, rod-shaped, intestinal bacterium | Genetic diversity; general microbiological lab skills | Petrie et al., 2005 |
| | Natural selection; antibacterial resistance | Welden and Hossler, 2003 |
| | Genotype/phenotype relationships; DNA transformation; DNA isolation | Guilfoile and Plum, 2000 |
| *Saccharomyces cerevisiae*<br>baker's/brewer's yeast | Gel electrophoresis; Cellular RNA content analysis; basic biochemical laboratory skills | Deutch and Marshall, 2008 |
| *Xenopus laevis*<br>African clawed frog | Endocrinology: hormone specificity; chemical nature of hormones | Heggland et al., 2000 |
| | Observation of heart beat and circulation | Hood and Witters, 1971 |

# Bibliography

Abadie V, Wiener-Vacher S, Morisseau-Durand MP, Poree C, Amiel J, Amanou L, Peigné C, Lyonnet S, Manac'h Y. 2000. Vestibular anomalies in CHARGE syndrome: investigations on and consequences for postural development. Eur J Pediatr. 159:569-574.

Abouheif E, Wray GA. 2002. Evolution of the gene network underlying wing polyphenism in ants. Science. 297:249-252.

Agrawal AA, Laforsch C, Tollrian R. 1999. Trans-generational induction of defences in animals and plants. Nature. 401:60-63.

Akisu M, Ozkinay F, Ozyurek R, Kucuktas A, Kultursay N. 1998. The CHARGE association in a newborn infant. Turk J Pediatr. 40:283-287.

Albertson RC, Yelick PC. 2005. Roles for fgf8 signaling in left-right patterning of the visceral organs and craniofacial skeleton. Dev Biol. 283:310-321.

Albertson RC, Kocher TD. 2006. Genetic and developmental basis of cichlid trophic diversity. Heredity. 97:211-221.

Albertson RC, Yan YL, Titus TA, Pisano E, Vacchi M, Yelick PC, Detrich III HW, Postlethwait JH. 2010. Molecular pedomorphism underlies craniofacial skeletal evolution in Antarctic notothenioid fishes. Evolutionary Biology. 10.

Allen MD, Religa TL, Freund SM, Bycroft M. 2007. Solution structure of the BRK domains from CHD7. J Mol Biol. 371:1135-1140.

Altaf M, Saksouk N, Cote J. 2007. Histone modifications in response to DNA damage. Mutat. Res. 618:81–90.

Alvarez Y, Alonso MT, Vendrell V, Zelarayan LC, Chamero P, Theil T, Bösl MR, Kato S, Maconochie M, Riethmacher D, Schimmang T. 2003. Requirements for FGF3 and FGF10 during inner ear formation. Development. 130:6329-6338.

Amack JD, Wang X, Yost HJ. 2007. Two T-box genes play independent and cooperative roles to regulate morphogenesis of ciliated Kupffer's vesicle in zebrafish. Developmental Biology. 15:196-210.

Amiel J, Attiee-Bitach T, Marianowski R, Cormier-Daire V, Abadie V, Bonnet D, Gonzales M, Chemouny S, Brunelle F, Munnich A, Manach Y, Lyonnet S. 2001. Temporal bone anomaly proposed as a major criteria for diagnosis of CHARGE syndrome. Am J Med Genet. 99:124-127.

Amores A, Force A, Yan YL, Joly L, Amemiya C, Fritz A, Ho RK, Langeland J, Prince V, Wang YL, Westerfield M, Ekker M, Postlethwait JH. Zebrafish hox clusters and vertebrate genome evolution. Science. 282:1711-1714.

Antunes AA, Leite KR, Reis ST, Sousa-Canavez JM, Camara-Lopes LH, Dall'oglio MF, Srougi M. 2009. GREB1 tissue expression is associated with organ-confined prostate cancer. Urol Oncol. Epub Nov 26.

Aramaki M, Udaka T, Kosaki R, Makita Y, Okamoto N, Yoshihashi H, Oki H, Nanao K, Moriyama N, Oku S, Hasegawa T, Takahashi T, Fukushima Y, Kawame H, Kosaki K. 2006. Phenotypic spectrum of CHARGE syndrome with CHD7 mutations. J Pediatr. 148:410-414.

Aramaki M, Kimura T, Udaka T, Kosaki R, Mitsuhashi T, Okada Y, Takahashi T, Kosaki K. 2007. Embryonic expression profile of chicken CHD7, the ortholog of the causative gene for CHARGE syndrome. Birth Defects Res A Clin Mol Teratol. 79:50-57.

Arduini BL, Bosse KM, Henion PD. 2009. Genetic ablation of neural crest cell diversification. Development. 136:1987-1994.

Aulehla A, Herrmann BG. 2004. Segmentation in vertebrates: clock and gradient finally joined. Genes and Development.18:2060-2067.

Batsukh T, Pieper L, Koszucka A, von Velsen N, Hoyer-Fender S, Elbracht M, Bergman JE, Hoefsloot LH, Pauli S. 2010. CHD8 interacts with CHD7, a protein which is mutated in CHARGE syndrome. Human Molecular Genetics. 19:2858-2866.

Bajpai R, Chen DA, Rada-Iglesias A, Zhang J, Xiong Y, Helms J, Chang CP, Zhao Y, Swigut T, Wysocka J. 2010. CHD7 cooperates with PBAF to control multipotent neural crest formation. Nature. 463:958-62.

Barrios A, Poole RJ, Durbin L, Brennan C, Holder N, Wilson SW. 2003. Eph/Ephrin signaling regulates the mesenchymal-to-epithelial transition of the paraxial mesoderm during somite morphogenesis. Curr Biol. 13:1571-1582.

Begemann G, Schilling TF, Rauch GJ, Geisler R, Ingham PW. 2001. The zebrafish neckless mutation reveals a requirement for raldh2 in mesodermal signals that pattern the hindbrain. Development. 128:3081-3094.

Ben Becher S, Ganouni S, Cheour M, Bouaziz A, Boudhina T. 1994. [CHARGE association]. Arch Pediatr. 1:1115-1117.

Bird NC, Mabee PM. 2003. Developmental morphology of the axial skeleton of the zebrafish, *Danio rerio* (Ostariophysi: Cyprinidae). Dev. Dynam. 228:337-357.

Blasiole B, Canfield VA, Vollrath MA, Huss D, Mohideen MA, Dickman JD, Cheng KC, Fekete DM, Levenson R. 2006. Separate Na,K-ATPase genes are required for otolith formation and semicircular canal development in zebrafish. Dev. Biol. 294:148-160.

Blake KD, Davenport SL, Hall BD, Hefner MA, Pagon RA, Williams MS, Lin AE, Graham JM Jr. 1998. CHARGE association: an update and review for the primary pediatrician. Clin Pediatr (Phila). 37:159-173

Blake KD, Prasad C. 2006. CHARGE syndrome. Orphanet J Rare Dis. 1:34.

Blankenberg D, Gordon A, Von Kuster G, Coraor N, Taylor J, Nekrutenko A; Galaxy Team. 2010. Manipulation of FASTQ data with Galaxy. Bioinformatics. 26:1783-1785.

Blasiole B, Canfield VA, Vollrath MA, Huss D, Mohideen MA, Dickman JD, Cheng KC, Fekete DM, Levenson R. 2006. Separate Na,K-ATPase genes are required for otolith formation and semicircular canal development in zebrafish. Dev. Biol. 294:148-160.

Bosman EA, Penn AC, Ambrose JC, Kettleborough R, Stemple DL, Steel KP. 2005 Multiple mutations in mouse Chd7 provide models for CHARGE syndrome. Human Molecular Genetics 14:3463-76.

Brand M, Heisenberg CP, Jiang YJ, Beuchle D, Lun K, Furutani-Seiki M, Granato M, Haffter P, Hammerschmidt M, Kane DA, Kelsh RN, Mullins MC, Odenthal J, van Eeden FJ, Nüsslein-Volhard C. 1996. Mutations in zebrafish genes affecting the formation of the boundary between midbrain and hindbrain. Development. 123:179-190.

Briegel JK, Joyner AL. 2001. Identification and Characterization of Lbh, a Novel Conserved Nuclear Protein Expressed during Early Limb and Heart Development. Dev. Biol. 233:291–304.

Bulman MP, Kusumi K, Frayling TM, McKeown C, Garrett C, Lander ES, Krumlauf R, Hattersley AT, Ellard S, Turnpenny PD. 2000. Mutations in the human delta homologue, DLL3, cause axial skeletal defects in spondylocostal dysostosis. Nat Genet. 24:438-41.

Burwell R, Dangerfield P, Freeman B. 2008. Concepts on the Pathogenesis of Adolescent Idiopathic Scoliosis. Bone Growth and Mass, Vertebral Column, Spinal Cord, Brain, Skull, Extra-Spinal Left-Right Skeletal Length Asymmetries, Disproportions and Molecular Pathogenesis. Stud Health Technol Inform. 135:3-52.

Byerly KA, Pauli RM. 1993. Cranial nerve abnormalities in CHARGE association. Am J Med Genet. 45:751-757.

Calie PJ, Lee S, Hicks EJ. 2007. The bioinformatic enhancement of exercises in Drosophila genetics. The American Biology Teacher. 68:482-487.

Carey JC. 2005. CHARGE syndrome: 2005. Am J Med Genet A. 133A:227.

Carroll SB, Grenier JK, Weatherbee SD. 2005. From DNA to Diversity. Malden, Massachusetts: Blackwell Publishing.

Chang W, Brigande JV, Fekete DM, Wu DK. 2004. The development of semicircular canals in the inner ear: role of FGFs in sensory cristae. Development. 131:4201-4211.

Cheng J, Tang S, Guo X, Chan C, Qin L. 2001. Osteopenia in Adolescent Idiopathic Scoliosis: A Histomorphometric Study. Spine. 26:C1-C5.

Childs S, Chen JN, Garrity DM, Fishman MC. 2002. Patterning of angiogenesis in the zebrafish embryo. Development. 129:973-82.

Christiansen HE, Lang MR, Pace JM, Parichy DM. 2009. Critical early roles for col27a1a and col27a1b in zebrafish notochord morphogenesis, vertebral mineralization and post-embryonic axial growth. PLoS One. 4:e8481.

Cibrian-Uhalte E, Langenbacher A, Shu X, Chen JN, Abdelilah-Seyfried S. 2007. Involvement of zebrafish Na+,K+ ATPase in myocardial cell junction maintenance. J. Cell Biol. 176:223-230.

Clapier CR, Cairns BR. 2009. The biology of chromatin remodeling complexes. Annu Rev Biochem. 78:273-304.

Clark, M. 2003. In situ Hybridization: Laboratory Companion. Wiley-VCH.

Conen KL, Nishimori S, Provot S, Kronenberg HM. 2009. The transcriptional cofactor Lbh regulates angiogenesis and endochondral bone formation during fetal bone development. Dev Biol. 333:348-358.

Connolly MH, Hall BK. 2008. Embryonic heat shock reveals latent hsp90 translation in zebrafish (Danio rerio). The International Journal of Developmental Biology. 52:71-79.

Daubresse G, Deuring R, Moore L, Papoulas O, Zakrajsek I, Waldrip WR, Scott MP, Kennison JA, Tamakun JW. 1999. The Drosophila kismet gene is related to chromatin-remodeling factors and is required for both segmentation and segment identity. Development. 126:1175-1187.

Davidson AJ, Zon LI. 2006. The caudal-related homeobox genes cdx1a and cdx4 act redundantly to regulate hox gene expression and the formation of putative hematopoietic stem cells during zebrafish embryogenesis. Dev Biol. 292:506-18.

D'Costa A, Shepherd IT. 2009. Zebrafish development and genetics: Introducing undergraduates to developmental biology and genetics in a large introductory laboratory class. Zebrafish. 6:169-177.

Deutch CE, Marshall PA. 2008. Analysis of the RNA content of the yeast Saccharomyces cerevisiae. The American Biology Teacher. 70:537-545.

Devriendt K, Swillen A, Fryns JP. 1998. Deletion in chromosome region 22q11 in a child with CHARGE association. Clin Genet. 53:408-410.

Doyle C, Blake K. 2005. Scoliosis in CHARGE: a prospective survey and two case reports. Am J Med Genet A. 133:340–343.

Du SJ, Frenkel V, Kindschi G, Zohar Y. 2001. Visualizing normal and defective bone development in zebrafish embryos using the fluorescent chromophore calcein. Dev Biol. 238:239-246.

Dubrulle J, McGrew MJ, Pourquié O. 2001. FGF signaling controls somite boundary position and regulates segmentation clock control of spatiotemporal Hox gene activation. Cell. 106:219-32.

Dunwoodie SL. 2009. Mutation of the fucose-specific beta1,3 N-acetylglucosaminyltransferase LFNG results in abnormal formation of the spine. Biochim Biophys Acta. 1792:100-11.

Eberhart JK, Swartz ME, Crump JG, Kimmel CB. 2006. Early Hedgehog signaling from neural to oral epithelium organizes anterior craniofacial development. Development. 133:1069-1077.

Eberharter A, Becker PB. 2004. ATP-dependent nucleosome remodelling: factors and functions. J. Cell Sci. 117:3707–3711.

Ellertsdottir E, Ganz J, Dürr K, Loges N, Biemar F, Seifert F, Ettl AK, Kramer-Zucker AK, Nitschke R, Driever W. 2006. A mutation in the zebrafish Na,K-ATPase subunit atp1a1a.1 provides genetic evidence that the sodium potassium pump contributes to left-right asymmetry downstream or in parallel to nodal flow. Dev Dyn. 235:1794-1808.

Emerging Model Organisms: A Laboratory Manual, Volume 1. 2008. Cold Spring Harbor, NY: Cold Spring Harbor Laboratory Press.

Emerging Model Organisms: A Laboratory Manual, Volume 2. 2010. Cold Spring Harbor, NY: Cold Spring Harbor Laboratory Press.

Enomoto A, Ping J, Takahashi M. 2006. Girdin, a novel actin-binding protein, and its family of proteins possess versatile functions in the Akt and Wnt signaling pathways. Ann N Y Acad Sci. 1086:169-184.

Erdmann B, Kirsch FP, Rathjen FG, More MI. 2003. N-cadherin is essential for retinal lamination in the zebrafish. Dev Dyn.226: 570-577.

Fauny JD, Thisse B, Thisse C. 2009. The entire zebrafish blastula-gastrula margin acts as an organizer dependent on the ratio of Nodal to BMP activity. Development. 136:3811-3819.

Feldner J, Becker T, Goishi K, Schweitzer J, Lee P, Schachner M, Klagsbrun M, Becker CG. 2005. Neuropilin-1a is involved in trunk motor axon outgrowth in embryonic zebrafish. Dev. Dyn. 234:535-549.

Fernandez-Funez P, Nino-Rosales ML, de Gouyon B, She WC, Luchak JM, Martinez P, Turiegano E, Benito J, Capovilla M, Skinner PJ, McCall A, Canal I, Orr HT, Zoghbi HY, Botas J. 2000. Identification of genes that modify ataxin-1-induced neurodegeneration. Nature. 408:101-6.

Fields S, Johnston M. 2005. Cell biology: Whither model organism research?. Science. 307:1885-1886.

Gangaraju VK, Bartholomew B. 2007. Mechanisms of ATP dependent chromatin remodeling. Mutat. Res. 618:3–17.

Gao X, Gordon D, Zhang D, Browne R, Helms C, Gillum J, Weber S, Devroy S, Swaney S, Dobbs M, Morcuende J, Sheffield V, Lovett M, Bowcock A, Herring J, Wise C. 2007. CHD7 gene polymorphisms are associated with susceptibility to idiopathic scoliosis. Am J Hum Genet. 80:957-965.

Garcia-Marcos M, Ghosh P, Farquhar MG. 2009. GIV is a nonreceptor GEF for G alpha i with a unique motif that regulates Akt signaling. Proc Natl Acad Sci U S A. 106:3178-3183.

Gaspar-Maia A, Alajem A, Polesso F, Sridharan R, Mason MJ, Heidersbach A, Ramalho-Santos J, McManus MT, Plath K, Meshorer E, Ramalho-Santos M. 2009. Chd1 regulates open chromatin and pluripotency of embryonic stem cells. Nature. 460:863-868.

Ge Q, Nilasena DS, O'Brien CA, Frank MB, Targoff IN. 1995. Molecular analysis of a major antigenic region of the 240 kDa protein of Mi-2 autoantigen. J. Clin. Invest. 96:1730–1737.

Geetha-Loganathan P, Nimmagadda S, Scaal M. 2008a. Wnt signaling in limb organogenesis. Organogenesis. 4:109-15.

Geetha-Loganathan P, Nimmagadda S, Scaal M, Huang R, Christ B. 2008b. Wnt signaling in somite development. Ann Anat. 190:208-22.

Giardine B, Riemer C, Hardison RC, Burhans R, Elnitski L, Shah P, Zhang Y, Blankenberg D, Albert I, Taylor J, Miller W, Kent WJ, Nekrutenko A. 2005. Galaxy: a platform for interactive large-scale genome analysis. Genome Res. 15:1451-1455.

Gilbert SF, Epel D. 2009. Ecological Developmental Biology: Integrating Epigenetics, Medicine, and Evolution. Sunderland, Massachusetts: Sinauer Associates Inc.

Goecks J, Nekrutenko A, Taylor J; Galaxy Team. 2010. Galaxy: a comprehensive approach for supporting accessible, reproducible, and transparent computational research in the life sciences. Genome Biol. 11:R86.

Gregory CA, Gunn WG, Peister A, Prockop DJ. 2004. An Alizarin red-based assay of mineralization by adherent cells in culture: comparison with cetylpyridinium chloride extraction. Anal Biochem. 329:77-84.

Grenier J, Teillet MA, Grifone R, Kelly RG, Duprez D. 2009. Relationship between neural crest cells and cranial mesoderm during head muscle development. PLoS One. 4:e4381.

Guilfoile P, Plum S. 2000. The relationship between phenotype & genotype. The American Biology Teacher. 62:288-291.

Hall JA, Georgel PT. 2007. CHD proteins: a diverse family with strong ties. Biochem Cell Biol. 85:463-76.

Hammond KL, Whitfield TT. 2006. The developing lamprey ear closely resembles the zebrafish otic vesicle: otx1 expression can account for all major patterning differences. Development. 133:1347-1357.

Hassoun L, Hable W, Payne-Ferreira T. 2008. Tissue regeneration in the classroom!. The American Biology Teacher. 70:546-549.

Heggland SJ, Lawless AR, Spencer LW. 2000. Visualizing endocrinology in the classroom. The American Biology Teacher. 62:597-601.

Hnatyszyn HJ, Liu M, Hilger A, Herbert L, Gomez-Fernandez CR, Jorda M, Thomas D, Rae JM, El-Ashry D, Lippman ME. 2010. Correlation of GREB1 mRNA with protein expression in breast cancer: validation of a novel GREB1 monoclonal antibody. Breast Cancer Res Treat. 122:371-380.

Ho L, Crabtree GR. 2010. Chromatin remodelling during development. Nature. 463:474-84.

Hohenlohe PA, Bassham S, Etter PD, Stiffler N, Johnson EA, Cresko WA. 2010. Population genomics of parallel adaptation in threespine stickleback using sequenced RAD tags. PLoS Genet. 6:e1000862.

Holley SA. 2007. The genetics and embryology of zebrafish metamerism. Dev Dyn. 236:1422-49.

Holstein TW, Watanabe H, Ozbek S. 2011. Signaling pathways and axis formation in the lower metazoa. Curr Top Dev Biol. 97:137-177.

Hood RD, Witters WL. 1971. Observation of heart beat and circulation in Xenopus laevis tadpoles. Journal of College Science Teaching. 1:38.

Hu Z, Bao J, Reecy JM. 2008. CateGOrizer: A Web-Based Program to Batch Analyze Gene Ontology Classification Categories. Online Journal of Bioinformatics. 9:108-112.

Huang S, Ma J, Liu X, Zhang Y, Luo L. 2011. Retinoic acid signaling sequentially controls visceral and heart laterality in Zebrafish. J Bio Chem. M111.244327.

Huang X, Saint-Jeannet JP. 2004. Induction of the neural crest and the opportunities of life on the edge. Dev Biol. 275:1-11.

Huelsken J, Behrens J. 2002. The Wnt signaling pathway. J Cell Sci. 15:3977-3978.

Hung V, Qin L, Cheung C, Lam T, Ng B, Tse Y, Guo X, Lee K, Cheng J. 2005. The Journal of Bone and Joint Surgery. 87:2709-2716.

Hurd EA, Capers PL, Blauwkamp MN, Adams ME, Raphael Y, Poucher HK, Martin DM. 2007. Loss of Chd7 function in gene-trapped reporter mice is embryonic lethal and associated with severe defects in multiple developing tissues. Mamm Genome. 18:94-104.

Hurd EA, Poucher HK, Cheng K, Raphael Y, Martin DM. 2010. The ATP-dependent chromatin remodeling enzyme CHD7 regulates pro-neural gene expression and neurogenesis in the inner ear. Development. 137:3139-3150.

Jacobs NL, Albertson, RC, and Wiles JR. 2011. Using Whole Mount in situ Hybridization to Link Molecular and Organismal Biology. J Vis Exp. 49: http://www.jove.com/details.php?id=2533 doi: 10.3791/2533

Jacobs-McDaniels NL, Albertson RC. 2011. Chd7 plays a critical role in controlling left-right symmetry during zebrafish somitogenesis. Dev Dyn. 240:2272-2280.

Jarman AP, Sun Y, Jan LY, Jan YN. 1995. Role of the proneural gene, atonal, in formation of Drosophila chordotonal organs and photoreceptors. Development. 121:2019-2030.

Jiang YH, Bressler J, Beaudet AL. 2004. Epigenetics and human disease. Annu Rev Genomics Hum Genet. 5:479-510.

Johnson R, Kennon T. 2009. Experimental population genetics in the introductory genetics laboratory using Drosophila as a model organism. Journal of College Science Teaching. 38:14-19.

Jongmans MCJ, Admiraal RJ, van der Donk KP, Vissers LELM, Baas BF, Kapusta L, van Hagen JM, Donnai D, de Ravel TJ, Veltman JA, Geurts van Kessel A, De Vries BBA, Brunner HG, Hoefsloot LH, van Ravenswaaij CMA. 2006. CHARGE syndrome: the phenotypic spectrum of mutations in the CHD7 gene. J. Med. Genet. 43: 306-314.

Jyonouchi S, McDonald-McGinn DM, Bale S, Zackai EH, Sullivan KE. 2009. CHARGE (coloboma, heart defect, atresia choanae, retarded growth and development, genital hypoplasia, ear anomalies/deafness) syndrome and chromosome 22q11.2 deletion syndrome: a comparison of immunologic and nonimmunologic phenotypic features. Pediatrics. 123:e871-877.

Karsenty G, Park RW. 1995. Regulation of type I collagen genes expression. International Reviews of Immunology. 12:177-185.

Kawakami Y, Raya A, Raya RM, Rodríguez-Esteban C, Belmonte JC. 2005. Retinoic acid signalling links left-right asymmetric patterning and bilaterally symmetric somitogenesis in the zebrafish embryo. Nature. 435:165-71.

Kawamura A, Koshida S, Hijikata H, Ohbayashi A, Kondoh H, Takada S. 2005. Groucho-Associated Transcriptional Repressor Ripply1 Is Required for Proper Transition from the Presomitic Mesoderm to Somites. Developmental Cell. 9:735-744.

Kim H, Kurth I, Lan F, Meliciani I, Wenzel W, Eom S, Kang G, Rosenberger G, Tekin M, Ozata M, Bick D, Sherins R, Walker S, Shi W, Gusella J, Layman L. 2008. Mutations in CHD7, Encoding a Chromatin-Remodeling Protein, Cause Idiopathic Hypogonadotropic Hypogonadism and Kallmann Syndrome. American Journal of Human Genetics. 83:511-519.

Kimmel CB, Ballard WW, Kimmel SR, Ullmann B, Schilling TF. 1995. Stages of embryonic development of the zebrafish. Dev Dyn. 203:253-310.

Knight RD, Schilling TF. 2006. Cranial neural crest and development of the head skeleton. Adv Exp Med Biol. 589:120-133.

Kodoyianni V, Maine EM, Kimble J. 1992. Molecular basis of loss-of-function mutations in the glp-1 gene of Caenorhabditis elegans. Molecular Biology of the Cell. 3:1199-1213.

Koensgen D, Mustea A, Klaman I, Sun P, Zafrakas M, Lichtenegger W, Denkert C, Dahl E, Sehouli J. 2007. Expression analysis and RNA localization of PAI-RBP1 (SERBP1) in epithelial ovarian cancer: association with tumor progression. Gynecol Oncol. 107:266-273.

Koizumi K, Nakajima M, Yuasa S, Saga Y, Sakai T, Kuriyama T, Shirasawa T, Koseki H. 2001. The role of presenilin 1 during somite segmentation. Development. 128:1391-1402.

Krauss S, Concordet JP, Ingham PW. 1993. A functionally conserved homolog of the Drosophila segment polarity gene hh is expressed in tissues with polarizing activity in zebrafish embryos. Cell. 75:1431-44.

Kulkarni S, Nagarajan P, Wall J, Donovan DJ, Donell RL, Ligon AH, Venkatachalam S, Quade BJ. 2008. Disruption of chromodomain helicase DNA binding protein 2 (CHD2) causes scoliosis. Am J Med Genet A. 146:1117-1127.

Lacombe D. 1994. Facial palsy and cranial nerve abnormalities in CHARGE association. Am J Med Genet. 49:351-353.

Lalani SR, Safiullah AM, Fernbach SD, Phillips M, Bacino CA, Molinari LM, Glass NL, Towbin JA, Craigen WJ, Belmont JW. 2005. SNP genotyping to screen for a common deletion in CHARGE syndrome. BMC Med Genet 6:8.

Lalani SR, Safiullah AM, Fernbach SD, Harutyunyan KG, Thaller C, Peterson LE, McPherson JD, Gibbs RA, White LD, Hefner M, Davenport SL, Graham JM, Bacino CA, Glass NL, Towbin JA, Craigen WJ, Neish SR, Lin AE, Belmont JW. 2006. Spectrum of CHD7 mutations in 110 individuals with CHARGE syndrome and genotype-phenotype correlation. Am J Hum Genet. 78:303-14.

Lang MR, Lapierre LA, Frotscher M, Goldenring JR, Knapik EW. 2006. Secretory COPII coat component Sec23a is essential for craniofacial chondrocyte maturation. Nat. Genet. 38:1198-1203.

Langenbacher AD, Huang J, Chen Y, Chen JN. 2011. Sodium pump activity in the yolk syncytial layer regulates zebrafish heart tube morphogenesis. Dev Biol. Dec 13. [Epub ahead of print]

Längst G, Becker PB. 2004. Nucleosome remodeling: one mechanism, many phenomena? Biochem. Biophys. Acta. 1677:58–63.

Larison KD, Bremiller R. 1990. Early onset of phenotype and cell patterning in the embryonic zebrafish retina. Development. 109:567-576.

Layman WS, McEwen DP, Beyer LA, Lalani SR, Fernbach SD, Oh E, Swaroop A, Hegg CC, Raphael Y, Martens JR, Martin DM. 2009. Defects in neural stem cell proliferation and olfaction in Chd7 deficient mice indicate a mechanism for hyposmia in human CHARGE syndrome. Hum Mol Genet. 18:1909-1923.

Lee JS, Smith E, Shilatifard A. 2010. The language of histone crosstalk. Cell. 142:682-685.

Lee P, Goishi K, Davidson AJ, Mannix R, Zon L, Klagsbrun M. 2002. Neuropilin-1 is required for vascular development and is a mediator of VEGF-dependent angiogenesis in zebrafish. Proc. Natl. Acad. Sci. USA. 99:10470-10475.

Lindblom T. 2006. A chemosensory adaptation module for the physiology laboratory from student-directed C. elegans research. The American Biology Teacher. 68:e72-e79.

Link BA, Fadool JM, Malicki J, Dowling JE. 2000. The zebrafish young mutation acts non-cell-autonomously to uncouple differentiation from specification for all retinal cells. Development. 127:2177-2188.

Linville A, Radtke K, Waxman JS, Yelon D, Schilling TF. 2009. Combinatorial roles for zebrafish retinoic acid receptors in the hindbrain, limbs and pharyngeal arches. Dev Biol. 315:60-70.

Liu DW, Hsu CH, Tsai SM, Hsiao CD, Wang WP. 2011. A variant of fibroblast growth factor receptor 2 (fgfr2) regulates left-right asymmetry in zebrafish. PLoS One. 6:e21793.

Long S, Ahmad N, Rebagliati M. 2003. The zebrafish nodal-related gene southpaw is required for visceral and diencephalic left-right asymmetry. Development. 130:2303-2316.

Lwigale PY, Bronner-Fraser M. 2009. Semaphorin3A/neuropilin-1 signaling acts as a molecular switch regulating neural crest migration during cornea development. Dev Biol. 336:257-265.

Lyu J, Jho EH, Lu W. 2011. Smek promotes histone deacetylation to suppress transcription of Wnt target gene brachyury in pluripotent embryonic stem cells. Cell Res. 21:911-921.

Mamanova L, Andrews RM, James KD, Sheridan EM, Ellis PD, Langford CF, Ost TW, Collins JE, Turner DJ. 2010. FRT-seq: amplification-free, strand-specific transcriptome sequencing. Nat Methods. 7:130-132.

Mara A, Holley SA. 2007. Oscillators and the emergence of tissue organization during zebrafish somitogenesis. Trends Cell Biol. 17:593-9.

Marfella CG, Ohkawa Y, Coles AH, Garlick DS, Jones SN, Imbalzano AN. 2006. Mutation of the SNF2 family member Chd2 affects mouse development and survival. J Cell Physiol. 209:162-71.

Marfella CG, Imbalzano AN. 2007. The Chd family of chromatin remodelers. Mutat Res. 618:30-40.

Marguerat S, Bähler J. 2010. RNA-seq: from technology to biology. Cell Mol Life Sci. 67:569-579.

Martin DM. 2010. Chromatin remodeling in development and disease: focus on CHD7. PLoS Genet. 6:e1001010.

Masai I, Lele Z, Yamaguchi M, Komori A, Nakata A, Nishiwaki Y, Wada H, Tanaka H, Nojima Y, Hammerschmidt M, Wilson SW, Okamoto H. 2003. N-cadherin mediates retinal lamination, maintenance of forebrain compartments and patterning of retinal neurites. Development. 130:2479-2494.

Melicharek D, Shah A, DiStefano G, Gangemi AJ, Orapallo A, Vrailas-Mortimer AD, Marenda DR. 2008. Identification of novel regulators of atonal expression in the developing Drosophila retina. Genetics. 180:2095-2110.

Melicharek DJ, Ramirez LC, Singh S, Thompson R, Marenda DR. 2010. Kismet/CHD7 regulates axon morphology, memory and locomotion in a Drosophila model of CHARGE syndrome. Hum Mol Genet. 19:4253-4264.

Michaut L, Jansen HJ, Bardine N, Durston AJ, Gehring WJ. 2011. Analyzing the function of a hox gene: An evolutionary approach. Dev Growth Differ. 53:982-993.

Miller CT, Maves L, Kimmel CB. 2004. moz regulates Hox expression and pharyngeal segmental identity in zebrafish. Development. 131:2443-61.

Moreno TA, Kintner C. 2004. Regulation of segmental patterning by retinoic acid signaling during Xenopus somitogenesis. Dev Cell. 6:205-218.

Morgan D, Bailey M, Phelps P, Bellman S, Grace A, Wyse, R. 1993. Ear-nose-throat abnormalities in the CHARGE association. Arch Otolaryngol Head Neck Surg. 119:49-54.

Mortazavi A, Williams BA, McCue K, Schaeffer L, Wold B. 2010. Mapping and quantifying mammalian transcriptomes by RNA-Seq. Nat Methods. 5:621-628.

Mueller MM. 2007. Malthus under a microscope: Using the soil nematode Caenorhabditis elegans to test Darwin's premises about populations. The American Biology Teacher. 69:219-225.

Mulero-Navarro S, Esteller M. 2008. Chromatin remodeling factor CHD5 is silenced by promoter CpG island hypermethylation in human cancer. Epigenetics. 3:210-215.

Nasevicius A, Ekker SC. 2000. Effective targeted gene 'knockdown' in zebrafish. Nat Genet. 26:216-220.

National Scoliosis Foundation (www.scoliosis.org)

Nie J, Wang H, He F, Huang H. 2010. Nusap1 is essential for neural crest cell migration in zebrafish. Protein Cell. 1:259-266.

Oates AC, Mueller C, Ho RK. 2005. Cooperative function of deltaC and her7 in anterior segment formation. Dev Biol. 280:133-49.

Osley MA, Tsukuda T, Nickoloff JA. 2007. ATP-dependent chromatin remodeling factors and DNA damage repair. Mutat. Res. 618:65–80.

Patten SA, Jacobs-McDaniels NL, Zaouter C, Drapeau P, Albertson RC, Moldovan F. 2012. Role of Chd7 in Zebrafish: A model for CHARGE syndrome. PLoS One. In press.

Peterson CL, Laniel MA. 2004. Histones and histone modifications. Curr. Biol. 14:R546-551.

Petrie A, Finkel SE, Erbe J. 2005. Use of long-term E. coli cultures to study generation of genetic diversity & teach general microbiology laboratory skills. The American Biology Teacher. 67:87-92.

Pizard A, Haramis A, Carrasco AE, Franco P, López S, Paganelli A. 2004. Whole-mount in situ hybridization and detection of RNAs in vertebrate embryos and isolated organs. Curr Protoc Mol Biol. Chapter 14:Unit 14.9.

Pourquié O. 2001. Vertebrate somitogenesis. Annu Rev Cell Dev Biol. 17:311-50.

Pray-Grant MG, Daniel JA, Schieltz D, Yates JR 3rd, Grant PA. 2005. Chd1 chromodomain links histone H3 methylation with SAGA- and SLIK-dependent acetylation. Nature. 433:434-438.

Rachinsky A, Hartfelder K. 1990. Corpora allata activity, a prime regulating element for caste-specific juvenile hormone titre in honey bee larvae (Apis mellifera carnica). Journal of Insect Physiology. 36:189-194.

Radman-Livaja M, Rando OJ. 2010. Nucleosome positioning: How is it established, and why does it matter?. Dev. Biol. 339:258-266.

Randall V, McCue K, Roberts C, Kyriakopoulou V, Beddow S, Barrett AN, Vitelli F, Prescott K, Shaw-Smith C, Devriendt K, Bosman E, Steffes G, Steel KP, Simrick S, Basson MA, Illingworth E, Scambler PJ. 2009. Great vessel development requires biallelic expression of Chd7 and Tbx1 in pharyngeal ectoderm in mice. J Clin Invest. 119:3301-10.

Reifers F, Böhli H, Walsh EC, Crossley PH, Stainier DY, Brand M. 1998. Fgf8 is mutated in zebrafish acerebellar (ace) mutants and is required for maintenance of midbrain-hindbrain boundary development and somitogenesis. Development. 125:2381-95.

Rogers SM, Matheson T, Despland E, Dodgson T, Burrows M, Simpson SJ. 2003. Mechanosensory-induced behavioural gregarization in the desert locust Schistocerca gregaria. The Journal of Experimental Biology. 206:3991-4002.

Rogers SM, Matheson T, Sasaki K, Kendsrick K, Simpson SJ, Burrows M. 2004. Substantial changes in central nervous system neurotransmitters and neuromodulators accompany phase change in the locust. The Journal of Experimental Biology. 207:3603-3617.

Sanlaville D, Etchevers HC, Gonzales M, Martinovic J, Clément-Ziza M, Delezoide AL, Aubry MC, Pelet A, Chemouny S, Cruaud C, Audollent S, Esculpavit C, Goudefroye G, Ozilou C, Fredouille C, Joye N, Morichon-Delvallez N, Dumez Y, Weissenbach J, Munnich A, Amiel J, Encha-Razavi F, Lyonnet S, Vekemans M, Attié-Bitach T. 2006. Phenotypic spectrum of CHARGE syndrome in fetuses with CHD7 truncating mutations correlates with expression during human development. J Med Genet. 43:211-217.

Satar B, Mukherji SK, Telian SA. 2003. Congenital aplasia of the semicircular canals. Otol Neurotol. 24:437-446.

Sato M, Tsai HJ, Yost HJ. 2006. Semaphorin3D regulates invasion of cardiac neural crest cells into the primary heart field. Dev. Biol. 298:12-21.

Sawada A, Fritz A, Jiang YJ, Yamamoto A, Yamasu K, Kuroiwa A, Saga Y, Takeda H. 2000. Zebrafish Mesp family genes, mesp-a and mesp-b are segmentally expressed in the presomitic mesoderm, and Mesp-b confers the anterior identity to the developing somites. Development. 127:1691-702.

Schimmang T. 2007. Expression and functions of FGF ligands during early otic development. Int J Dev Biol.51: 473-481.

Schmitt EA, Dowling JE. 1999. Early retinal development in the zebrafish, Danio rerio: light and electron microscopic analyses. J Comp Neurol. 404:515-536.

Schmitt S, Aftab U, Jiang C, Redenti S, Klassen H, Miljan E, Sinden J, Young M. 2009. Molecular characterization of human retinal progenitor cells. Invest Ophthalmol Vis Sci. 50:5901-5908.

Schmoldt A, Forecki J, Hammond DR, Udvadia AJ. 2009. Exploring differential gene expression in zebrafish to teach basic molecular biology skills. Zebrafish. 6:187-199.

Schnetz MP, Bartels CF, Shastri K, Balasubramanian D, Zentner GE, Balaji R, Zhang X, Song L, Wang Z, Laframboise T, Crawford GE, Scacheri PC. 2009. Genomic distribution of CHD7 on chromatin tracks H3K4 methylation patterns. Genome Res.19:590-601.

Schnetz MP, Handoko L, Akhtar-Zaidi B, Bartels CF, Pereira CF, Fisher AG, Adams DJ, Flicek P, Crawford GE, Laframboise T, Tesar P, Wei CL, Scacheri PC. 2010. CHD7 targets active gene enhancer elements to modulate ES cell-specific gene expression. PLoS Genet. 6:e1001023.

Schoenwolf GC. 2008. Laboratory Studies of Vertebrate and Invertebrate Embryos: Guide and Atlas of Descriptive and Experimental Development (9th Edition). Upper Saddle River, NJ: Pearson Education- Benjamin Cummings.

Schwanbeck R, Martini S, Bernoth K, Just U. 2011. The Notch signaling pathway: Molecular basis of cell context dependency. European Journal of Cell Biology. 90:572-581.

Scimone ML, Meisel J, Reddien PW. 2010. The Mi-2-like Smed-CHD4 gene is required for stem cell differentiation in the planarian Schmidtea mediterranea. Development. 137:1231-41.

Sekulic A, Kim SY, Hostetter G, Savage S, Einspahr JG, Prasad A, Sagerman P, Curiel-Lewandrowski C, Krouse R, Bowden GT, Warneke J, Alberts DS, Pittelkow MR, DiCaudo D, Nickoloff BJ, Trent JM, Bittner M. 2010. Loss of inositol polyphosphate 5-phosphatase is an early event in development of cutaneous squamous cell carcinoma. Cancer Prev Res. 3:1277-1283.

Sewell W, Kusumi K. 2007. Genetic analysis of molecular oscillators in mammalian somitogenesis: clues for studies of human vertebral disorders. Birth Defects Res C Embryo Today. 81:111-120.

Shaw KM, Castranova DA, Pham VN, Kamei M, Kidd KR, Lo BD, Torres-Vasquez J, Ruby A, Weinstein BM. 2006. fused-somites-like mutants exhibit defects in trunk vessel patterning. Dev Dyn. 235:1753-1760.

Shilatifard A. 2006. Chromatin modifications by methylation and ubiquitination: implications in the regulation of gene expression. Annu Rev Biochem. 75:243-69.

Shimizu T, Bae YK, Muraoka O, Hibi M. 2005. Interaction of Wnt and caudal-related genes in zebrafish posterior body formation. Dev Biol. 279:125-41.

Shu X, Cheng K, Patel N, Joseph E, Tsai HJ, Chen JN. 2003. Na,K-ATPase is essential for embryonic heart development in the zebrafish. Development. 130:6165-6173.

Sif S. 2004. ATP-dependent nucleosome remodeling complexes: enzymes tailored to deal with chromatin. J. Cell. Biochem. 91:1087–1098.

Smith A, Avaron F, Guay D, Padhi BK, Akimenko MA. 2006. Inhibition of BMP signaling during zebrafish fin regeneration disrupts fin growth and scleroblasts differentiation and function. Dev Biol. 299:438-454.

Souriau J, Gimenes M, Blouin C, Benbrik I, Benbrik E, Churakowskyi A, Churakowskyi B. 2005. CHARGE syndrome: developmental and behavioral data. Am J Med Genet A. 133A:278-281.

Sparrow DB, Chapman G, Turnpenny PD, Dunwoodie SL. 2007. Disruption of the somitic molecular clock causes abnormal vertebral segmentation. Birth Defects Res C Embryo Today. 81:93-110.

Srinivasan S, Dorighi K, Tamkun J. 2008. Drosophila Kismet Regulates Histone H3 Lysine 27 Methylation and Early Elongation by RNA Polymerase II. Plos Genetics. 4:e1000217.

Stickney HL, Barresi MJ, Devoto SH. 2000. Somite development in zebrafish. Dev Dyn. 219:287-303.

Stockdale C, Flaus A, Ferreira H, Owen-Hughes T. 2006. Analysis of nucleosome repositioning by yeast ISWI and CHD1 chromatin remodeling complexes. J. Biol. Chem. 281:16279-16288.

Takada I, Mihara M, Suzawa M, Ohtake F, Kobayashi S, Igarashi M, Youn MY, Takeyama K, Nakamura T, Mezaki Y, Takezawa S, Yogiashi Y, Kitagawa H, Yamada G, Takada S, Minami Y, Shibuya H, Matsumoto K, Kato S. 2007. A histone lysine methyltransferase activated by non-canonical Wnt signalling suppresses PPAR-gamma transactivation. Nat Cell Biol. 9:1273-85.

Takahashi Y, Koizumi K, Takagi A, Kitajima S, Inoue T, Koseki H, Saga Y. 2000. Mesp2 initiates somite segmentation through the Notch signalling pathway. Nat Genet. 25:390-396.

Tang F, Barbacioru C, Nordman E, Li B, Xu N, Bashkirov VI, Lao K, Surani MA. 2010. RNA-Seq analysis to capture the transcriptome landscape of a single cell. Nat Protoc. 5:516-535.

Tellier AL, Cormier-Daire V, Abadie V, Amiel J, Sigaudy S, Bonnet D, de Lonlay-Debeney P, Morrisseau-Durand MP, Hubert P, Michel JL, Jan D, Dollfus H, Baumann C, Labrune P, Lacombe D, Philip N, LeMerrer M, Briard ML, Munnich A, Lyonnet S. 1998. CHARGE syndrome: report of 47 cases and review. Am J Med Genet. 76:402-409.

Thisse B, Heyer V, Lux A, Alunni A, Degrave A, Seiliez I, Kirchner J, Parkhill J-P, Thisse C. 2004. Spatial and Temporal Expression of the Zebrafish Genome by Large-Scale In Situ Hybridization Screening. Meth. Cell. Biol. 77:505-519.

Thomas IT, Frias JL. 1987. The heart in selected congenital malformations. A lesson in pathogenetic relationships. Ann Clin Lab Sci. 17:207-210.

Thompson BA, Tremblay V, Lin G, Bochar DA. 2008. CHD8 is an ATP-dependent chromatin remodeling factor that regulates beta-catenin target genes. Mol Cell Biol. 28:3894-904.

Thompson PM, Gotoh T, Kok M, White PS, Brodeur GM. 2003. CHD5, a new member of the chromodomain gene family, is preferentially expressed in the nervous system, Oncogene. 22:1002–1011.

Tran HG, Steger DJ, Iyer VR, Johnson AD. 2000. The chromo domain protein chd1p from budding yeast is an ATP-dependent chromatin-modifying factor. Embo J. 19:2323–2331.

Trapnell C, Salzberg SL. 2009. How to map billions of short reads onto genomes. Nat Biotechnol. 27:455-457.

Trapnell C, Williams BA, Pertea G, Mortazavi A, Kwan G, van Baren MJ, Salzberg SL, Wold BJ, Pachter L. 2010. Transcript assembly and quantification by RNA-Seq reveals unannotated transcripts and isoform switching during cell differentiation. Nat Biotechnol. 28:511-515.

Twine NA, Janitz K, Wilkins MR, Janitz M. 2011. Whole transcriptome sequencing reveals gene expression and splicing differences in brain regions affected by Alzheimer's disease. PLoS One. 6:e16266.

Uemura O, Okada Y, Ando H, Guedj M, Higashijima S, Shimazaki T, Chino N, Okano H, Okamoto H. 2005. Comparative functional genomics revealed conservation and diversification of three enhancers of the isl1 gene for motor and sensory neuron-specific expression. Dev Biol. 278:587-606.

Van Meter TD, Weaver DD. 1996. Oculo-auriculo-vertebral spectrum and the CHARGE association: clinical evidence for a common pathogenetic mechanism. Clin Dysmorphol. 5:187-196.

Vissers LE, van Ravenswaaij CM, Admiraal R, Hurst JA, de Vries BB, Janssen IM, van der Vliet WA, Huys EH, de Jong PJ, Hamel BC, Schoenmakers EF, Brunner HG, Veltman JA, van Kessel AG. 2004. Mutations in a new member of the chromodomain gene family cause CHARGE syndrome. Nat. Genet. 36:955–957.

Voskoboynikova OS. 1993. Evolution of the visceral skeleton and phylogeny of Nototheniidae. Journal of Ichthyology. 33:23-47.

Voskoboynikova OS. 1994. Rates of individual development of the bony skeleton of eleven species of the family Nototheniidae. Journal of Ichthyology. 34:108-120.

Voskoboynikova OS, Tereshchuk OY, Kellermann A. 1994. Osteological development of the Antarctic silverfish Pleuragramma antarcticum (Nototheniidae). Cybium. 18:251-271.

Vuorela P, Ala-Mello S, Saloranta C, Penttinen M, Poyhonen M, Huoponen K, Borozdin W, Bausch B, Botzenhart EM, Wilhelm C, Kääriäinen H, Kohlhase J. 2007. Molecular analysis of the CHD7 gene in CHARGE syndrome: identification of 22 novel mutations and evidence for a low contribution of large CHD7 deletions. Genet Med. 9:690-694.

Walker MB, Kimmel CB. 2007. A two-color acid-free cartilage and bone stain for zebrafish larvae. Biotechnic & Histochemistry. 82:23-28.

Wang HB, Zhang Y. 2001. Mi2, an auto-antigen for dermatomyositis, is an ATP-dependent nucleosome remodeling factor, Nucl. Acid Res. 29:2517–2521.

Weinberg ES, Allende ML, Kelly CS, Abdelhamid A, Murakami T, Andermann P, Doerre OG, Grunwald DJ, Riggleman B. 1996. Developmental regulation of zebrafish MyoD in wild-type, no tail and spadetail embryos. Development. 122:271–280.

Welden CW, Hossler RA. 2003. Evolution in the lab: Biocide resistance in E. coli. The American Biology Teacher. 65:56-61.

Wessels K, Bohnhorst B, Luhmer I, Morlot S, Bohring A, Jonasson J, Epplen JT, Gadzicki D, Glaser S, Göhring G, Mälzer M, Hein A, Arslan-Kirchner M, Stuhrmann M, Schmidtke J, Pabst B. 2010. Novel CHD7 mutations contributing to the mutation spectrum in patients with CHARGE syndrome. Eur J Med Genet. 53:280-285.

White PS, Thompson PM, Gotoh T, Okawa ER, Igarashi J, Kok M, Winter C, Gregory SG, Hogarty MD, Maris JM, Brodeur GM. 2005. Definition and characterization of a region of 1p36.3 consistently deleted in neuroblastoma. Oncogene. 24:2684–2694.

Wirtz P. 1973. Differentiation in the honeybee larva. Medelingen Landbouwhogeschool Wageningen. 73-75:1-66.

Wincent J, Schulze A, Schoumans J. 2009. Detection of CHD7 deletions by MLPA in CHARGE syndrome patients with a less typical phenotype. Eur J Med Genet 52:271-272.

Windhorst S, Minge D, Bähring R, Hüser S, Schob C, Blechner C, Lin HY, Mayr GW, Kindler S. 2012. Inositol-1,4,5-trisphosphate 3-kinase A regulates dendritic morphology and shapes synaptic Ca(2+) transients. Cell Signal. 24:750-757.

Workman JL. 2006. Nucleosome displacement in transcription. Genes Dev. 20:2009–2017.

Wyatt S, Ballard HE. 2007. Arabidopsis ecotypes: A model for course projects in plant biology & evolution. The American Biology Teacher. 69:477-481.

Yelon D, Horne SA, Stainier DY. 1999. Restricted expression of cardiac myosin genes reveals regulated aspects of heart tube assembly in zebrafish. Dev. Biol. 214:23–37.

Yokoi H, Yan YL, Miller MR, BreMiller RA, Catchen JM, Johnson EA, Postlethwait JH. 2009. Expression profiling of zebrafish sox9 mutants reveals that Sox9 is required for retinal differentiation. Dev Biol.329: 1-15.

Yoon YS, Lee MW, Ryu D, Kim JH, Ma H, Seo WY, Kim YN, Kim ss, Lee CH, Hunter T, Choi CS, Montminy MR, Koo SH. 2010. Suppressor of MEK null (SMEK)/protein phosphatase 4 catalytic subunit (PP4C) is a key regulator of hepatic gluconeogenesis. Proc Natl Acad Sci USA. 107:17704-17709.

Yu HH, Moens CB. 2005. Semaphorin signaling guides cranial neural crest cell migration in zebrafish. Dev Biol. 280:373-85.

Zentner GE, Hurd EA, Schnetz MP, Handoko L, Wang C, Wang Z, Wei C, Tesar PJ, Hatzoglou M, Martin DM, Scacheri PC. 2010. CHD7 functions in the nucleolus as a positive regulator of ribosomal RNA biogenesis. Hum Mol Genet. 19:3491-501.

Zhang L, Kendrick C, Jülich D, Holley SA. 2008. Cell cycle progression is required for zebrafish somite morphogenesis but not segmentation clock function. Development, 135:2065-2070.

Zheng Z. 2006. Use of the gl1 Mutant & the CA-rop2 Transgenic Plants of Arabidopsis thaliana in the Biology Laboratory Course. The American Biology Teacher. 68:e148-e153.

# Biographical Data

Name of Author: Nicole Lynn Jacobs McDaniels

Place of Birth: Utica, New York

Date of Birth: Jaunary 25, 1986

Graduate and Undergraduate Schools Attended:

Syracuse University, Syracuse New York
SUNY University at Buffalo, Buffalo, New York

Degrees Awarded:

Bachelors of Science in Biological Sciences with a concentration in Cellular and Molecular Biology, 2007, SUNY University at Buffalo

Awards and Honors:

Syracuse University Certificate in University Teaching, 2011
Syracuse University Graduate Student Association Travel Grant, 2010
Syracuse University Biology Department Travel Grant, 2009
Syracuse University Department of Biology Teaching Assistantship 2007-2011
Christopher White Award for combined excellence in scholarship and outstanding contributions to the community, 2007
Phi Beta Kappa, 2007
Golden Key National Honor Society, 2006
UB Launch Chapter of the Mortar Board, 2006
National Society for Collegiate Scholars, 2005
Excellence in General Chemistry, 2005
University at Buffalo Dean's List, 2004-2007
University at Buffalo Scholars Program, 2004-2007

Professional Experience:

Science Instructor, Herkimer County Community College, 2011-present
Instructor, Department of Biology, Syracuse University, 2009-2010
Teaching Assistant, Department of Biology, Syracuse University, 2007-2011
Laboratory Intern, Prevalere Life Sciences, 2007